# IMPROVING THERMAL STABILITY AND INTRATRACHEAL DELIVERY OF VIRAL-VECTORED DRY POWDER VACCINES

IMPROVING THERMAL STABILITY AND INTRATRACHEAL DELIVERY OF VIRAL-VECTORED DRY POWDER VACCINES

By: MYLA M. MANSER, B. ENG. BIOSCI

A thesis submitted to the School of Graduate Studies in Partial Fulfillment of the Requirements for the Degree of Master of Applied Science



April 2022

MASTER OF APPLIED SCIENCE (2022) Chemical Engineering

MCMASTER UNIVERSITY Hamilton, Ontario

**TITLE:** IMPROVING THERMAL STABILITY AND INTRATRACHEAL DELIVERY OF VIRAL-VECTORED DRY POWDER VACCINES

**AUTHOR:** Myla M. Manser

B.Eng.Biosci (McMaster University)

**SUPERVISORS:** Professor Michael R. Thompson

Professor Emily D. Cranston

**NUMBER OF PAGES:** xii, 127

## Lay Abstract

Most vaccines currently available on the market must be stored and transported at temperatures ranging from 2-8 ºC to properly maintain their function, with some vaccine requiring temperatures as low as -80 ºC. The equipment required to maintain such temperatures is costly and is a significant limitation for developing nations trying to secure vaccine access. As an alternative to traditional liquid vaccine formulations, dry powder vaccines offer stability at room temperature without the need for expensive equipment and can also be administered through inhalation. Using a processing method called spray drying, an active vaccine component can be encapsulated in a carefully selected sugar formulation which forms a protective coating as the particles dry to provide stabilization. Since the efficacy of such dry powder vaccines must be first evaluated with mouse models, the focus of this work was to improve an existing blend of sugars to produce a dry vaccine powder that contains high enough dosage for mouse testing. Processing losses from spray drying were minimized through careful selection of vaccine cryoprotective agents, in addition to optimizing the blend ratio and molecular weight of sugars used for encapsulation. Successful delivery of the optimized powder to the lungs of mice was also accomplished after analyzing the suitability of a variety of custom-made handheld devices. This work shows that inhalable dry powder vaccine delivery is a promising solution to help improve temperature stability and achieve more equitable access to vaccines globally.

**Abstract**

As the global public health community continues to strive for more equitable vaccine access, thermal instability of liquid vaccines continues to be a significant challenge due to strict cold-chain temperature requirements. Dry powder vaccines offer a favourable alternative, with the ability to retain vaccine efficacy at ambient temperature conditions. In the form of dry powder, vaccines against respiratory diseases can also be administered via inhalation for targeted delivery to the lung tissue. A processing technique known as spray drying is particularly promising for the development of thermally stable and inhalable dry powder vaccines, offering a method of continuous and scalable production. Spray drying is widely used in the pharmaceutical industry and can effectively encapsulate and immobilize labile biologics, like adenoviral vectors, within a glassy carbohydrate matrix to help retain biologic function. However, pulmonary delivery of a thermally stable, viral vectored dry powder vaccine has yet to be demonstrated.

This thesis focuses on improving the formulation of a carbohydrate excipient blend of mannitol and dextran encapsulating a human serotype 5 adenovirus (AdHu5), with the goal of producing an inhalable vaccine with sufficient viral potency for *in vivo* murine testing. First, the impact of cryoprotective agents used for frozen storage of the stock adenovirus was investigated with respect to viral activity retention, thermal stability and inhalation properties of the dry powder after spray drying. Trehalose was considered a preferred cryoprotective agent, compared to glycerol traditionally used for adenoviral cryo-storage, allowing for the preparation of a high potency viral dry powder with 1.5 log loss of viral titre after processing and thermal aging. Further investigation of the dextran mass ratio and dextran molecular weight used within the excipient blend revealed that incorporating mannitol in a 1:3 ratio with 500 kDa dextran can further improve viral activity to achieve 0.8 log loss of viral titre after aging. Through controlled drying dynamics,

this formulation led to improved activity retention and thermal stability, in addition to desirable aerosolization properties for pulmonary delivery. Using this optimized formulation, custom-made intratracheal dosator devices were evaluated for pulmonary powder delivery in mice. The method of powder loading in the device was found to be a significant factor of device performance *in vivo* when determining if the critical powder mass dosage could be delivered. Successful intratracheal delivery of the AdHu5-vectored dry powder was achieved with a pipette-tip loading dosator and led to a strong bioactive response. Overall, this work indicates the feasibility of murine pulmonary delivery and immunological testing of a thermally stable, adenoviral-vectored vaccine in dry powder form.

**Acknowledgements**

I would like to sincerely thank my supervisors Dr. Michael R. Thompson and Dr. Emily D. Cranston for all of their support and guidance over these past few years. Your approach to problem solving and scientific discovery has been so motivational to me. It has been such a pleasure learning from both of you. The passion I have for this work is just as strong as the day I started and I feel so grateful to have be part of this important area of research.

I also extend thanks to Dr. Zhou Xing for all of his guidance from the adenovirus perspective, as well as all of my research colleagues within his research group in the McMaster Immunology Research Centre. Thank you to Mathy Jeyanathan, Xueya Feng, Anna Zganiacz, Sam Afkhami, Mike D'Agostino, Dominik Fritz for your assistance with all that was virus/cell culture related and for always making me feel welcome. To Vidthiya Jeyanathan, thank you for all of your time and commitment towards mastering the art of intratracheal powder delivery. Wishing you all the best as you finish up your degree!

To my fellow grad students in our Spray Dry Team and CAPPA-D group, your support throughout this process has made it such a joy. Dr. Blair A. Morgan, your mentorship during my time as an undergrad summer student and into my Master's was so appreciated – thank you for fielding my numerous questions and never hesitating to share advice. Varsha Singh, thank you for showing me the ropes on the spray dryer/aerosol testing, best wishes for your PhD defense!

Additional thanks to Dr. Myrna B. Dolovich for her thoughtful project guidance and to everyone who offered additional technical support over the past few years, in particular: Rod Rhem, Marcia Reid, Mark Mackenzie, Zoya Tabunshchyk, Heera Marway, James Mayo, Sahar Esmaeili Samani and Jen Newton.

To my friends and family, thank you from the bottom of my heart for all of your love and support throughout my entire educational career. Mom, Dad, Shayna you are my greatest source of inspiration and my most cherished teachers. Thank you for always bringing wisdom and balance into my life whenever I need it most. And finally Carter, my rock, thank you for your unwavering support as I have journeyed through grad school while weathering a pandemic. I can't wait for the adventures we have ahead of us!

## Table of Contents

## Table of Figures

## Table of Tables

**Nomenclature**

| | |
|---|---|
| AdHu5 | human serotype 5 adenovirus |
| API | active pharmaceutical ingredient |
| DNA | deoxyribonucleic acid |
| DPI | dry powder inhaler |
| DSC | differential scanning calorimeter |
| D50 | median particle diameter |
| EDTA | ethylenediaminetetraacetic acid |
| FPF | fine particle fraction |
| GFP | green fluorescent protein |
| MD | mannitol-dextran excipient blend |
| MMAD | mass median aerodynamic diameter |
| mRNA | messenger ribonucleic acid |
| MW | molecular weight |
| PBS | phosphate buffered saline |
| pDMI | pressurized metered dose inhaler |
| PFA | paraformaldehyde |
| PFU | plaque forming units |
| RH | relative humidity |
| SEM | scanning electron microscopy |
| SARS-CoV-2 | severe acute respiratory syndrome coronavirus 2 |
| $T_g$ | glass transition temperature |
| TGA | thermogravimetric analysis |

## Declaration of Achievement

The research presented herein is original work with all original drafts completed by myself, Myla M. Manser, with editorial assistance from my supervisors Dr. Michael R. Thompson and Dr. Emily D. Cranston and Dr. Zhou Xing. The role of co-authors is described fully in the respective chapters.

## Chapter 1: Introduction and Research Objectives

### 1.1 Introduction

Vaccination is widely considered one of the most life-saving public health interventions against infectious diseases over the past century [1]. In light of the COVID-19 pandemic, however, shortfalls of the current global vaccine supply chain are even more apparent. Commercial vaccine distribution is strictly reliant on a traditional storage temperature range between 2 ºC and 8 ºC, known as the cold-chain, to ensure therapeutic effectiveness [2]. For more sensitive vector-based vaccine products, storage temperatures as low as -80 ºC can be required [3]. Inequities in global vaccine access are largely influenced by the high cost of cold-chain storage infrastructure to maintain temperature during transportation and storage which are less readily available in developing nations [4,5]. Costly equipment maintenance is a critical limitation in many global regions, with equipment failure and insufficient storage space leading to high rates of vaccine wastage [2]. According to the World Health Organization, nearly 2.8 million vaccine doses were wasted in 2011 in five countries as direct result of cold-chain equipment failure, which is costly to both government programs and vaccine manufacturers [6]. Maintaining cold-chain requirements are even more challenging in warm climate zones, necessitating the development of thermally stable vaccines that do not require refrigeration or freezing temperatures to maintain potency and clinical effectiveness.

Vaccine thermal stability is especially relevant to adenovirus-based vaccine strategies, due to the high temperature sensitivity these labile biologics. Clinical relevance of adenovirus vaccines has continued to grow from the recent development of human vaccines targeting lung diseases like tuberculosis and COVID-19 [7,8]. With tuberculosis being more prominent in the global regions

that already suffer from the challenges of vaccine distribution [9], manufacturing vaccines in a thermally stable form is particularly important. To tackle this challenge, a technique known as spray drying has been used to thermally stabilize adenovirus in powder form [10]. As a cost-effective and scalable processing method, spray drying has become extensively used within the pharmaceutical industry [11]. The process of spray drying involves atomizing a liquid feed of dissolved excipients and the active pharmaceutical ingredient (API), followed by contact with heated air and rapid particle drying to produce a stable dry powder encapsulation.

Beyond thermal stability, another benefit to producing a vaccine in spray dried form is the potential for administration via pulmonary delivery. Pulmonary delivery via inhalation has long been considered an effective administration route for therapeutic drug delivery. Applications that have incorporated inhalation strategies range widely from asthma therapy [12], cancer therapeutics [13] and insulin delivery [14] to pulmonary vaccination. Delivering vaccines through inhalation is especially appealing for respiratory diseases, where targeting the lungs directly may induce a specific mucosal immune response [15,16]. In fact, respiratory mucosal vaccination has been shown to induce an immune response that is equivalent or stronger than observed via intramuscular injection [17,18,19].

Current publications have yet to successfully demonstrate the immunogenic response of a thermally stable, viral-vectored spray dried vaccine administered through *in vivo* pulmonary delivery. With this end goal in mind, this work builds upon a previously determined mannitol-dextran formulation to improve the encapsulation of an human serotype 5 adenoviral vector (AdHu5) and more effectively retain its viral activity after exposure to elevated temperatures. This work offers new insights into the factors that can improve a thermally stable and inhalable vaccine

formulation while also providing guidance towards achieving successful *in vivo* pulmonary delivery of dry powder pharmaceutics in mice.

### 1.2 Research Objectives

Overall, the goal of this thesis is to improve the viral potency and aerosol delivery of a thermally stable and inhalable, viral-vectored spray dried powder to achieve an *in vivo* immunogenic response upon intratracheal delivery in mice. This work utilizes AdHu5 expressing either green fluorescent protein (GFP) for *in vitro* activity evaluation or luciferase for assessing *in vivo* bioactivity. This work was divided into three main areas of investigation:

1) *Analyzing the impacts of cryoprotective agents on AdHu5 stabilization*

The aim of this project was to understand how cryoprotective agents used in biologic frozen storage impact viral activity retention during spray drying of a high potency AdHu5-vectored dry powder for pulmonary delivery. Through this work, we indicate that (1) the inclusion of glycerol within a spray dried mannitol-dextran encapsulation of AdHu5 has a negative impact on both viral activity and process yield and (2) trehalose is an appropriate cryogenic alternative that improves viral activity retention after spray drying to produce an inhalable dry powder with high viral potency.

2) *Determining the role of mass ratio and molecular weight of excipients in spray dried encapsulation of AdHu5*

Using trehalose as the cryoprotective agent for adenoviral storage, the goals of this project were to analyze the effect of the dextran mass ratio (relative to mannitol) and dextran molecular

weight on the stabilization and aerosolization of AdHu5 in a spray dried powder. By developing a deeper understanding of the dynamic roles of mannitol and dextran during particle drying, we were able to optimize the binary excipient formulation to minimize AdHu5 activity loss during processing and thermal aging while achieving appropriate powder properties for inhalation.

*3) Evaluating dosator devices for intratracheal delivery of AdHu5 dry powder in mice*

This project aimed to develop a reliable dosator device for intratracheal delivery to allow for the *in vivo* assessment of the optimized AdHu5-vectored dry powder in mice. We correlated dosator needle tip materials (including stainless-steel, polypropylene and polytetrafluoroethylene) and operational parameters like loaded mass, syringe air volume and storage conditions with overall device performance *in vitro* to help address the current challenges of testing dry powder pharmaceutics in mice and guide future developments. We also investigated three custom-made dosator device designs for murine intratracheal delivery, including tamp-loading, chamber-loading and pipette tip-loading designs, to successfully deliver a bioactive dose of spray dried AdHu5 powder *in vivo*.

## 1.3 Thesis Outline

This thesis is divided into six chapters, beginning with the current chapter. A review of the current published literature is provided in Chapter 2 to summarize recent advances in the areas of adenovirus vaccination strategies, stabilization through vitrification and pulmonary delivery methods of dry powder vaccines. Chapter 3 includes a study published in the *International Journal of Pharmaceutics* that analyzes the impact of cryoprotective agents on activity retention of AdHu5 encapsulated in a mannitol-dextran spray dried powder. Excipient formulation parameters are

further optimized in Chapter 4, in which dextran mass ratio and dextran molecular weight are both correlated to viral activity retention and aerosolization behaviour of the inhalable dry powder. Chapter 5 assesses the design and performance of custom-made intratracheal dosator devices and compatibility with the optimized mannitol-dextran formulation, while also providing *in vivo* validation of the AdHu5-vectored dry powder formulation via intratracheal delivery in mice. Overall conclusions are presented in Chapter 6 along with suggested directions for the future of this work.

## Chapter 2: Background and Literature Review

### 2.1 Adenovirus Functionality and Stabilization

For decades, adenoviruses have been studied for their application in recombinant vaccine development [20] by providing the biologic machinery for gene transduction to mammalian cells. Adenoviruses act as the delivery vessel, carrying targeted genetic sequences that allow for localized antigen expression to induce an immune response. With a non-enveloped and complex icosahedral structure [21], see Figure 2.1, an adenovirus has a large diameter of approximately 150 nm and is comprised of a variety of outer capsid and core proteins that protect its genome of double-stranded DNA [22,23]. The capsid shell consists of 3 major proteins known as hexons, pentons and fibres [22]. Upon infection, adenoviruses do not incorporate their genetic material into the host genome but instead induce transient gene expression [24]. They are commonly modified to be non-replicating, which also increases their safety profile as a vaccine vector. Thanks to their genetic stability, ease of infectivity and high efficiency of gene transduction, adenoviruses have become increasingly popular for both gene therapy and vaccination in the clinical setting [24]. Compared to live-attenuated pathogens, adenoviruses offer mild pathogenicity while being able to express highly immunogenic antigens [25]. For this reason, recombinant adenovirus vaccines are considered a safer and more cost-effective option when designing vaccines for highly pathogenic diseases.

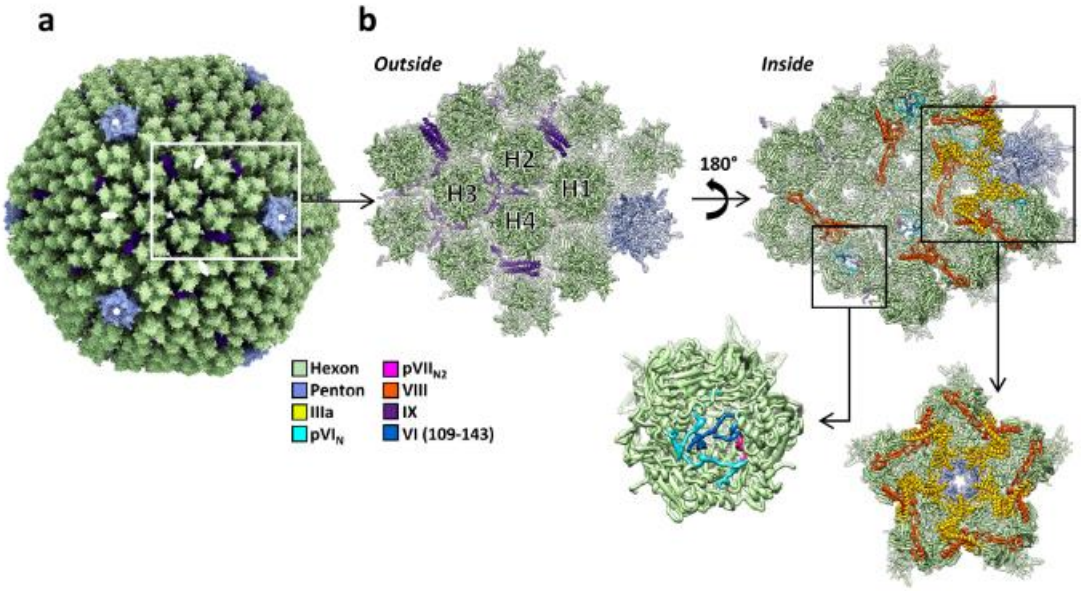


**Figure 2.1**. Structural rendering of an adenovirus capsid where (a) indicates the general view and (b) represents a zoomed in view of one asymmetric unit from both the outside and inside of the capsid. Hexon trimers are labelled H1- H4 and associated proteins are colour-coded based on the legend above. Figure reproduced from: [23]

Adenovirus-based vaccination strategies have been effectively demonstrated against a wide range of infectious diseases including rabies [26,27], tuberculosis [7] and Ebola [28]. There are currently 86 adenovirus species recognized by the International Committee for the Taxonomy of Viruses [23], with human and chimpanzee adenovirus species being among the more commonly used in vaccine development [27,28,29]. In light of the current COVID-19 pandemic, a commercialized chimpanzee adenovirus vaccine against SARS-CoV-2 was developed though a collaboration between University of Oxford and AstraZeneca and has been widely used in global vaccination efforts [30]. A next generation COVID-19 vaccine has also built upon a similar adenovirus platform by encoding for a range of antigens that induce more widespread protective immunity through the respiratory mucosal route [18].

Despite the great therapeutic potential of adenoviruses, these vectors are highly susceptible to deactivation and degradation due to thermal stresses, repeated freeze-thaw cycles, low pH and viral aggregation [31,32,33]. Since an adenovirus is composed of highly specialized proteins, denaturation is of high concern and can ultimately lead to impaired viral function. Adenoviruses are highly labile materials, particularly at temperatures above 56 °C at which structural changes can occur [31,33]. Since viral vectors are incredibly sensitive to environmental changes, overall viability can change greatly between the time of production to final administration [34]. As a result, the stability of a therapeutic adenovirus is highly dependent on the formulation in which it is stored.

Most commonly, adenovirus vectors are stored in a frozen liquid suspension with 10% glycerol (v/v) at cryogenic temperatures as low as -80 °C [35]. Glycerol is well known for its ability to stabilize globular proteins under cryogenic conditions through thermodynamic interactions that favour the folded, native state of a protein [36]. By reducing the freezing point of water and preventing eutectic crystallization, glycerol helps to immobilize the adenovirus in an amorphous, glass-like state to keep the viral proteins in their native form [37]. This immobilization process within an amorphous solid is often referred to as vitrification and ultimately prevents damage caused by viral agglomeration or ice crystal formation. However, such ultralow storage temperatures greatly hinder therapeutic transportation and administration efforts in areas of the world that do not have access to the necessary infrastructure and equipment. The risk of thawing and refreezing from fluctuating temperatures is also worrisome, given the potential for adenoviral deactivation due to repeated freeze-thaw cycling [38]. Producing a pharmaceutically robust adenovirus therapeutic therefore requires improved thermal stability.

Initial efforts to improve the temperature stability of viral vectors heavily focused on the development of stable liquid formulations and excipient concentrations. To further understand the

role of excipient formulation and temperature stability, Rexroad et al. demonstrated that the secondary and tertiary protein structure of a human serotype 5 adenovirus (AdHu5) could be stabilized in the presence of 10% sucrose at 45 °C, but quaternary structure could not be maintained at this temperature [33]. Comparatively, a 2% sucrose formulation led to rupture of the adenovirus's icosahedral vertices and total capsid disassembly after exposure to 45 °C [33]. At refrigeration temperatures, Evans et al. were highly successful in optimizing a liquid formulation for long-term stabilization of a human immunodeficiency virus (HIV) vaccine using AdHu5 with a blend of sucrose, glycerol and polysorbate-80 among other components [39]. Within the field, this formulation is often considered the gold standard for achieving long-term stability of a liquid adenovirus vaccine in the typical cold-chain temperature range between 2-8 °C [28]. However, this formulation is still limited to refrigeration storage and resulting vaccines can only be administered through traditional needlestick injections.

## 2.2 Alternative Vitrification Methods for Thermal Stability

### 2.2.1 Amorphous Solid Dispersion and Excipient Selection

Recently, the pharmaceutical industry has shifted focus towards using vitrification methods without water to achieve thermal stability of active pharmaceutical ingredients and biologics. By entrapping labile biologics like adenoviruses within a solid amorphous powder, storage temperatures can be much higher than using water-based cryogenic vitrification. Producing amorphous solids is of particular interest as they lack long-term molecular packing order, unlike crystalline solids, but do display some short-range molecular order [40]. This distinction can give amorphous solids improved solubility and dissolution properties since they exhibit greater free

energy than in the crystalline state [40,41]. From a kinetic perspective, amorphous behavior is characterized based on the degree of polymer mobility or available free volume within the matrix. When polymer mobility is very low, with minimum free volume, the amorphous material is in a glassy and highly viscous state [41]. Entrapping adenovirus within this state helps to prevent viral aggregation or damage from thermal stresses, thereby preserving the native protein structure and ensuring that viral activity is retained.

Carbohydrates are particularly useful excipients for the solid vitrification of biologics due to their low toxicity, accessibility in a purified state, improved biocompatibility and biodegradation [40,42,43]. Despite most sugars being thermodynamically more stable in their crystalline form, transition to the amorphous state can be achieved under specific processing conditions [44]. Within an amorphous solid, the glass transition temperature ($T_g$) describes the point above which molecular mobility has increased to allow for a decrease in viscosity to form a rubbery state [41]. By immobilizing components within a glassy amorphous matrix, the bioactivity and stability of an API can be maintained at elevated storage temperatures as long as the $T_g$ is sufficiently high. Since the ideal storge temperature of an amorphous solid drug encapsulation is approximately 50 ºC below the glass transition temperature [45], achieving thermostability at room temperature requires $T_g$ values of at least 75-80 ºC. Carbohydrates including sucrose, lactose and trehalose all have relatively high glass transition temperatures, thus making them common excipient selections. Table 2.1 includes a summary of commonly researched carbohydrates and their reported glass transition temperature.

**Table 2.1**. Reported $T_g$ values of common carbohydrates used in amorphous solid applications.

| CARBOHYDRATE | CLASSIFICATION | REPORTED $T_G$ | REFERENCE |
|---|---|---|---|
| **LACTOSE** | Reducing Disaccharide | $T_g$ = 101 ºC | [46] |
| **MALTOSE** | Reducing Disaccharide | $T_g$ = 87 ºC | [46] |
| **SUCROSE** | Non-reducing Disaccharide | $T_g$ = 62 - 70 ºC | [46,47] |
| **TREHALOSE** | Non-reducing Disaccharide | $T_g$ = 100 ºC | [48] |
| **RAFFINOSE** | Non-reducing Trisaccharide | $T_g$ = 70 - 80 ºC | [47,48] |
| **DEXTRAN** ($\boldsymbol{40\ kDa}$) | Polysaccharide | $T_g$ = 223 ºC | [49] |

Eliminating the need for cryogenic storage conditions could have huge implications on the global vaccine supply chain. This is of particular importance for developing nations that have faced great challenges in the roll-out of mass vaccination programs due to the cost of securing and maintaining cold-chain infrastructure [5]. Beyond thermal stability improvements, there are many other benefits to dry solid vitrification. Removing water leads to a weight and volume reduction of the final solid dispersion, which can lower costs associated with transportation and storage [50]. Since APIs are entrapped in powder form, alternative vaccine delivery methods can also be explored. For example, dry powder vaccines can be aerosolized for inhalable delivery [51], delivered intranasally [52] or used for oral administration [53]. For vaccines targeting respiratory diseases, direct delivery to lungs could ultimately initiate stronger mucosal immunity compared to traditional intramuscular injection [18,55]. Alternatively, reconstitution of dry powders prior to intramuscular delivery is another common strategy that takes advantage of increased thermal stability.

### 2.2.2 Lyophilization

To produce solid amorphous encapsulations, lyophilization or freeze-drying has been commonly used to achieve long term API stability. The lyophilization process typically consists of three main steps: a freezing step followed by primary and secondary dryings steps [55]. Beginning as a liquid, the freezing step cools the formulation until ice nucleation and growth occurs such that ice crystals separate from a glassy matrix [56]. Primary drying allows ice crystals to sublimate while secondary drying promotes water desorption under increased temperature and low pressure [56]. Geeraedts et al. found that a freeze-dried inactivated virus vaccine could be stored for one year at ambient temperature without losing its immunogenic effect in mice [57]. However, lyophilization must be conducted in batch operation, which can be a lengthy process and more complicated to scale up [50]. It is also an energy intensive and expensive process, which is especially detrimental for vaccine manufacturing that already suffers from high development costs. Although strong thermal stability has been achieved using this technique, for relevance in vaccine manufacturing the production process must have the potential to scale up efficiently.

### 2.2.3 Spray Drying

Spray drying is a method used to create amorphous solid dispersions that is becoming increasingly popular for biologic entrapment. Heavily used within the food industry for additive and nutraceutical encapsulation [59,60], spray drying has also become a popular choice in the pharmaceutical industry due to its scalability and continuous mode of operation [60]. The spray drying process pumps a liquid feed, consisting of dissolved excipient and API, through a nozzle upon which it atomizes into tiny droplets within a preheated chamber for rapid particle drying [61]. The high temperature and relatively low humidity environment of the drying chamber drives

evaporation from the droplet, causing solute concentration to increase on the droplet surface or diffuse towards the interior and eventually precipitate once saturated [50]. Figure 2.2 shows a schematic of a typical laboratory-scale spray dryer set up. Compared to lyophilization which can require additional milling or secondary sieving, spray drying offers much higher control over the final properties of particles [50]. Milling could also be harmful to highly sensitive APIs like adenoviruses and is therefore not a suitable processing technique [62]. Entrapment of sensitive and labile biologics requires a high degree of process control which makes spray drying a promising production method.

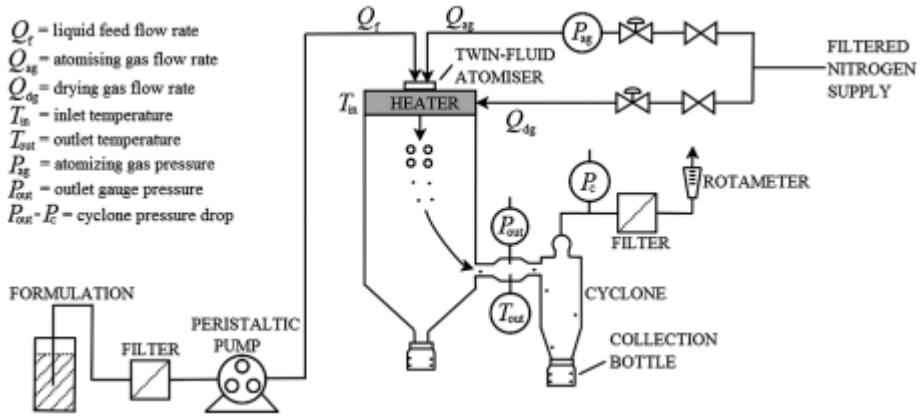


**Figure 2.2**. Schematic example of a typical laboratory-scale spray dryer set-up. Reproduced from [143]**.**

To date, there have been a number of successful reports of biologic entrapment using spray drying, ranging from protein antigens [51] to drugs with poor water solubility [60]. Many labile APIs have also been effectively spray dried to retain activity at elevated temperatures. Ohtake et al. spray dried a live-attenuated measles virus to find that processing losses were only 0.2 log loss and viral titre could be maintained for 8 weeks at 37 ºC [63]. Saboo et al. used a similar approach to produce a thermally stable vaccine using virus-like particles targeting human papillomavirus

and saw an immunogenic response in mice after exposure to 37 °C for one year [64]. Within our group, LeClair et al. demonstrated that spray drying could be used to successfully retain viral activity of a serotype 5 human adenovirus (AdHu5) by entrapping the adenovirus within a mannitol-dextran excipient matrix [10,65] and lea to an immunological response *in vivo* after reconstitution [29]. However, there has yet to be a report in the literature showing successful pulmonary delivery of a thermally stable encapsulated adenovirus powder, prepared through spray drying.

### 2.3 Dry Powder Administration

#### 2.3.1 Strategies and Benefits of Pulmonary Delivery

Pulmonary delivery is a well-established administration route for drug delivery and extensive developments have been made in this area over the past few decades. This approach has been widely studied for a vast range of applications including diabetic insulin delivery [66], cancer therapeutics [13,67] and pulmonary vaccination [51,62,68]. Physiologically, the lungs offer large surface area for absorption with a thin epithelial layer that is highly vascularized [69]. Since inhaled drug therapies are delivered directly to the target lung tissue, it is expected that the API dosage required to initiate a mucosal immune response is lower for inhaled delivery compared to a systemic delivery method like injection [70]. Delivering highly localized doses of a therapeutic could also reduce reactogenicity or unwanted systemic side effects [71]. Inhaled delivery is non-invasive and allows for relatively easy self-administration, which are highly advantageous features in a clinical setting. In vaccine development against respiratory disease like tuberculosis, targeting mucosal lung tissue has been found to offer a stronger immune response compared to standard intradermal injection [54]. However, inhaled delivery is notoriously challenging because the lungs

are highly sensitive to foreign particles and can remove inhaled particulate through mucociliary clearance, mediated by phagocytotic immune cells on the epithelial lining [69,72].

There are three main categories of established pulmonary drug delivery methods in humans including: liquid nebulizers, pressurized metered dose inhalers (pMDIs) and dry powder inhalers (DPIs) [13,73]. Nebulizers convert a liquid therapeutic into fine aerosol particles or mist, often using compressed air, that can be inhaled by a patient through a mouthpiece. Despite widespread clinical application, aerosol generation with a nebulizer is only suitable for liquid formulations which functionally limits the use of thermally stable dry powder formulations and prevents long-term storage [67,70]. Comparatively, pMDIs are hand-held devices with a valve, mouthpiece and chamber from which the therapeutic formulation is released with a propellant upon actuation [74]. There are currently a number of commercially approved pMDIs on the market but these devices contain a known greenhouse gas, hydrofluoroalkane, as a propellent chemical [74]. Based on the limitations of both nebulizers and pMDIs, current research efforts continue to focus on dry powder inhalers as a promising option for achieving dry powder pulmonary delivery. DPIs have gained significant attention as a lower cost option, while also being highly portable, easy to handle and free of environmentally harmful propellants [13].

### 2.3.2 Dry Powder Requirements for Inhalation

When developing inhalable powders for pulmonary delivery, aerosol properties like particle size, morphology, moisture content and flowability are critical aspects to consider in an effective particle design strategy. In general, particles are considered inhalable if they have an aerodynamic diameter within the range of 1-5 µm. Particles below 3 µm are commonly referred to as the fine particle faction (FPF) of an aerosolized powder [69]. Particle size can be reported in terms of geometric diameter, as well as mass median aerodynamic diameter (MMAD) which

determines size based on aerodynamic behaviour within an airstream [75]. Acknowledging that powder production methods like spray drying tend to produce particles that can range in size, geometric particle size is often described in terms of the median diameter of the total distribution (D50). The D50 value represents the particle diameter at 50% in the cumulative distribution of dry powder distributed from a delivery device [69]. In other words, 50% of the population has a particle diameter that is either above or below the measured D50 value. Span of the distribution is another important parameter to inform about the size heterogeneity within a powder. Larger calculated span is associated with a larger range of sizes within a powder sample.

Aerodynamic diameter ($d_{ae}$) or MMAD can be experimentally determined using equipment like cascade impactors, which are composed of separated plates or stages that correspond to increasingly smaller aerodynamic diameter [75]. Particles travel through an airstream until they become impacted at a specific stage, upon which the mass of powder collected at each stage is measured and used to calculate a cumulative mass distribution [75]. There have also been theoretical attempts to determine ($d_{ae}$) based on the relationship between physical diameter of the particle ($d_p$) and bulk density of a powder ($\rho$) by the following equation [76]:

$$d_{ae} = d_p * \left( \frac{\left(\frac{\rho}{\rho_{ref}}\right)^{0.5}}{\gamma} \right) \quad (2.1)$$

From the above equation (2.1), particles are assumed to be spherical in shape, making the particle shape factor ($\gamma$) equal to 1. The density of water (1 g/cm$^3$) can be used as the reference density. The D50 value is assumed to be representative of the median geometric particle size and is determined experimentally through laser diffraction methods.

Achieving appropriate respiratory deposition of inhaled powders is largely based on aerodynamic diameter, since smaller particles have greater capacity to reach the more peripheral airways of the lung. Figure 2.3 highlights this negative correlation between particle size and the fraction of lung deposition of aerosolized powders observed in both mice and rats, as adapted from the work of Kuehl et al. [72]. This work demonstrated that as particle size decreased from 5 to 0.5 μm, the fraction of aerosol deposition observed in the lungs of mice increased from 2% to 12% respectively [72]. Particles above 5 μm in size are more likely to deposit in the oral cavity or upper airways and therefore more easily removed through clearance mechanisms [76]. However, there has also been a report by Edwards et al. of successful distal lung delivery and increased lung retention using low density, porous particles containing insulin that had larger geometric diameters up to 20 μm [77]. Other reports have similarly suggested that particles with geometric diameters above 10 μm experience prolonged retention time at the lung surface [78]. To achieve prolonged drug release, increased retention time at the lung and avoidance of macrophage phagocytosis is

preferred [79]. Comparatively, vaccination requires fast and effective macrophage activation to mount a strong immune response.

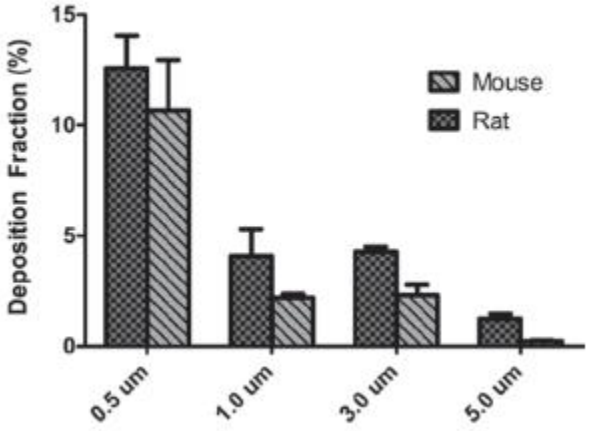


**Figure 2.3.** Aerosolized particle deposition fraction in lungs of mice and rats based on known particle size. Error bars represent the standard error between four animal replicates. Adapted directly from [72].

## 2.4 Pulmonary Delivery in Murine Models

Within the preclinical stages of vaccine development, murine models are considered the "go-to" mechanistic model when testing *in vivo* immunogenicity of new vaccine candidates [80]. Mice are relatively inexpensive and have a short growth period, which is advantageous during the initial screening stages of vaccine testing [51,81]. However, the administration of dry powders in mice presents many additional challenges due to the small anatomical scale and difficulty achieving consistent powder dispersion. Since mouse lungs cannot handle high amounts of aerosolized powder, the API must be of sufficient concentration or potency within a powder formulation to limit the amount of powder mass required per dose. A typical dose of dry powder administered to a mouse can range depending on the concentration of API and the administration device or method used. Based on the small scale of mouse lungs, it is common to test inhaled

powders with slightly smaller particle size at the preclinical stage compared to the larger particle size used in the formulations intended for humans. Typically mouse studies require the use of inhalable particles with an aerodynamic diameter between 2-3 μm [82].

For dry powders intended for inhalation in rodents, pulmonary delivery is commonly achieved through passive inhalation, intratracheal instillation or endotracheal administration, also called insufflation. Since mice are obligatory nose-breathers, passive inhalation implies that aerosolized particles will travel through the nasal cavity, into the trachea and through the pulmonary bronchi [83]. Delivery of aerosolized powder through passive inhalation is often referred to as a "nose-only" method, requiring the mouse to be appropriately restrained within an inhalation chamber [51,68]. This method typically requires a customized set-up and has been demonstrated with and without the use of animal sedation [72,84]. For example, Gomez et al. tested a spray dried tuberculosis vaccine powder in mice with an aerodynamic diameter between 1-2 μm using a custom nose-only aerosol exposure chamber and observed an antigen specific immune response similar to intramuscular delivery [51]. Comparatively, Wang et al. delivered an amorphous immunosuppressant agent by using a rotating brush generator (Figure 2.4) to produce powder aerosols that flowed into a nose-only chamber for rats to achieve high pulmonary bioavailability [78]. A more simplified, hand-held system was utilized by Kaur et al. which consisted of a nose-only exposure chamber made from a plastic centrifuge tube and an air inlet tube connected to a pipette bulb to fluidize the loaded powder [68]. Overall, the nose-only delivery

strategy is associated with high levels of material loss and poor delivery efficiency. In cases where the API is produced in low volume or at high cost, this delivery strategy is not ideal.

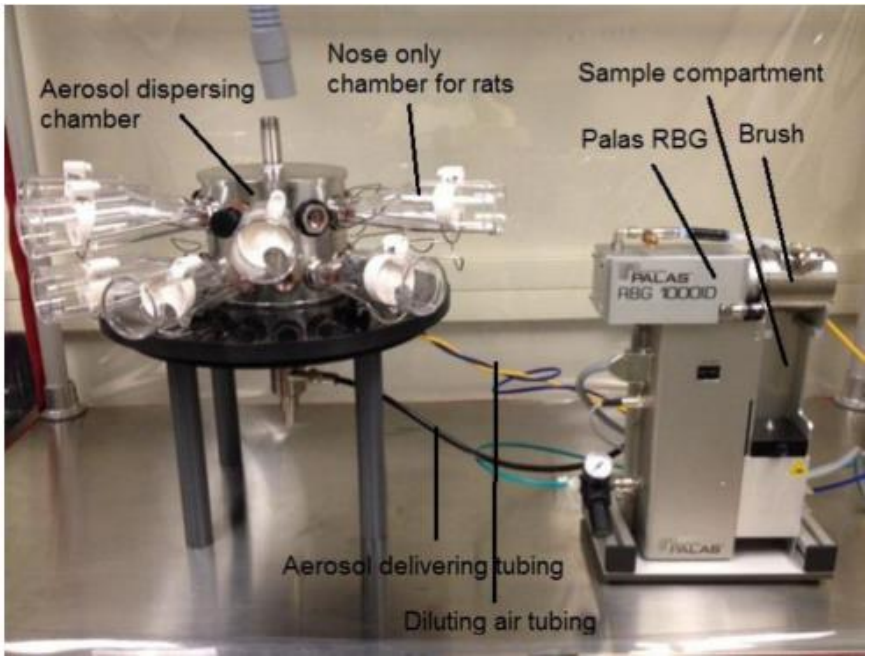


**Figure 2.4.** Rotating brush generator (RBG) set up for nose-only dosing in rats. Adapted directly from [78].

Alternatively, dry powders can also be reconstituted and delivered as aerosolized liquid using commercially available nebulizers or aerosolizers. This strategy was used by Qiu et al. to deliver a reconstituted, spray dried mRNA vector using a liquid Microsprayer® Aerosolizer (Penn-Century Inc.) which successfully expressed luciferase in the distal lungs of mice 24 hours after transfection (Figure 2.5) [85]. Compared to non-reconstituted spray dried powder, their work showed higher luciferase expression (and therefore a higher rate of transfection) with reconstitution [85]. Solid lipid nanoparticles containing insulin have also been delivered to the pulmonary system using a scaled-up method of nebulization in larger rats with a nebulization efficiency of 63% [66]. Despite this demonstrated efficiency in mice, reconstituting dry powders for nebulization still leads to challenges and limitations when transferring to human pulmonary delivery.

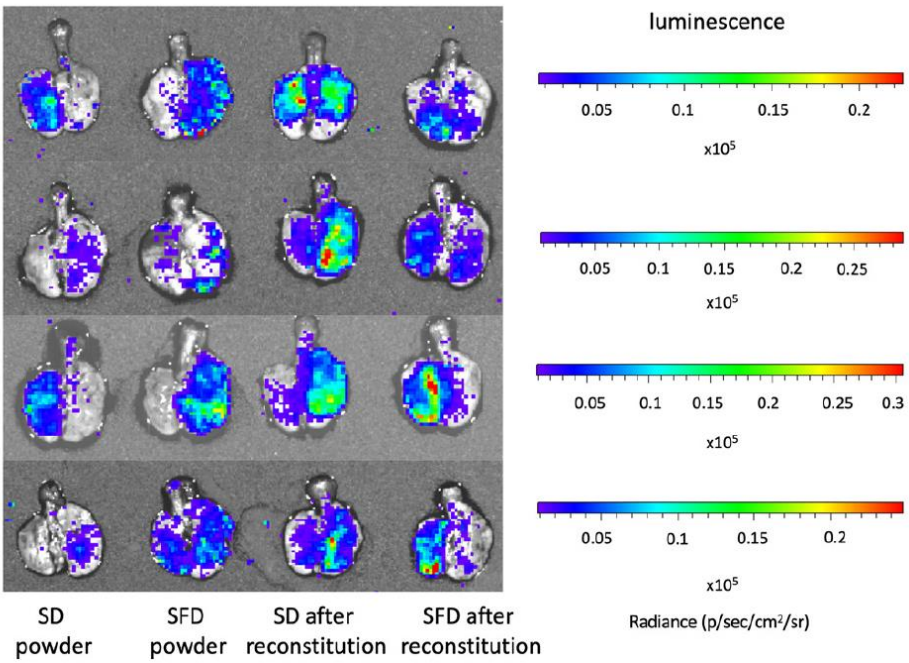


**Figure 2.5.** Luminescence observed in mice lungs 24 hours following intratracheal delivery and transfection of reconstituted spray dried (SD) and spray-freeze dried (SFD) mRNA expressing luciferase. Adapted directly from: [85].

Inhaled dry powder delivery in mice is also challenging because of the significant lack of commercially available devices that can be used for powder administration. Most commonly cited is the Penn-Century Dry Powder Insufflator™, which is a hand-held device used for pulmonary powder delivery in rodents and uses positive pressure to dispel material from the device into the trachea [68]. Despite being a commonly used device for dry powder administration, the Penn-Century Dry Powder Insufflator™, is no longer sold commercially as the company shut down production in 2016. The Penn-Century device also suffered from limitations, including significant differences between emitted dose achieved *in vitro* compared to *in vivo* [73]. As a result, many groups have published details of custom-made dry powder insufflator designs often fabricated from easily accessible components [84,86,87].

For larger dosage capacity, Durham et al. described the assembly of an easily disposable dosator for endotracheal delivery using a syringe, microcentrifuge tube with holes drilled at both ends and a 18 Ga needle tip [87]. However, the application of this device was demonstrated as an aerosol generator within a nose-only dosing chamber for passive inhalation in guinea pigs, rather than direct endotracheal delivery in murine models [87]. To scale down this dosator design for administration in mice, Stewart et al. used an alternative approach by tamping powder into a shortened 21 Ga needle tip which was then inserted into a 20 Ga Teflon needle and sprayed into a mouse trachea with a 1 mL syringe to deliver a spray dried anti-tuberculosis multidrug [88]. This method is limited by the mass powder capacity within the dosator needle tip, which is on the order of micrograms of powder. For applications that require larger powder doses (on the order of milligrams rather than micrograms) powder delivery may be insufficient to observe an appropriate response *in vivo*.

In contrast, Ihara et al. assembled a dosator using a 1 mL syringe, 3-way stopcock and a disposable pipette tip connected to a 22 Ga needle for successful pulmonary delivery of siRNA to the lungs of mice [86]. Figure 2.6 illustrates a similar set-up from Qiu et al. who also used a 3-way stopcock in conjunction with a gel-loading pipette tip, 1 mL syringe and guiding cannula for pulmonary delivery of spray freeze dried mRNA powder [84]. In both of these cases, the 3-way stopcock served as a way to protect the powder dosage prior to administration while also allowing airflow during actuation. These strategies also permit ease of device assembly, since there is no additional machining required to retrofit components and offer a functional method of intratracheal powder delivery in murine models.

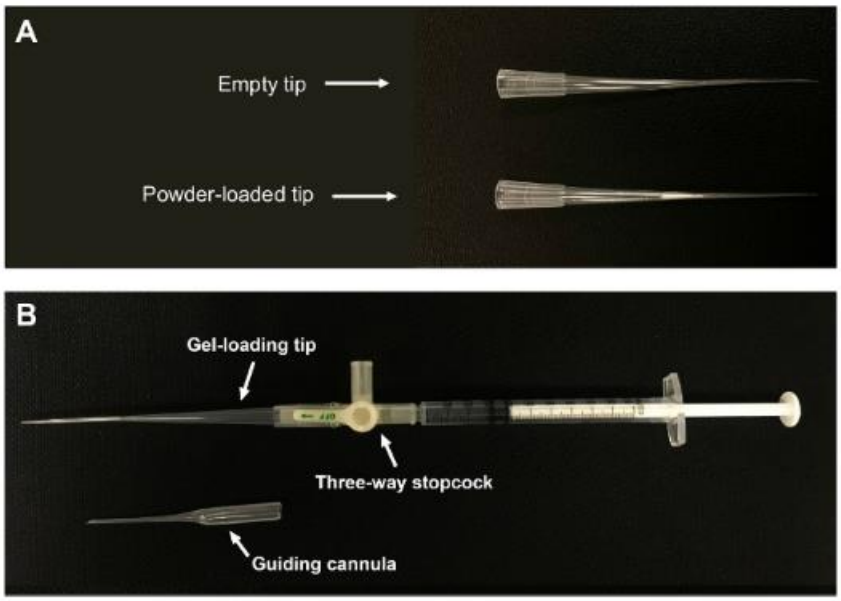


**Figure 2.6.** Dry powder delivery device showing (A) powder packed towards end of the gel-loading. Panel (B) shows the full device assembly along with the guiding cannula used for intratracheal administration. Directly adapted from: [84].

## Chapter 3: Cryoprotective Agents Influence Viral Dosage and Thermal Stability of Inhalable Dry Powder Vaccines



Within this chapter, the experimental design, viral activity testing, thermal property characterization and data analysis was all conducted by myself. Varsha Singh conducted the SEM imaging and particle sizing. Sahar Esmaeili Samani conducting moisture analysis via Karl Fisher titration. Co-author Xueya Feng prepared the adenoviral vector used in this work. The manuscript was drafted by myself and edited by supervisors Dr. Michael Thompson, Dr. Emily Cranston and Dr. Zhou Xing. Approval was given by all authors prior to submission.

**Manser, M.M.,** Feng, X., Xing, Z., Cranston, E.D., Thompson, M.R., 2022. Cryoprotective agents influence viral dosage and thermal stability of inhalable dry powder vaccines. Int. J. Pharm. 617, 121602. https://doi.org/10.1016/j.ijpharm.2022.121602

**Abstract**

Increasing viral dosage within dry powder vaccines reduces the powder mass required to elicit an immune response through pulmonary delivery. This work analyzes how cryoprotective agents affect viral activity, particle properties and thermal stability of a spray dried, inhalable vaccine vector under high viral loading. Stock suspensions of a human serotype 5 adenovirus (AdHu5) vector in either neat phosphate buffered saline (PBS), 10% glycerol in PBS, or 5% trehalose in PBS were added to a mannitol-dextran formulation prior to spray drying. At high viral loading, spray dried powder containing glycerol had a viral titre log loss of 2.8 compared to 0.7 log loss using neat PBS. Powders containing glycerol had a lower glass transition temperature ($T_g$) compared to all other formulations, permitting greater viral mobility and exposure to heat damage. Inclusion of glycerol also promoted particle cohesion during spray drying and lower yields. Using 5% trehalose as a cryogenic alternative, viral powders had a viral log loss of 1.5 and the highest displayed thermal stability over time. Additionally, trehalose-containing powders had smaller particles with lower water moisture content and higher powder yield compared to glycerol-containing powders. These findings demonstrate the importance of cryoprotective agent selection when developing thermostable vaccine powders.

**Key Words**

adenovirus, spray drying, inhalation, glycerol, thermal stability, cryoprotective agent

## 3.1 Introduction

One of the greatest challenges in securing global vaccine access is the need for a reliable and economical temperature control infrastructure. Traditional vaccine storage and transport requires that temperatures be kept between 2 ºC to 8 ºC at all times, a protocol commonly referred to as the cold-chain [34,89]. Depending on the biologic, ultra-low temperature storage down to -80 ºC may also be required to ensure vaccine stability [16]. Failure to meet these rigorous protocols can result in vaccine wastage or risk of healthcare workers administering vaccines with decreased potency [5]. This requirement is particularly limiting for developing nations in tropical or semiarid climates that deal with unreliable power supply and frequent equipment failure [6,90]. These global regions are also disproportionately more impacted by the spread of infectious diseases such as tuberculosis (TB). The World Health Organization estimates that over 95% of all TB cases and resulting deaths occur in developing countries [9]. To reduce both disease prevalence and infrastructure limitations, scientific efforts are now focusing on developing vaccines that can maintain efficacy under elevated temperature conditions [63,91]. Thermostable vaccines will reduce global cold-chain dependency, offering a solution to the supply challenges in regions with limited resources.

One of the new TB vaccine strategies has focused on adenoviral vectors as effective modes for gene transfer and antigen delivery [7,29,92,93]. Although adenoviral vectors are highly unstable at and above room temperature, our group has previously shown that spray drying technology can effectively encapsulate adenovirus and maintain thermal stability in powder form by using a mannitol-dextran excipient blend [10,94,95]. Immobilization of viral vectors or proteins within a glassy particle matrix prevents aggregation and denaturation to preserve biologic activity *in vitro* [10,95,96] and *in vivo* [29,97]. Excipient formulations used in spray dried micro-encapsulations

must exhibit strong compatibility with the entrapped biologic to retain its activity, while also displaying appropriate particle morphology and thermal stability [95,98].

Formulation selection in the context of spray drying typically refers to the excipients used for viral vector encapsulation, but the stock adenovirus suspension also has specific formulation requirements. Adenoviruses are highly susceptible to deactivation, therefore long-term storage protocols recommend the use of cryoprotective agents to prevent damage induced by freezing and thawing [39]. These cryoprotective agents are often selected based on adenovirus purification procedures [99], with many protocols specifying 10% glycerol in PBS due to the historical use of glycerol for cryopreservation of viruses and proteins [37,100,101]. Sucrose is another commonly used cryoprotective agent, known to achieve long term AdHu5 stability in liquid formulations stored between 2-8 ºC [39,102]. Although sucrose is effective at maintaining adenovirus infectivity under refrigeration conditions, relatively high concentrations of the excipient are required to achieve stability at elevated temperatures [33,102,103]. As a non-reducing sugar, trehalose has interesting potential as a cryogenic alternative that can stabilize viral vectors under frozen conditions but has not been as extensively studied to date [104]. Adenovirus stability has been well documented in the context of cryopreservation and liquid vaccine formulation, but the impacts of stock viral suspension within spray dried powders has not been previously reported in literature.

Administering spray dried powders as inhalable vaccines is particularly advantageous for respiratory diseases like TB as they can reach the distal lung for a targeted immune response [62]. For inhalable solid dosages, it is crucial that the powder has correct particle size for distal lung penetration and contains sufficient viral potency to elicit an immune response *in vivo*. Viral losses will occur during the spray drying process and within the lungs during pulmonary delivery, so initial viral loading (i.e., the volume of adenovirus stock suspension added to an excipient

formulation) must account for anticipated losses as well as the necessary dose to achieve efficacy. However, increasing viral potency of a spray dried vaccine powder for stronger immunogenic response *in vivo* requires that adenoviral stock suspension be carefully considered for its impact on created particles. Initial trials by the authors to increase potency by 3-10 times, simply through increasing the quantity of added adenoviral stock, produced vaccine powders with very low yields and poor adenovirus activity, contrary to the intent of increasing viral dosage. This study explores the influence of cryoprotective agents within adenovirus stock suspension on the spray drying of a human serotype 5 adenovirus vector expressing GFP (AdHu5-GFP) encapsulated in a mannitol-dextran excipient blend. The goal of this work was to create a vaccine powder of higher viral potency, while also maintaining thermal stability and inhalable powder properties at higher viral loading.

## 3.2 Materials and Methods

### *3.2.1 Chemicals and Biologics*

Dextran ($M_r$ 40000 Da) and D-mannitol were sourced as USP grades from Millipore-Sigma (Ontario, Canada). D-(+)-trehalose dihydrate and glycerol were also purchased from Millipore-Sigma (Ontario, Canada). Water was purified in house utilizing a Barnstead GenPure Pro purification system operating at a resistivity of 18.2 MΩ-cm from ThermoFisher Scientific (Waltham, MA, USA). Cell culturing was performed using A-549 epithelial lung tumor cells grown in α-minimum essential media (α-MEM) combined with 10% fetal bovine serum and 1% streptomycin/penicillin, as prepared based on Life Technologies protocols from Invitrogen (ON, Canada). A recombinant, replication-deficient human serotype 5 adenovirus vector was prepared locally in the vector facility within the McMaster University Immunology Research Centre and modified to express Green Fluorescent Protein (GFP), referred to as AdHu5-GFP. Stock

suspensions of the adenoviral vector were prepared in parallel using either phosphate buffered saline (PBS), 10% glycerol in PBS or 5% trehalose in PBS. Initial viral titres were determined via plaque forming assay and were found to be $5.7 \times 10^8\ pfu/mL$ (PBS buffer), $1.4 \times 10^{10}\ pfu/mL$ (10% glycerol in 1X PBS) and $4.4 \times 10^8\ pfu/mL$ (5% trehalose in 1X PBS).

*3.2.2 Sample Preparation*

Excipient solution was prepared at a concentration of 1% solids by weight containing a mixture of mannitol and dextran (3:1 ratio by weight respectively) dissolved in purified water. This ratio of excipients was selected based on previous work reporting successful viral encapsulation and thermal stability of the AdHu5-GFP vector [10]. All physical characterizations were conducted on placebo powders, in which a 60 µL solution of cryoprotective agent in PBS (referred to as the placebo storage solution) was added to 10 mL of excipient feed solution and subsequently spray dried. The placebo powders used for particle characterization did not contain AdHu5-GFP vector. Placebo storage solutions were prepared by adding cryoprotective agents to autoclave sterilized PBS at the concentrations outlined in Table 3.1; the table includes calculated relative weight contributions of cryoprotective agents and salt residuals within the spray dried powders. Calculated compositions do not account for any residual moisture that may be retained in the powder after spray drying. The calculated dry composition values were determined based on spray drying a 10 mL excipient batch size loaded with 60 µL of placebo storage solution.

Powders containing AdHu5-GFP were prepared by spray drying a 10 mL excipient feed solution containing 10 µL, 30 µL, 60 µL or 90 µL of the adenoviral stock suspensions described in Section 3.2.1. Spray drying small batch volumes in these trials was intended to conserve usage of the viral vector.

**Table 3.1.** Placebo storage solutions used to prepare spray dried mannitol-dextran placebo powder and the calculated relative contributions of cryoprotective agents and salt residuals within the final dry powder.

| **Placebo Storage Solution** | **Cryoprotective Agent Composition** | **Composition in Dry Powder (wt.%)** | |
|---|---|---|---|
| | ***% Glycerol in 1X PBS (by weight)*** | ***Glycerol*** | ***Salts*** |
| 1 | 0 | 0.0 | 1.2 |
| 2 | 2 | 1.5 | 1.1 |
| 3 | 5 | 3.6 | 1.1 |
| 4 | 10 | 7.0 | 1.0 |
| 5 | 15 | 10.1 | 0.9 |
| | ***% Trehalose in 1X PBS (by weight)*** | ***Trehalose*** | ***Salts*** |
| 6 | 5 | 2.9 | 1.1 |
| 7 | 10 | 5.6 | 0.5 |

*3.2.3 Spray Drying Parameters*

All spray dried powders were produced using a B-290 Mini Spray Dryer manufactured by Büchi (Switzerland) using a 0.7 mm nozzle. To ensure processing consistency, all spray dryer settings were the same for each batch. A feed flow rate of 234 mL/h (pump setting 13%) was used with a spray gas flow rate of 357 L/h (rotameter reading 30 mm), an aspirator flow rate of 35 $m^3$/h (100% aspiration) and inlet temperature of 120 ℃. These conditions were selected to optimize yield, viral activity and particle size [65]. Outlet temperature was maintained between 56-62 ℃. Upon completion, powders were transferred from the collection tube of the spray dryer into microcentrifuge tubes within containment of the biosafety cabinet.

*3.2.4 Collected Yield and Handling of Dry Powder*

Collected yield was calculated as the percentage of removable powder mass recovered from the collection vial compared to the total mass of mannitol-dextran excipient in the feed

solution prior to atomization. Low collected yields indicate that powder residual was stuck to the walls of both the cyclone and collection vial, limiting powder removal. Following powder collection, all powders were stored in the presence of Drierite® anhydrous indicating desiccant (W.A Hammond Drierite Company Ltd.) in sealed tubes within a benchtop desiccator at room temperature. To avoid exposure to ambient humidity during transport between workspaces, samples were stored in a vacuum sealed container containing additional desiccant.

### *3.2.5 A549 Cell Culturing*

A batch suspension of low passage A549 cells were thawed from cryo-storage in liquid nitrogen. Cells were added to α-MEM that was pre-warmed to 37 ºC and immediately spun down in a centrifuge at 1400 rpm for 5 min. After discarding the supernatant, the cell pellet was resuspended in media to form a single cell suspension before plating in T150 flask. The flask was incubated overnight in a $CO_2$ water jacketed incubator from Forma Scientific Inc. (Marietta, OH, USA) at 37 ºC and 5% $CO_2$. Cell media was changed the next day to remove dead cells and residual dimethyl sulfoxide (DMSO) from the media used in cryo-storage. Cells revived from cryo-storage were passaged twice before *in vitro* testing was conducted. Upon reaching 80-90% confluency, cells were plated in a 96-well plate for viral activity testing and passaged into a fresh T150 culture flask.

### *3.2.6 Viral Activity Testing via Flow Cytometry*

Viral activity was tested in vitro by infecting 40,000 confluent A549 cells with spray dried vaccine powders, as described previously [105]. Each spray dried sample was reconstituted in α-MEM to a 1% solids concentration. Cell infection took place within one hour of spray drying to neglect the influence of varying storage conditions in our analyses. Following infection, culture

plates were incubated at 37 ℃ for approximately 24 h. Media was then aspirated from each well and cells were washed with 1X PBS prior to trypsinization. Each sample was transferred as a single cell suspension to a 4 mL tube and spun for 5 min at 1400 rpm in a centrifuge. After decanting, 1 mL of 1X PBS/ 2 mM EDTA (prepared in house) was added to each sample before centrifuging again at 1400 rpm for 5 min and decanting. To facilitate cell fixation, 1 mL of 1% paraformaldehyde (PFA) prepared in house was added to each sample. This was followed by a 10-min incubation period at room temperature. A third and final spin at 1800 rpm was performed and remaining liquid was decanted before adding 200 µL of flow cytometry staining buffer (FACS buffer, prepared in house) to each sample.

Flow cytometry was performed using a CytoFlex LX flow cytometer from Beckman Coulter Life Sciences (Indianapolis, IN, USA) with CytExpert software used for data acquisition. A minimum of 10,000 events were analyzed per sample, representing at least 25% of cells plated. GFP expression was determined using FlowJo® software from BD (New Jersey, USA). Auto-gating of the data was used to identify the live cell population and remove artifacts of cellular debris and doublet formation that could skew the results. The overall percentage of GFP expression was compared to a negative control. A representative gating process is included in Figure A3.1 in the Supplementary Material. A calibration curve was then used to correlate the percentage of GFP to the viral multiplicity of infection (MOI) which represents the ratio of plaque forming units to the number of cells tested (see Figure A3.2 in Supplementary Material). A viral titre was calculated in terms of pfu/mL, followed by pfu/mg to normalize based on collected powder weight. Results were discussed in terms of viral titre log loss to compare final titres with the initial amount of virus loaded in each sample. Flow cytometry scatterplots and corresponding event histograms of positive GFP expression can be found in Figures A3.3-A3.5 in Supplementary Material.

### *3.2.7 Aging and Thermal Stability of Viral Vector Powder*

The impact of each stock viral suspension on spray dried powder thermal stability was assessed using accelerated aging conditions. Each vaccine powder was incubated at 45 ºC in a water bath (ThermoFisher Scientific, Waltham, MA, USA) for 72 hours prior to testing viral activity via flow cytometry. To prevent any moisture uptake during the aging process, samples were stored in microcentrifuge tubes sealed with Parafilm®, which were placed within a plastic bag containing desiccant [95]. The bag was stored in a glass jar sealed with Parafilm® containing additional desiccant and finally placed into a larger plastic bag before placing in the water bath. After the 72-hour incubation period, samples were removed from the water bath and diluted in α-MEM for subsequent cell infection. Viral activity testing via flow cytometry was conducted the following day. Replicate testing was conducted for all sample points, with a minimum of two true replicates per cryogenic agent tested.

### *3.2.8 Particle Characterization*

#### *3.2.8.1 Thermal Properties of Spray Dried Powder*

Thermograms for each spray dried placebo powder were generated using a Q200 Differential Scanning Calorimeter (DSC) from TA Instruments (New Castle, DE, USA). Between 6-12 mg of sample stored on desiccant was weighed into an aluminum pan that was hermetically sealed. The best technique found to highlight the glass transition temperature ($T_g$) of the simple and complex carbohydrates in the formulation involved two normal heat-cool cycles, first between 20-120 ºC and then 20-160 ºC with a ramp rate of 25 ºC/min. This was followed by a third pass slowly heating the sample up to 200 ºC at 2 ºC/min under modulation with an amplitude of $\pm$1 ºC and a period of 60 s. The $T_g$ was quantified using Universal Analysis 2000 software from TA

Instruments (New Castle, DE, USA). All placebo powders were tested in duplicate as true replicates.

*3.2.8.2 Moisture Content of Spray Dried Powder*

Retained moisture content of a spray dried powder was determined using a C10SX coulometric Karl Fisher titrator (Mettler Toledo, Columbus, OH, USA). The placebo powder was weighed in a glove box configured with a dry nitrogen flush to maintain a relative humidity of <10%. Samples were dissolved in 2 mL of anhydrous formamide prior to titration. A volume of 0.1 mL sample solution was injected in the titrator for measurement. After applying blank corrections, the moisture content was determined within each sample.

*3.2.8.3 Particle Sizing*

Placebo powder was dispersed from an ICOone® inhaler that was generously provided by Iconovo (Lund, Sweden). Particle size distribution was detected and analyzed using a Helos R-series laser diffraction sensor from Sympatec GmbH (Pulverhaus, Germany) outfitted with a R2 lens with a focal length of 50 mm. Reliable detection for the R2 lens ranges from 0.45 – 87.5 µm. Cumulative distributions of particle sizes were generated for powder samples of weighed mass between 8-11 mg. Stated particle size was based on the median particle diameter of the distribution (D50), representing the $50^{th}$ percentile of the distribution. The $10^{th}$ (D10), $50^{th}$ (D50) and $90^{th}$ (D90) percentiles of the particle size distribution were used to calculate span, shown in Eq.3.1.

$$Span = \frac{D90 - D10}{D50} \tag{3.1}$$

*3.2.8.4 Imaging of Spray Dried Particles*

To visualize particle morphology and relative aggregation, spray dried placebo powders were imaged using a Tescan Vega II LSU scanning electron microscope from Tescan Orsay Holding, a.s. (Brno, Czech Republic). Prior to imaging, samples were placed on double-sided carbon tape and sputter-coated with a layer of 24 nm of gold using a Polaron E5100 sputter coater from Quorum Technologies Limited (Laughton, UK). All images were captured using an electron accelerating voltage of 5 kV with a working distance ranging from 17.03-17.33 mm and a magnification of 4000.

*3.2.9 Freeze-Thaw Stability of AdHu5 Vector Stock Suspensions*

Freeze-thaw stability of AdHu5-GFP stock suspension was tested by thawing a single vial of AdHu5-GFP viral vector suspended in PBS. It should be noted that this vial had been thawed once before commencing freeze-thaw studies. Prior to storage at -85 ºC, the vial of AdHu5-GFP vector had an initial viral titre of $5.7x10^8$ pfu/mL. Once thawed, 10 µL aliquots of viral stock suspension were diluted in PBS by a factor of 100 and each respective cryoprotective agent was added to achieve the following concentrations by weight: 0% glycerol (PBS only), 5% glycerol, 10% glycerol, 5% trehalose and 10% trehalose. From this viral buffer dilution, 100 µL was removed for viral titre determination via flow cytometry using the protocol outlined in Section 2.6. Remaining samples were frozen at -85 ºC for 7 days before thawing at room temperature and repeating the activity test. For each subsequent freeze-thaw cycle, 100 µL was removed from each respective storage buffer. This process was repeated four times. Sample dilution was accounted for in the calculation of viral titre at each freeze-thaw cycle.

## 3.3 Results and Discussion

### *3.3.1 Impacts of Buffer Composition on Viral Activity*

Preparing a vaccine powder for inhalable delivery requires that the adenovirus is active and is delivered at sufficient concentration to elicit an immune response. Our previous work focused on stabilizing the viral vector but only studied *in vivo* immunogenicity of reconstituted powders prepared with 10 µL adenoviral stock suspension per 100 mg excipient, resulting in a viral titre of ~$10^6$ pfu/mg in the spray dried powder [29]. Although this viral dosage was sufficient for intramuscular delivery in mice, evaluation of this powder through pulmonary delivery requires an increased dosage up to 9-fold to achieve a detectable response. Following conventional purification and cryo-storage protocols for AdHu5, the adenoviral stock suspension contained 10% glycerol in PBS in our initial trials to increase dosage. It was not initially anticipated that increasing the volume of stock adenoviral suspension in the excipient solution would have a negative impact on viral activity in the spray dried product. However, Figure 3.1 shows that increased loading of the adenoviral stock suspension containing 10% glycerol led to substantially increased viral titre log losses upon spray drying up to 3.3 log loss at a high viral loading of 90 µL added to 100 mg of excipient.

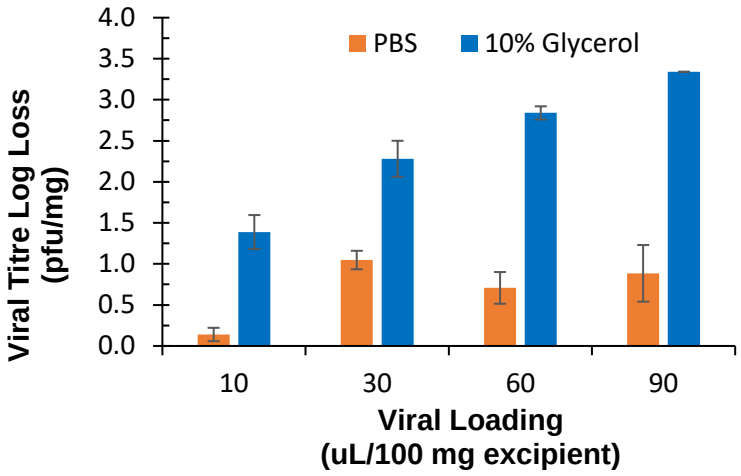


**Figure 3.1.** AdHu5-GFP viral activity log loss in spray dried powders as a function of viral loading with either neat PBS (no glycerol) or 10% glycerol in PBS as the adenoviral stock suspension. Error bars represent the standard error between averaged duplicates.

In contrast, when the PBS adenovirus stock suspension was added to the formulation, spray dried powders showed more acceptable changes in viral titre log loss when viral loading was increased from 10 to 30 µL/100 mg excipient. Viral activity then remained relatively constant at 1 log loss up to the highest viral loading of 90 µL/100 mg. For both stock adenoviral suspensions used, an increased viral loading corresponded to an increase in the amount of buffer salt within the spray dried matrix composition. Viral activity was essentially preserved during spray drying with increased PBS stock adenoviral suspension, suggesting that the buffer salts are much less detrimental to viral stability in the powder product compared to the cryoprotective agent glycerol. Ohtake et al. similarly found that viral titre process losses did not increase significantly by adding a potassium phosphate buffer in concentrations between 25-50 mM to an excipient solution prior to spray drying measles virus [63]. For comparison, all tested adenoviral stock suspensions in the present study contained a low concentration of potassium phosphate of 1.76 mM in addition to 134 mM sodium chloride and 100 mM disodium phosphate salts. The slight increase in AdHu5-GFP

titre log loss observed for PBS loading of 30 µL/100 mg and higher could indicate the need for buffer salt optimization in the adenoviral stock suspension, but this was beyond the focus of the present study.

### *3.3.2 Impact of Increasing Stock Viral Suspension on Collected Yield*

Using the adenoviral stock suspensions with and without glycerol, Figure 3.2 reveals that the cryoprotective agent presented significant challenges in collecting adequate process yields. We observed that increasing the volume of glycerol in the feed solution resulted in a strong negative correlation with the yield collected. Qualitatively, the higher glycerol content caused the powder to become increasingly adhesive on the glassware of the spray dryer. Much of these yield losses occurred due to particle adhesion on the walls of the spray dryer's cyclone and drying chamber which limited the amount of powder that could be collected. In comparison, by removing glycerol from the adenoviral stock suspension, the collected yields remained constant across all loadings of PBS adenoviral stock suspension. Similar findings have been reported by another group who experienced decreased yield when adding glycerol to a zein-based spray dried encapsulation of an antimicrobial peptide [58]. With batch yields often used as an indicator of process efficiency, this data further highlights the importance of investigating cryoprotective agents for their impact on spray drying viral encapsulations effectively. The adenovirus was assumed to be evenly distributed within the excipient feed solution, meaning that increased yield losses proportionally reduced the amount of adenovirus recovered in the collection vial. It should be noted that small volume batches were prepared for this study which accounts for the low yields overall, but we still consider the trend meaningful. Process yields from a laboratory spray dryer are expected to increase as batch volumes are scaled up [60].

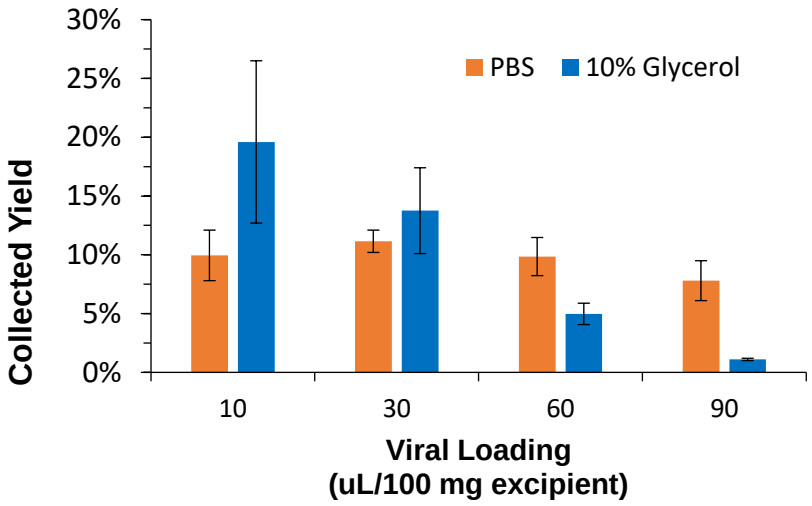


**Figure 3. 2.** Percent yield of spray dried powder recovered from the spray dryer collection chamber based on a 10 mL batch volume with 1% solids concentration. Increased loadings of AdHu5-GFP (suspended in either PBS or 10% glycerol) were added to the feed solution prior to spray drying. Error bars represent the standard error between averaged duplicate samples.

It should be noted that there was no significant difference in average viscosity of the feed solutions containing placebo storage solutions with and without glycerol in Figures 3.1 and 3.2 (tested using a U-tube viscometer, data not shown). Wan et al. similarly reported no significant change in viscosity of a 1% *w/v* hydroxypropyl methylcellulose solution with 30% glycerol added prior to spray drying [106]. Since our feed solution viscosity did not significantly change with the addition of glycerol, self-diffusion of the primary mannitol-dextran excipients and virus as well as the initial droplet drying dynamics are all expected to be consistent between formulations.

*3.3.3 Influence of Cryoprotective Agents of Powder Properties*

To further understand the direct impact of glycerol on powder properties, the amount of added glycerol in the spray dried powder was varied while keeping the concentration of excipients, virus, and salt constant, according to Table 3.1. Figure 3.3 shows that as glycerol content in the dry powder increased from 0 wt.% to 10 wt.%, there was a corresponding increase in viral titre log loss of 0.7. For reference, the dry powders previously discussed in Figures 3.1 and 3.2 contained 10 wt.% glycerol at a loading of 90 µL/100 mg excipient. Discrete ranges of error did not overlap between the 0 wt.% glycerol and 10 wt.% glycerol dry powder formulations, thus indicating a statistical difference between these datasets. Since viral load and salt concentration were consistent for all preparations in Figure 3.3, glycerol content was the fundamental difference between particle composition in this case. Although glycerol represented a minor component of the overall particle matrix, it hindered the ability to produce a viral powder of sufficient AdHu5-GFP activity.

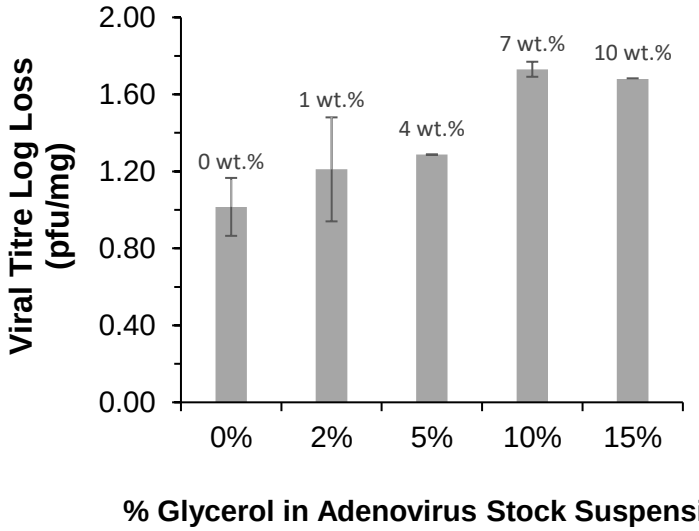


**Figure 3.3.** Log loss (pfu/mg) of AdHu5-GFP viral titre in spray dried powder as a function of increasing glycerol concentration within the adenovirus stock suspension. Data labels refer to the wt.% of glycerol incorporated within the spray dried particle matrix. All samples contain the same viral loading of 60 µL/100 mg excipient and equivalent salt content. Error bars represent the standard error between averaged duplicate samples.

Placebo powders were produced with either glycerol or trehalose as the cryoprotective agent and the resulting powder properties were characterized (Table 3.2). Trehalose was selected as an alternative to glycerol, based on its ability to participate in thermal stabilization of the powder [10] and prevention of adenovirus deactivation due to freeze-thaw damage [37]. In terms of thermal properties, the spray dried powders containing glycerol were found to have decreased $T_g$ values compared to those containing trehalose or PBS storage solution alone. For example, incorporating the 10% glycerol placebo storage solution led to a $T_g$ that was 20 ºC lower than the preparation using PBS, whereas the powder prepared with a 5% trehalose placebo storage solution resulted in a $T_g$ of 120 ºC (the highest of all samples tested). A plasticization effect was observed with the addition of glycerol that caused a decrease in particle $T_g$ [50]. Considering the Kauzmann temperature is 50 ºC below the $T_g$, formulations that have a $T_g$ of 100 ºC or below are more likely to experience virus mobility and are less desirable for long term room temperature storage [95]. Since the spray dryer outlet temperature typically ranged from 55-65 ºC, particles containing 5% and 10% glycerol stock suspension could experience more viral deactivation while sitting in the collection tube during spray drying. Virus located at the particle surface seems especially vulnerable to heat damage and deactivation during spray drying [65][65]. AdHu5 is particularly susceptible to capsid rupture and can experience a 3 log loss in viral titre after only one minute of exposure to 56 ºC if freely mobile [31]. Using 5% trehalose as an alternative cryogenic storage solution maintained the Tg high enough with respect to the Kauzmann temperature, impeding viral mobility in the dry powder and effectively preserving adenovirus functionality. Plasticization was not detectable in the trehalose formulation as compared to the formulations containing glycerol. As both a cryogenic agent and a non-reducing sugar, trehalose promotes adenovirus stability by helping to prevent stresses caused by dehydration during the drying process [107]. Since trehalose

is able to form hydrogen bonds, it replaces the role of water during the drying process to offer adenovirus stability as the glassy matrix forms [63,95].

**Table 3.2.** Summary of spray dried mannitol-dextran particle properties based on the addition of placebo storage solution added at a loading of 60 µL/100 mg excipient. Placebo storage solutions refer to the percentage of each cryogenic component in PBS before addition to the excipient formulation.

| Placebo Storage Solution | Cryogenic Composition in Dry Powder | Glass Transition Temperature | Water Content [%] | Median Particle Diameter, D50 [µm] | Span [µm] |
|---|---|---|---|---|---|
| *5% Trehalose in PBS* | 3 wt.% | 120 ± 10 ºC | 3.76 ± 0.09% | 4.3 ± 0.3 | 1.8 ± 0.1 |
| *PBS Buffer* | 0 wt.% | 118 ± 5 ºC | 3.73 ± 0.09% | 5.6 ± 0.3 | 1.9 ± 0.1 |
| *5% Glycerol in PBS* | 4 wt.% | 103 ± 4 ºC | 4.89 ± 0.09% | 6.6 ± 0.3 | 2.1 ± 0.1 |
| *10% Glycerol in PBS* | 7 wt.% | 98 ± 4 ºC | 5.39 ± 0.09% | 6.6 ± 0.3 | 2.0 ± 0.1 |

Particle size and residual water content are important characteristics to be considered for spray dried powders intended for inhalation. Ideally, particles should be 5 µm or smaller to reach the distal lung region [108]. All tested powders had particle sizes near or under the target median diameter and the span was relatively constant (Table 3.2). Particles containing 5% trehalose displayed an ideal median diameter of 4.3 µm which is highly suitable for pulmonary delivery. On the other hand, glycerol-containing particles were 1-2 µm larger than particles with trehalose or PBS alone. This trend was supported by SEM (Figure 4) where powders containing 5% and 10% glycerol placebo storage solutions both appeared to contain slightly larger particles than powders with PBS and 5% trehalose.

One of the contributing factors for the larger particle size was water content. Powders containing 5% trehalose or PBS storage solutions had low water content, around 3.75%, while the

powders containing glycerol had higher levels of absorbed water after being stored at comparable conditions. Water retention increased by approximately 1.5% for the glycerol containing particles, compared to preparations with trehalose or PBS alone. Glycerol is highly hygroscopic and has been noted to cause high moisture absorption within polymeric-protein microstructures [109]. Due to this affinity for water, glycerol-containing powder experienced moisture swelling which was indicated by larger particles. Inhalable powders containing glycerol could have limited functionality in an inhaler due to moisture-related particle cohesion.

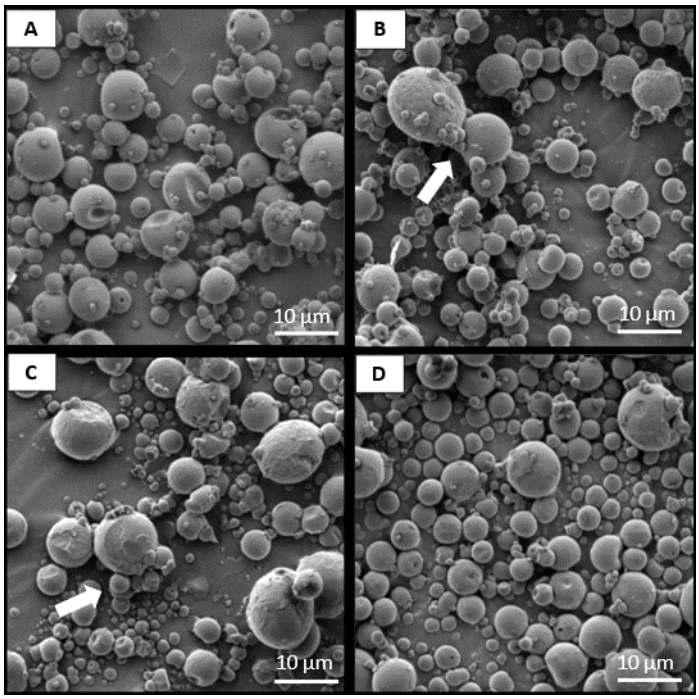


**Figure 3.4.** Scanning electron microscope (SEM) images of mannitol-dextran spray dried powders showing particle morphology for placebo powder samples with 60 µL/100mg excipient of the following storage solutions: (A) 0% glycerol, (B) 5% glycerol, (C) 10% glycerol, (D) 5% trehalose. Arrows indicate areas of particle bridging caused by cohesion. All images were captured at 4000X magnification with a scale bar representing 10 µm in length.

SEM micrographs suggested the particles were more cohesive for those powders containing either 5% or 10% glycerol storage solution, due to clumping shown in Figure 3.4. In contrast, powders that contained only PBS or the 5% trehalose placebo solution did not display

notable cohesive behaviour. Work conducted by Wan et al. has shown that spray drying plasticizers, such as glycerol, along with polymers for drug microencapsulation led to similar particle cohesion and agglomeration [106]. The observed result of cohesion within powders containing glycerol directly affected the process yield from the spray dryer, as reported in Figure 3.2. During drying, glycerol-plasticized particles are more likely to display a viscous nature and high surface tension while maintained near their depressed glass transition temperature, resulting in high apparent cohesive strength or "stickiness". This stickiness facilitates low yields as the particles come into contact with glass surfaces in the spray dryer [106,110,111]. Foster et al. have demonstrated that in amorphous sugars the rate of cohesion is proportional to the value of $T - T_g$, such that liquid bridge formation is faster at temperatures exceeding the $T_g$ [110]. Since the outlet temperature and residence time in the spray dryer were constant for each batch of powder, the depressed $T_g$ associated with glycerol-containing powders led to an increase in the $T\text{-}T_g$ value and a higher rate of cohesion.

In addition to glassware adhesion and yield loss during spray drying, there was also concern that particle cohesion will reduce the respirable fraction dispersed from an inhaler based on prior reported experiences for dry powders with higher water content [112]. To achieve efficacious delivery *in vivo*, residual moisture and subsequent cohesion must therefore be minimized. Based on these results, using 5% trehalose or neat PBS as a cryoprotective stock prevented particle cohesion appropriately within the spray dried powder.

### *3.3.4 Viral Buffer Freeze-Thaw Stability*

Removing glycerol entirely from the stock viral suspension led to stronger viral activity, better powder properties and improved spray drying yield. However, the reason for including a cryoprotective agent within an adenoviral stock suspension must also be addressed to prevent

issues during powder processing. A viral suspension often undergoes repeated freeze-thaw cycling prior to batch powder preparation, making cryoprotective agents crucial for maintaining adenovirus integrity. Figure 3.5 compares the viral titre of adenoviral stock suspensions containing either PBS, glycerol (5% and 10%) or trehalose (5% and 10%) during repeated freeze-thaw cycles. Each adenoviral stock suspension tested appeared to offer nearly identical cryoprotective behaviour as there were no significant differences at any of the sampling timepoints. However, it should be noted that these buffers were prepared by adding each cryoprotective agent to a thawed aliquot of virus originally suspended in pure PBS. This aliquot had an initial titre of $5.7\times 10^{8} pfu/mL$ but underwent one freeze-thaw cycle prior to commencing the freeze-thaw study. The drop in PBS viral titre to $3.3\times 10^{7} pfu/mL$ by the second freeze-thaw cycle was attributed to the lack of added cryoprotective agent. Adding a cryoprotective agent after an initial freeze-thaw did not appear to substantially alter the progression of additional viral damage. Without a cryoprotective agent (using only PBS), the viral titre decreased by 0.7 log between the second and fifth freeze-thaw cycle.

As an alternative to glycerol, trehalose has previously been used to protect viruses against damage due to freeze-thaw cycling [37]. Based on identical performance between glycerol and trehalose as cryoprotective agents in this work, trehalose was considered a robust alternative to glycerol for cryo-storage of adenovirus intended for dry powder vaccine preparation. Moving forward, a concentration of 5% trehalose was preferred because it minimized the amount of cryoprotective agent added, while also maintaining cryogenic effectiveness compared to 10% trehalose which did not appear to offer additional freeze-thaw stability. Incorporating trehalose as a cryoprotective agent at high concentrations will impact the excipient formulation intended to immobilize the virus within the spray dried powder. Although trehalose has robust stabilization

behavior with most viral vectors upon spray drying, lower cryoprotective agent content will allow for more optimization opportunities. As noted above, spray dried powders formulated with 5% trehalose placebo storage solution offered ideal particle sizing for inhalation, a high $T_g$ and low moisture content.

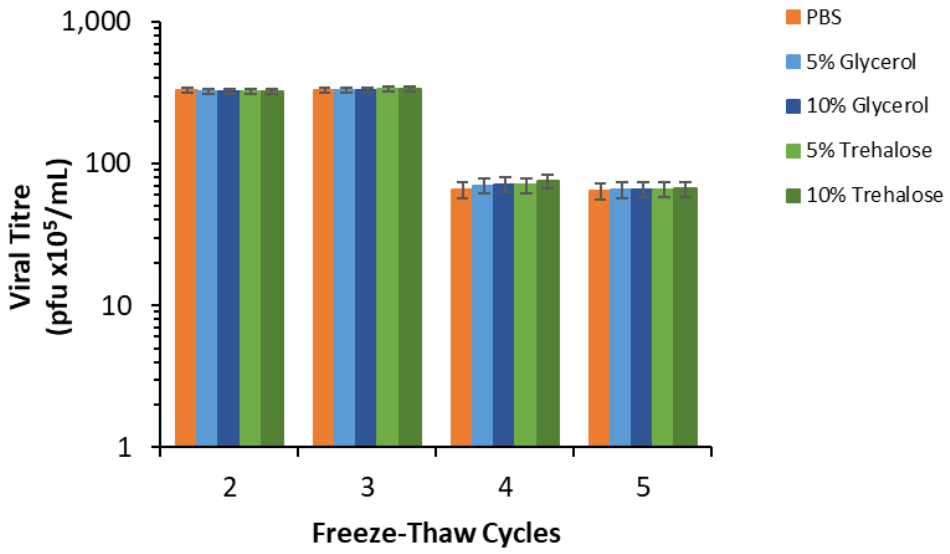


**Figure 3.5.** Viral titre of AdHu5 following progressive freeze-thaw cycling of adenoviral stock solutions containing PBS only, 5% glycerol, 10% glycerol, 5% trehalose and 10% trehalose, respectively.

*3.5 Thermal Stability of Spray Dried Powder*

To test the impacts of selected cryoprotective agents on thermal stability of the spray dried powder, viral activity was assessed after 72-hour exposure to 45 ºC (Table 3.3). These accelerated aging conditions are robust and comparable to the degradation tests set forth by the World Health Organization to test viral stability of the oral poliomyelitis vaccine [2]. For accurate comparison, a high viral loading of 60 µL/100 mg excipient was used for each of the formulations tested. Viral

losses related to the spray drying process were captured by the viral activity log loss of each 'fresh' sample. Losses related to the aging process and subsequent thermal stability of a formulation were indicated by the differences between viral log loss in fresh and aged samples. In all tested cases, the range of error for fresh and aged activity values did not overlap and therefore indicated significant statistical difference. Larger standard error was observed with larger sample sizes and was associated with natural variability between environmental conditions and cell culture.

**Table 3.3.** Viral titre log loss observed in mannitol-dextran spray dried powder with a viral loading of 60 µL/100 mg excipient of AdHu5-GFP stored in 5% trehalose in PBS, neat PBS and 10% glycerol in PBS adenoviral stock suspension. Samples were tested immediately after spray drying (fresh) and after exposure to accelerated aging conditions (aged).

| ***Adenoviral Stock Suspension*** | **Collected Yield (%)** | **Sample Type** | **Viral Titre Log Loss (pfu/mg)** | **Sample Size (n)** |
|---|---|---|---|---|
| ***5% Trehalose in PBS*** | $13 \pm 2$ | Fresh | $1.5 \pm 0.3$ | n = 5 |
| | | Aged | $2.0 \pm 0.2$ | n = 2 |
| ***PBS*** | $10 \pm 2$ | Fresh | $0.7 \pm 0.2$ | n = 3 |
| | | Aged | $1.98 \pm 0.03$ | n = 2 |
| ***10% Glycerol in PBS*** | $5 \pm 1$ | Fresh | $2.84 \pm 0.08$ | n = 2 |
| | | Aged | $3.4 \pm 0.0$ | n = 2 |

Addition of a 5% trehalose viral stock suspension allowed for relatively low process losses (1.5 log loss) and excellent thermal stability with an additional 0.5 log loss due to high temperature aging. In combination with higher collected yields, 5% trehalose stock viral suspension helped to maintain the intended thermal stability and preserved activity under high viral dosage. Without a cryoprotective agent, the formulation containing only PBS showed the lowest thermal stability, with an additional 1.3 log loss of viral titre during the aging process. Despite having lower initial process losses, removing the cryoprotective agent appeared to hinder adenovirus stability during prolonged exposure to high temperatures. In comparison, the addition of a 10% glycerol stock viral

suspension only resulted in an additional viral titre log loss of 0.6 following aging but was also associated with low collected yields and high process losses. The order of decreasing thermal stability coincided with the decrease in respective $T_g$ presented in Table 3.2, reiterating that the formulation with 5% trehalose adenoviral stock suspension experienced less molecular mobility and less viral damage under thermal stress. Targeted losses in adenovirus vaccine processing were around 0.5 log loss [39], which indicated the need for further processing improvements to reach pharmaceutically acceptable limits for this formulation. It is understood that with additional process optimization [65], viral losses occurring during spray drying can be further reduced.

### 3.4. Conclusions

Despite the necessity of cryoprotective agents for long-term freeze-thaw viral stability, the consequences of their addition within thermally stable vaccine preparations cannot be overlooked. It has been shown that introducing small volumes of glycerol into an excipient blend had a plasticizing effect on the excipient carrier in a spray dried powder. This impacted viral immobilization, consequently causing a reduction of adenovirus activity under high viral load. Although this work only focuses on the encapsulation of an AdHu5 vector, it is expected that the plasticizing effect of glycerol could also impact the yield and activity of other spray dried vectors. Interactions between glycerol and a particle matrix are applicable to most excipient sugars, suggesting that processing efficiency of other spray dried formulations may be hindered by the inclusion of glycerol. Removing the cryoprotective agent entirely from the adenoviral stock suspension improved the viral activity of spray dried powder, but this method also negatively impacted freeze-thaw stability and decreased thermal stability. As a cryoprotective alternative to glycerol, it was demonstrated that a 5% trehalose adenoviral stock suspension did not depress the

$T_g$ of a mannitol-dextran spray dried powder and retained viral activity and thermal stability. Sucrose is another cryogenic alternative that could be further explored for this purpose. Though not considered in the present study, our initial testing showed that 5% and 10% sucrose could provide freeze-thaw stability similar to 5% trehalose (data not shown). However, the impact of incorporating sucrose within a mannitol-dextran spray dried encapsulation remains unknown. Cryoprotective agents may account for less than 10 wt.% of the overall spray dried particle composition, but they are shown in this study to play significant roles as matrix components and influence viral encapsulation, particularly at high viral loading. Improving viral load in spray dried vaccines to optimize *in vivo* delivery and immunogenic response must therefore consider the impacts of all ingredients, even those in the stock viral suspension.

**Appendix 3 – Chapter 3 Supplementary Material**

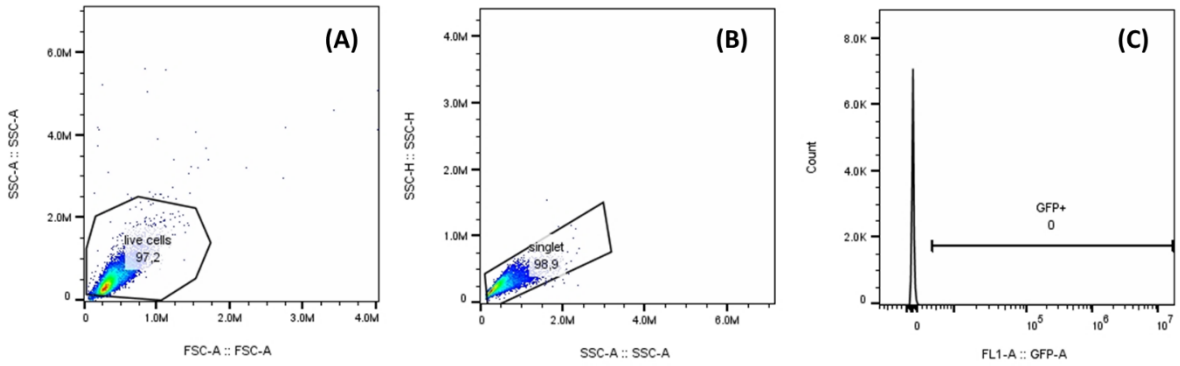


**Figure A3.1.** Cell population gating process of an uninfected negative control sample using FlowJo software. The autogating tool was used to select the live cell population from the scatterplot (A), followed by a user-defined gate to seperate live cell singlet events from non-singlet events (B) and a final user-defined gate to determine positive GFP expression in live cells as compared to the negative control population (C). For infected cell populations, viral titre is normalized based on mass of reconstituted powder as well as volume and intial titre of stock suspension.

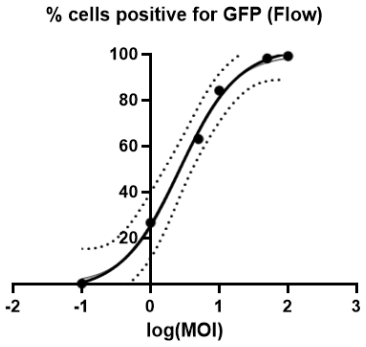


**Figure A3.2.** Standard curve used to convert the percentage of cells expressing green fluorescent protein (GFP), determined via flow cytometry, to a corresponding modality of infection (MOI). Calibration was determined based on measuring GFP expression of samples with known MOI of 0.1, 1, 5, 10, 50, 100.

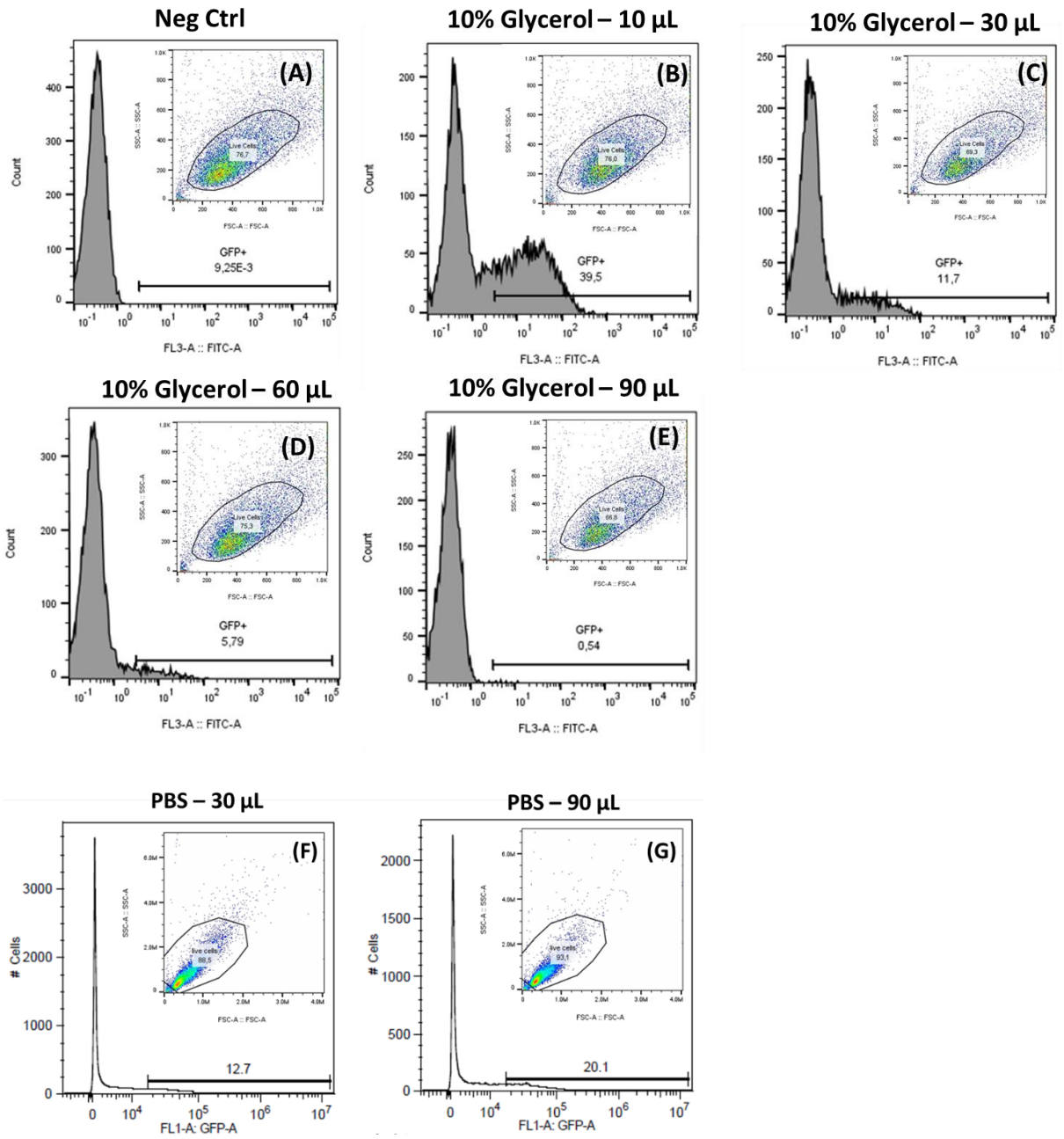


**Figure A3.3.** Histogram counts of cells expressing GFP and corresponding event scatterplot (inset) for each sample analyzed via flow cytometry. Panel (A) represents an uninfected cell population as a negative control. Samples shown were infected with reconstituted spray dried powder prepared with either a 10% glycerol AdHu5 stock suspension added at volumes of (B) 10 µL, (C) 30 µL, (D) 60 µL and (E) 90 µL or a PBS-only AdHu5 stock suspension added at (F) 30 µL and (G) 90 µL.

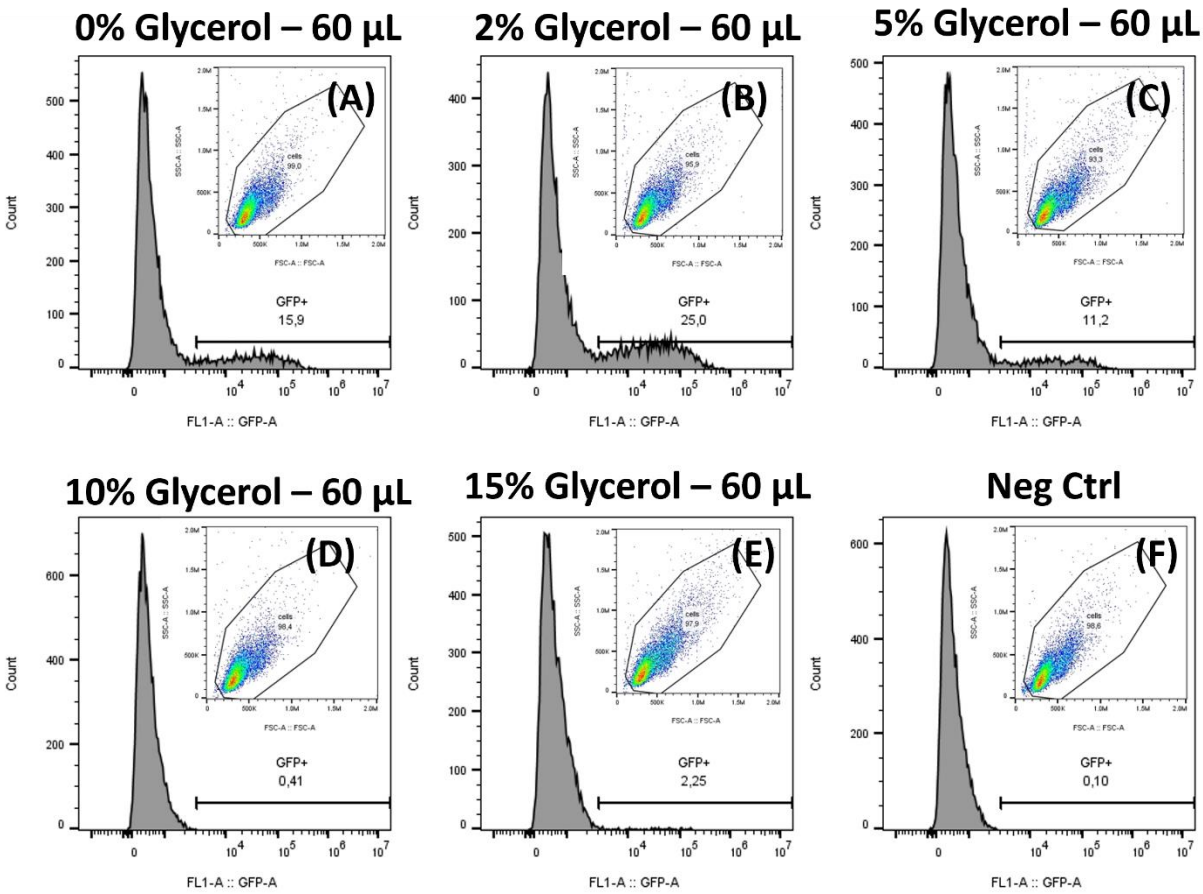


**Figure A3.4.** Histogram counts of cell GFP expression and corresponding event scatterplot (inset) in samples analyzed via flow cytometry where cells were infected with reconstituted powder spray dried with 60 µL of AdHu5 stock suspensions containing (A) 0% glycerol, (B) 2% glycerol, (C) 5% glycerol, (D) 10% glycerol and (E) 15% glycerol. Panel (F) represents an uninfected cell population as the negative control.

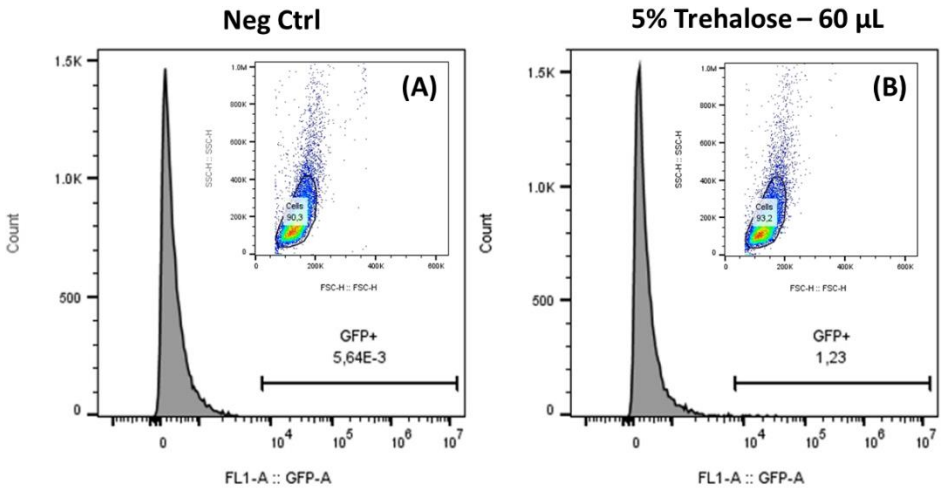


**Figure A3.5.** Histogram counts of positive GFP expression and corresponding event scatterplot (inset) analyzed via flow cytometry where cells were either uninfected (A) or infected with reconstituted powder spray dried containing 60 µL of 5% trehalose AdHu5 stock suspensions.

## Chapter 4: Dextran Mass Ratio Controls Particle Drying Dynamics in a Thermally Stable Dry Powder Vaccine for Pulmonary Delivery

**Manser, M.M.,** Morgan B.A., Feng, X., Rhem, R.G., Dolovich M.B., Xing, Z., Cranston, E.D., Thompson, M.R., 2022. Dextran mass ratio controls particle drying dynamics in a thermally stable dry powder vaccine for pulmonary delivery. Submitted to *Pharmaceutical Research*. Submission ID: PHAM-D-22-00378

Within this chapter, the experimental design, viral activity testing, thermal property characterization and data analysis was all conducted by myself. James Mayo conducted moisture analysis via TGA and Varsha Singh assisted with particle sizing. Co-author Xueya Feng prepared the adenoviral vector used in this work. Co-author Rod Rhem produced the STL file used in 3D printing the mouse trachea and Mark MacKenzie facilitated all 3D printing. The manuscript was drafted by myself and edited by supervisors Dr. Michael Thompson, Dr. Emily Cranston and Dr. Zhou Xing. Additional editing was provided by co-authors Rod Rhem and Dr. Myrna B. Dolovich, as well as Mikael Ekstrom of Iconovo. This chapter was submitted to *Pharmaceutical Research*.

**Abstract**

Thermally stable, spray dried vaccines targeting respiratory diseases are promising candidates for pulmonary delivery, requiring careful excipient formulation to effectively encapsulate and protect labile biologics. This study investigates the impact of dextran mass ratio and molecular weight on activity retention, thermal stability and aerosol behaviour of a labile adenoviral vector (AdHu5) encapsulated within a spray dried mannitol-dextran blend. Comparing formulations using 40 kDa or 500 kDa dextran at ratios of 1:3 and 3:1 mannitol to dextran, processing-related activity losses were significantly higher in formulations with a lower dextran mass ratio. Incorporating mannitol in a 1:3 ratio with 500 kDa dextran reduced viral titre processing losses below 0.5 log loss and displayed strong thermal stability under accelerated aging conditions. Dextran-rich formulations increased viscosity during drying, which slowed self-diffusion and favorably hindered viral partitioning at the particle surface. Reducing mannitol content also minimized AdHu5 exclusion from crystalline regions that can force the vector to an air-solid interface where deactivation occurs. Increased dextran molecular weight improved activity retention at the 1:3 ratio but was less influential than the ratio parameter itself. Moisture absorption and agglomeration was higher in dextran-rich formulations, but under low humidity the 1:3 ratio with 500 kDa powder had the lowest mass median aerodynamic diameter of 4.4 μm and 84% available dose from an intratracheal dosator to indicate its suitability for inhalation. Demonstrating more effective encapsulation ultimately allows inhalable vaccines to be prepared at higher potency, requiring less powder mass per inhaled dose and higher delivery efficiency overall.

## 4.1 Introduction

Vaccine thermal sensitivity is one of the largest hurdles currently facing global immunization efforts. In low-income countries, particularly those with tropical or semi-arid climates, access to the necessary cold-chain infrastructure is limited and incredibly expensive. The resulting immunization programs in these regions suffer from insufficient storage capacity and cold-chain equipment failure, leading to vaccine wastage or reduced vaccine potency due to poor temperature control [5,6]. To reduce this geographical discrepancy and improve global vaccine access, development efforts have started using processing methods such as spray drying to achieve thermal stability of active vaccine components in dry powder form [29,62,64,113,114].

Thermal stabilization of a spray dried biologic is based upon the *water replacement hypothesis*, where its proteins favorably interact with the hydroxyl groups of excipients like carbohydrates to retain the native protein structure and prevent denaturation [15]. Careful excipient formulation is a critical aspect in the successful encapsulation of highly labile biologics such as adenoviruses [95]. Although recombinant adenoviral (Ad) vectors such as human serotype 5 Ad vector (AdHu5) have been utilized to develop human vaccines against respiratory infectious diseases including COVID-19 [8] and tuberculosis [8][7], they are particularly labile at elevated temperatures and prone to structural damage [31,33]. This functional limitation highlights the value of developing thermally stable, dry powder preparation for pulmonary delivery of Ad-vectored vaccines.

A blend of mannitol and dextran has been previously shown to successfully retain viral activity of AdHu5 through spray drying, in addition to providing thermal stabilization [10,95,115]. Of these previous studies, the most successful formulation blended mannitol and dextran in a 3:1 mass ratio using a moderately low molecular weight dextran of 40 kDa [65]. Within this blend, dextran

acts as the major amorphous component known to effectively stabilize the matrix through vitrification [10].

During particle drying dextran diffuses slowly and increases the viscosity of the solution, while encouraging surface-active components mannitol and AdHu5 to diffuse towards the droplet center away from the air-liquid interface and dextran-rich particle surface [116,117]. By preventing viral partitioning at the air-solid particle interface, dextran can effectively shield the adenovirus from the high heat environment in the drying chamber of the spray dryer. Once the particle is dry, dextran helps to minimize adenovirus mobility within the matrix to prevent viral aggregation, which is a known cause of viral deactivation and activity loss [32]. Dextran exhibits a relatively high glass transition temperature ($T_g$) making it a preferred choice for encapsulating and stabilizing an adenovirus at elevated temperatures [95]. However, dextran alone does not show good water replacement characteristics with the adenovirus resulting in high activity losses [95]. As a hygroscopic amorphous solid, dextran is moisture sensitive under elevated humidity conditions leaving it susceptible to $T_g$ depression [118].

Comparatively, mannitol is much smaller than a dextran polymer and more readily forms hydrogen bonds with the protein capsid of the adenovirus which can prevent denaturation [95]. Although mannitol interacts strongly with the protein capsid layer of an adenovirus, anchoring it within the particle matrix during particle drying, it also has the tendency to crystallize. Crystalline regions formed by this sugar impede moisture absorption and are associated with lower surface energy and increased thermodynamic stability of produced dry powders [119]. However, these crystalline regions can also lead to viral exclusion which limits the extent of viral encapsulation [116,120]. Fine particle crystalline materials are also known to experience high inter-particulate cohesion, leading to poor dissolution and reduced absorption efficiency in the lungs upon

inhalation [119,120]. Particle cohesion also reduces aerosolization and must therefore be controlled. We hypothesize that our previously identified mannitol-dextran excipient blend could be further improved by reducing the relative amount of mannitol within the blend. This would reduce the negative impact of crystal formation within an inhalable product and allow the adenovirus to remain fully encapsulated within the interior of the particle, minimizing viral deactivation in an inhalable spray dried vaccine. This study investigates the role of molecular weight and mass ratio of dextran on the retained activity, thermal stability and powder flowability of a spray dried AdHu5 adenoviral vector intended for pulmonary dry powder delivery.

## 4.2 Materials & Methods

### *4.2.1 Chemical and Biologics*

D-mannitol, xylitol and dextran ($M_r$ 40000 Da) were all sourced from Millipore-Sigma (ON, Canada) as USP grades. High molecular weight dextran ($M_r$ 500000 Da) was purchased from ThermoFisher Scientific (Waltham, MA, USA). Milli-Q® water was purified with a Barnstead GenPure Pro system from ThermoFisher Scientific (Waltham, MA, USA) using a resistivity of 18.2 MΩ cm. A-549 epithelial lung tumor cells were used for all cell culturing experiments and were grown in a culture media described in a Life Technologies protocol from Invitrogen (ON, Canada) which consisted of α-minimum essential media (α-MEM) mixed with 1% streptomycin/penicillin and 10% fetal bovine serum (FBS). A recombinant human serotype 5 adenovirus expressing Green Fluorescent Protein (AdHu5) was prepared in the McMaster University Immunology Research Centre vector facility and was modified to be replication

deficient. Upon purification, the adenoviral vector stock was stored in a 5% trehalose storage buffer at -80 ºC and had a titre of $4.4 \times 10^8$ pfu/mL [115].

### *4.2.2 Modelling Excipient Distribution in Spray Dried Particles*

A diffusion-based single droplet drying model developed and validated by Morgan et al. [116] was used to predict the distribution of dextran and AdHu5 within a dry particle for each of the mannitol-dextran blends using MATLAB (Mathworks, Inc; Natick, MA, USA). Although the model was validated based on acoustically levitated particles with radii on the scale of 200 µm, it has been previously demonstrated that acoustic levitation and spray drying can produce particles with similar morphologies, thermal properties and viral activity trends due to comparable drying kinetics [98]. Therefore, we expect that this model is an appropriate approximation for excipient diffusion and the relative component distribution experienced during spray drying. Component distribution was plotted across the radius of a drying particle by dividing the particle into 40 shells spanning the radial axis. The weight fraction of each component at a specific shell is reported as a mass%, normalized based on the total amount of that specific component added to the excipient blend.

### *4.2.3 Sample Preparation and Spray Drying*

Excipient solutions were prepared using a mannitol-to-dextran (MD) mass ratio of either 3:1 or 1:3 by dissolving excipients in purified Milli-Q® water to a concentration of 1% solids. Either low molecular weight dextran (40 kDa) or high molecular weight dextran (500 kDa) was used to prepare each formulation ratio. For comparison, a xylitol-dextran formulation was also prepared at a 1:3 ratio using 40 kDa dextran. Details and corresponding notations for all five

excipient formulations are summarized in Table 4.1. A volume of 60 µL AdHu5 stock vector with 5% trehalose was added per 100 mg of excipient based on our previous work that improved viral activity retention at high loading via appropriate selection of the cryoprotective storage solution [115]. In all physical characterization and flowability tests described in Section 2.6, a placebo solution of 5% trehalose was added at 60 µL/100 mg of excipient instead of the viral stock, as particle size and morphology of mannitol-dextran spray dried powder is the same with and without AdHu5 present [65].

**Table 4.1.** Formulation notation and preparation details of each excipient blend, based on component weight percent and molecular weight.

| **Formulation Notation** | **Excipient Weight Percent** | | **Molecular Weight of Dextran** |
|---|---|---|---|
| | ***Mannitol*** | ***Dextran*** | |
| MD (1:3)- 40 kDa | 25 wt.% | 75 wt.% | 40 kDa |
| MD (1:3)-500 kDa | 25 wt.% | 75 wt.% | 500 kDa |
| MD (3:1)- 40 kDa | 75 wt.% | 25 wt.% | 40 kDa |
| MD (3:1)- 500 kDa | 75 wt.% | 25 wt.% | 500 kDa |
| | ***Xylitol*** | ***Dextran*** | |
| XD (1:3)- 40 kDa | 25 wt.% | 75 wt.% | 40 kDa |

Once the excipients were fully dissolved in solution, spray dried powders were produced using a a B-290 Mini Spray Dryer from Büchi (Switzerland) outfitted with a 0.7 mm nozzle. It should be noted that excipient solutions with 500 kDa dextran were refrigerated at 4 ºC for at least 30 minutes to achieve full dissolution prior to spray drying. For accurate comparison between each excipient formulations, all spray dryer settings were kept consistent for each batch. Based on previous process optimization of yield, particle size and viral activity [65], the following settings were used: 120 ºC inlet temperature, 217.5 mL/h feed flow rate (pump setting 13%), 439.11 L/min spray gas flow rate (30 mm rotameter reading) and 35 m/h aspirator flow rate (100% aspiration).

The outlet temperature ranged between 55-65 ºC. Immediately after drying, powder was collected into microcentrifuge tubes within a biosafety cabinet and transferred to a benchtop desiccator for storage at room temperature on Drierite® anhydrous indicating desiccant (W.A Hammond Drierite Company Ltd.). Powders were transported between lab spaces using a vacuum sealed storage container that contained additional desiccant to avoid exposure to ambient humidity.

### *4.2.4 Cell Culturing*

Stock suspension of A-549 cells was stored in liquid nitrogen under cryo-storage conditions. Once thawed, cells were added to pre-warmed α-MEM and centrifuged for 5 minutes at 1400 rpm to obtain a cell pellet. A single cell suspension was prepared by resuspending the pellet in α-MEM and plating in a T-150 flask for overnight incubation at 37 ºC and 5% $CO_2$ in a water jacketed incubator (Forma Scientific Inc., Marietta, OH, USA). Dead cells and remaining dimethyl sulfoxide from cryo-storage were removed the following day by exchanging cell media and passaging the confluent culture twice before *in vitro* testing on a 96-well plate.

### *4.2.5 Viral Activity Testing via Flowcytometry*

Viral activity testing of each spray dried powder formulation was tested *in vitro* by following the same protocol described in our previous work [115]. Briefly, α-MEM was used to reconstitute each spray dried sample to a solids concentration of 1% immediately before infecting 40,000 confluent A-549 cells on a 96-well plate and incubating overnight at 37 ºC. Cell washing, trypsinization and fixation with 1% paraformaldehyde was performed prior to flowcytometry analysis with a Beckman Coulter Life Sciences CytoFlex LX flow cytometer (Indianapolis, IN, USA). At least 10,000 events were analyzed per sample to account for 25% of the plated cell population using CytExpert software. FlowJo® software (BD, New Jersey, USA) was used to

quantify GFP expression within the live cell population, excluding cellular debris and artifacts using the auto-gating tool. A calibration curve was used to convert GFP expression to viral multiplicity of infection (MOI). Viral titre was then calculated based on the MOI and normalized based on sample mass of the spray dried powder. Processing losses in viral titre due to spray drying are discussed on the log scale via viral titre log loss.

### *4.2.6 Thermal Aging*

Each spray dried formulation was stored under accelerated aging conditions to determine the impact of excipient formulation on thermal stability of the encapsulated adenovirus. Using a previously described protocol [115], each powder formulation was stored in a water bath at 45 ºC for 72 hours prior to GFP quantification via flowcytometry. Moisture uptake was prevented during the aging process by storing the spray dried powder within microcentrifuge tubes that were sealed with Parafilm® wax, placed within a plastic bag containing desiccant and added to a sealed glass jar with additional desiccant. Immediately after the 72-hour aging process, samples were removed from the water bath and resuspended in α-MEM for cell infection and viral activity tested as in Section 4.2.5. Viral activity for all aged samples was tested in duplicate and error bars represent the standard error between samples.

### *4.2.7 Particle Flowability and Characterization*

#### *4.2.7.1 Moisture Content via Thermogravimetric Analysis*

Thermogravimetric analysis (TGA) was used to determine total moisture content in each spray dried powder formulation following processing and thermal aging. Moisture analysis was conducted on samples stored under accelerated aging conditions at 45 ºC for 72 hours. Between 5-10 mg of sample was loaded into an alumina crucible and heated in a TGA/DSC 3+ LF/1100

instrument from Mettler Toledo (Columbus, Ohio, USA) at a rate of 5 ºC/min until reaching 150 ºC where the temperature was held constant for 10 minutes under argon gas. Mass was monitored over the tested temperature range using STARe software from Mettler Toledo (Columbus, Ohio, USA). Moisture content was determined based on the percentage of mass change from 25 ºC to approximately 110 ºC, when the sample mass had stabilized. Standard error was determined based on duplicate sample measurement.

#### *4.2.7.2 Scanning Electron Microscopy (SEM)*

A Tescan Vega II LSU scanning electron microscope (Tescan Orsay Holding, a.s., Brno, Czech Republic) was used for qualitative analysis of the spray dried particle morphology. To prepare samples for imaging, a Polaron E5100 sputter coater (Quorum Technologies Limited, Laughton, UK) was used to coat a 24 nm layer of gold on top of sample secured by double-sided carbon tape. An electron accelerating voltage of 20 kV and magnification of 2000 were used to capture micrographs at a working distance range between 10.12 - 10.14 mm.

#### *4.2.7.3 Geometric Particle Sizing*

Geometric particle sizing was conducted with a Helos R-series laser diffraction sensor from Sympatec GmbH (Pulverhaus, Germany) using an R2 lens with a 50 mm focal length for a reliable detection range between 0.45 – 87.5 µm in size. Powder samples with mass weighed between 7-12 mg were loaded into and dispensed from an ICOone inhaler provided generously by Iconovo (Lund, Sweden). A cumulative particle size distribution was generated, with median particle diameter represented by the $50^{th}$ percentile (D50) of the distribution. Span of the particle size distribution was determined with the values of the $10^{th}$ (D10), $50^{th}$ and $90^{th}$ (D90) percentiles based

on Eq 4.1. All samples were measured in duplicate and error bars represent standard error between samples.

$$Span = \frac{D90 - D10}{D50} \tag{4.1}$$

*4.2.7.4 Aerodynamic Particle Size*

Aerodynamic particle size distribution was experimentally determined using a Next Generation Impactor (NGI) from Copley Scientific Limited (Nottingham, UK). Filter paper was used to line each of the impactor stages for gravimetric analysis of particle mass deposition. Five ICOone inhalers were loaded with 8-12 mg of spray dried powder, for a total nominal dose of approximately 50 mg, and immediately dispersed into the impactor drawing a flow rate of 60 L/min. The mass median aerodynamic diameter (MMAD) was calculated based on the cumulative particle size distribution from gravimetric measurements.

*4.2.7.5 Bulk Density, Tapped Density and Carr's Index*

Bulk density of spray dried powder was determined using a method loosely based on a scaled down USP protocol for powder bulk density measurement published in the International Pharmacopoeia [121]. By pouring a known mass of powder into a graduated cylinder with minimal agitation, the volume was recorded and used to determine bulk density. Although the USP protocol for bulk density testing in the European pharmacopeia states that a scaled down test can utilize a 25 mL graduated cylinder for bulk volume measurement, this would still require powder mass in quantities far larger than feasibly produced with the lab scale spray dryer. Hughes et al. have shown that a material sparing testing method for bulk density using a 10 mL cylinder produced acceptable results comparable to the USP method [122]. Here, the bulk density testing method was further

scaled down to a 1 mL graduated cylinder, readable to 0.1 mL, using 200 mg of powder per measurement to save needing additional material.

Tapped density was determined by manually tapping a syringe filled with approximately 200 mg of powder for 1 minute at a rate of 2 taps/s. Tapping height was approximately 2 cm. The powder mass was divided by the difference between recorded volume before and after tapping to determine tapped density. As an indicator of powder flowability, the percentage of powder compressibility (Carr's Index) was calculated based on Eq. 4.2. Prior to data collection, the experimental method was validated based on a standard Carr's Index scale for flowability. Further details on experimental set-up and method validation can be found in Figure A4.1 and Table A4.1 of the Supplementary Material. All spray dried powder formulations were tested in triplicate using the described method and error bars represent standard error between measurements.

$$Carr's\ Index = \frac{\rho_{tapped} - \rho_{bulk}}{\rho_{tapped}} \tag{4.2}$$

*4.2.7.6 Intratracheal Delivery Device (Dosator)*

An intratracheal dosator device intended for *in vivo* testing with a murine animal model was assembled based on similar custom designs described by Ihara et al. and Qui et al. which both used a 3-way stopcock to control airflow from a syringe through a gel-loading pipette or needle tip [84,86]. Briefly, our intratracheal dosator consisted of a 1 mL syringe with a male luer lock connection that twists onto a complementary luer inlet on a 3-way stopcock purchased from Cole-Parmer (Montreal, Canada). An air volume of 0.6 mL was pre-drawn in the syringe prior to securing the luer lock connection. Between 3-4 mg of powder was weighed onto weigh paper and carefully poured into a 10 µL Rainin LiteTouch System pipette tip (Mettler-Toledo, Oakland, CA,

USA) before tightly fastening the pipette tip on the opposite end of the 3-way stopcock. After ensuring the valve was correctly oriented, powder was dispersed through the tip by quickly depressing a pre-drawn syringe. A new pipette tip with freshly loaded powder was used when each sample was sprayed. Individual components of the intratracheal dosator, as well as the final assembly loaded with powder, can be visualized in Figure 4.1.

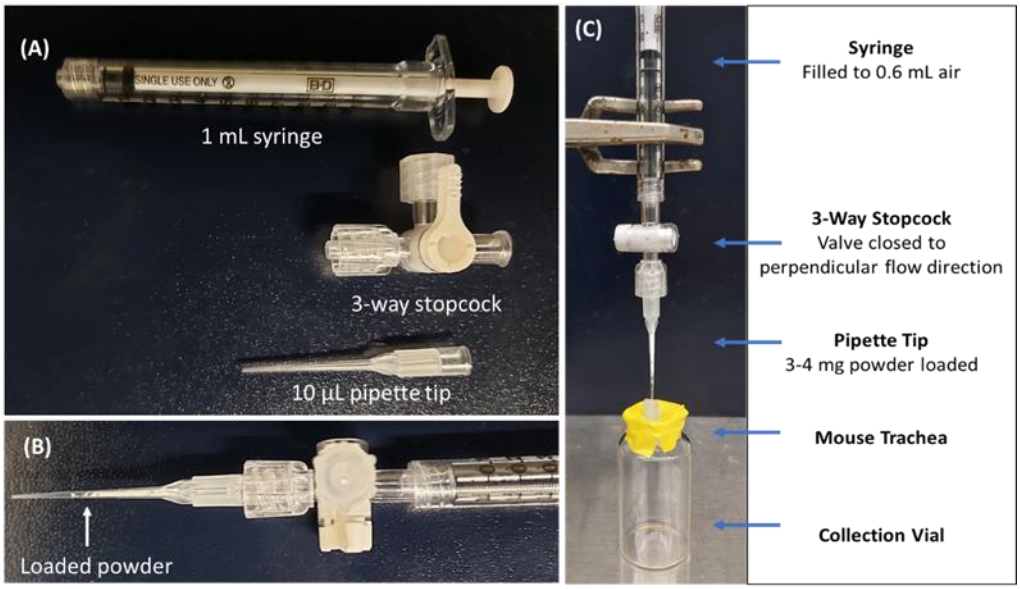


**Figure 4.1.** Custom made intratracheal dosator intended for in vivo delivery to mice using assembled components (Panel A) including: a 1 mL syringe with luer lock connection, 3-way stopcock and a 10 µL pipette tip. Spray dried powder is loaded into the pipette tip and all components are assembled tightly together (Panel B). A full experimental set up is pictured in Panel C, showing the syringe, dosator assembly, 3D mouse trachea model and a powder collection vial.

#### *4.2.7.7 Available and Delivered Dose*

To test the functionality of this intratracheal dosator and compatibility with each spray dried powder formulation, powder was loaded into the dosator and released through a 3D printed model of a mouse trachea and into a glass collection vial (Figure 4.1). The 3D trachea model was developed using CT scans from mice, which were converted into binary images in MATLAB (Mathworks, Inc; Natick, MA, USA) and used to produce a CAD rendering. To improve the durability, the wall thickness of the printed trachea was increased to 2.5 mm while keeping the internal geometry printed to scale. See Figure A4.2-A4.7 in Supplementary Material for further details. The 3D trachea was printed with a ProJet® MJP 2500 Plus from 3D Systems (South Carolina, USA) using the ultra high-definition printing mode with VisiJet M2R-CL rigid plastic (3D Systems, South Carolina, USA). Figure 4.1 (panel C) shows the experimental set up used for device testing. The dosator was tested in a vertical orientation for all measurements to closely represent the needle positioning used during *in vivo* intratracheal delivery of dry powder to mice. This orientation also minimized any variation during repeated device set-up and actuation. A retort stand with clamp was used to secure the dosator assembly above the collection vial for consistency between actuations. Available dose from the intratracheal dosator was determined after loading the tip with a known mass of powder and measuring the mass of the dosator assembly before and immediately after actuation. This difference was divided by the total powder loaded in the tip and expressed in terms of percentage, as indicated in Eq. 4.3. The calculated available dose accounted for all powder losses within the pipette tip and at the luer lock connection point. Triplicate measurements were performed, with error bars representing the standard error. It is expected that there will be significant differences in available dose between bench top testing, in vivo murine testing and testing in human subjects.

$$Available\ Dose = \frac{Dosator\ Mass_{Before} - Dosator\ Mass_{After}}{Powder\ Loaded} \times 100\% \quad (4.3)$$

To approximate the amount of powder that could be effectively delivered through a mouse trachea and into the lungs, the tip of the intratracheal dosator was sprayed directly into the 3D printed mouse trachea. The other end of the trachea was secured on top of a glass collection vial. By measuring the mass of the collection vial before and after powder administration from the dosator, delivered dose was calculated (Eq. 4.4). In this context, the delivered dose refers to the percentage of powder that successfully flows through the 3D printed mouse trachea for delivery into the lungs with respect to total powder loaded. All measurements were performed in triplicate, with error bars representing standard error.

$$Delivered\ Dose = \frac{Vial\ Mass_{After} - Vial\ Mass_{Before}}{Powder\ Loaded} \times 100\% \quad (4.4)$$

## 4.3 Results & Discussion

### *4.3.1 Predicted Component Distribution in Spray Dried Particles*

We used our previously established mannitol-dextran formulation, MD (3:1) with 40 kDa dextran, as a baseline to compare the impacts of increasing the relative dextran content and molecular weight of dextran. Using a diffusion-based drying droplet model, the relative distribution of AdHu5 was predicted with respect to the radial distance to the particle surface (Figure 4.2). The displayed AdHu5 mass% was normalized by the total concentration of AdHu5 added to the excipient blend, not the total mass of all excipient components. It should be noted that the particle was treated as a series of finite thick shells to predict the distribution of components throughout.

Based on the model output, the baseline formulation of MD (3:1)-40 kDa led to the highest amount of adenovirus located at the particle surface and had the lowest predicted amount of adenovirus throughout the solid inner layers of the particle. In comparison, the formulation with lowest predicted adenovirus on the particle surface was MD (1:3)-500 kDa. The molecular weight of dextran was predicted to significantly influence adenovirus surface concentration, as both formulations containing 500 kDa dextran showed lower AdHu5 mass% on the particle surface compared to the 40 kDa counterparts. A similar prediction was previously reported with this model for levitated particles and was verified experimentally with fluorescently tagged-protein coated silica nanoparticles as adenovirus analogues [116]. Higher molecular weight dextran at a higher concentration experiences much slower self-diffusion of dextran entanglements and creates an obstruction effect on the smaller solutes within the droplet [123,124]. With dextran acting as a physical obstacle, diffusion of mannitol and AdHu5 within the bulk droplet is hindered and may explain why AdHu5 is less likely to partition on the particle surface. Previous reports have noted that increased viral concentration on or near the surface of a drying particle can lead to reduced viral activity [10,116]. Consequently, we anticipate that vaccine formulations with lower predicted viral mass at the surface are likely more effective at retaining biologic activity under experimental conditions.

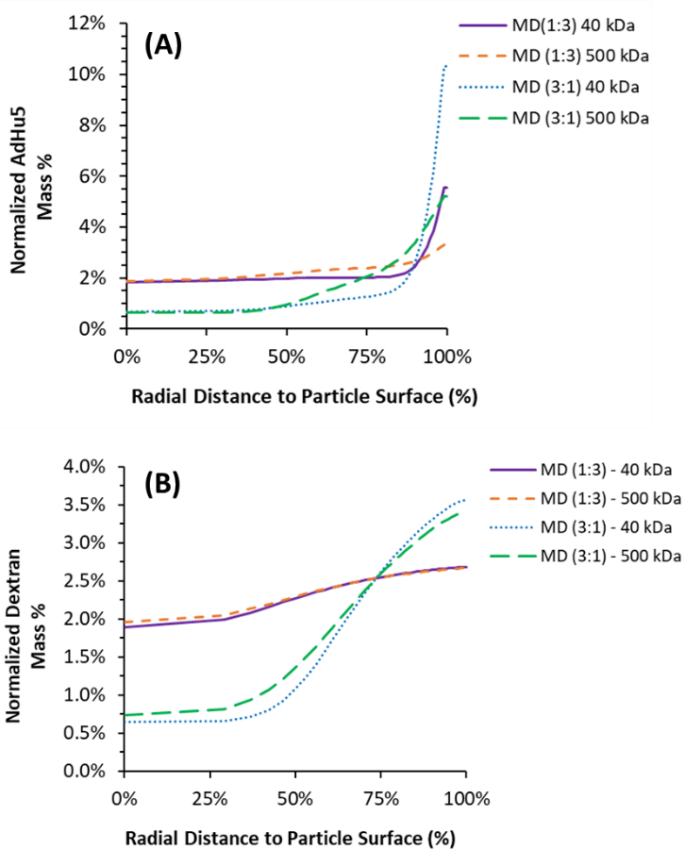


**Figure 4.2.** Model predicted, normalized mass distribution of (A) AdHu5 adenoviral vector and (B) dextran within a mannitol-dextran particle. Radial distance refers to the percentage of distance between the particle core (0%) and the particle surface (100%). Mass% of each component was normalized based on the total amount of that component added to the formulation. Excipient formulations include mannitol and dextran in a ratio by mass of either 1:3 or 3:1, respectively, and a dextran molecular weight of either 40 kDa or 500 kDa.

Furthermore, both formulations containing a 1:3 ratio of mannitol-to-dextran had a higher predicted mass% of AdHu5 at the particle core compared to the formulations using a 3:1 ratio. These 1:3 formulations also have a more uniform distribution of dextran throughout the particle, in contrast to the dextran-enriched particle surface seen for 3:1 formulations. Dextran has a substantially larger impact on viscosity, compared to mannitol and AdHu5, resulting in a much lower diffusion coefficient in water [125]. This effect is particularly relevant in the 3:1 formulations, as dextran becomes enriched on the droplet surface during solvent evaporation where

it reaches saturation and precipitates [116]. Since increasing dextran concentration in water has been found to increase the solution viscosity [126], incorporating more dextran within the formulation physically prevented mannitol from diffusing towards the droplet surface. As a result, mannitol can closely interact with AdHu5 in the particle core to provide stabilization though hydrogen bonding. It should also be noted that encapsulating AdHu5 in 40 kDa dextran alone has been experimentally shown to yield poor viral activity, likely due to the inability of dextran to effectively stabilize AdHu5 through water-replacement hydrogen bonding [95]. Overall, these model predictions suggest that the formulation with higher molecular weight and mass ratio of dextran favors more viral entrapment at the particle core, which should be verifiable by activity testing.

### *4.3.2 Viral Activity and Thermal Aging*

To validate the model predictions, viral activity was experimentally tested immediately after spray drying as well as after accelerated thermal aging for each powder formulation (Figure 4.3). Here we compare results to a xylitol-dextran blend where xylitol is chemically similar to the structure of mannitol and has previously been shown to retain high viral activity through spray drying [98]. In terms of activity losses attributed to processing, minimal viral titre log losses were observed immediately after spray drying when a 1:3 ratio was used for either mannitol or xylitol blends. Processing loss for the MD (1:3)-500 kDa and XD (1:3)-40 kDa were both below the acceptable threshold of 0.5 log loss, indicating very favorable results. The MD (1:3)-40 kDa was slightly above the target threshold with viral titre log losses that were slightly below 0.8 log loss. Processing losses were significantly higher for the powders formulated with a 3:1 mannitol-to-dextran ratio, exceeding 1.7 log loss. These results generally reflect the model prediction, in that viral activity was the highest for the MD (1:3)-500 kDa formulation with the lowest amount of

AdHu5 predicted at the air-particle interface. Likewise, MD (3:1)-40 kDa had the highest predicted AdHu5 at the air-particle interface and had low viral activity after processing. A slight deviation between modelled distributions and experimental activity was observed in the MD (3:1)-500 kDa, giving the highest overall activity loss. However, the model does not currently account for crystallinity or void formation within dry particles, which may have contributed to the different experimental outcome. It should be noted that formal process optimization was only conducted for the baseline MD (3:1)-40 kDa formulation, as the process yield was similar for all other mannitol-dextran formulations (data not shown). Since yield can be an indicator of spray drying process efficiency, this suggested that additional optimization of processing parameters was not necessary for the purposes of this study.

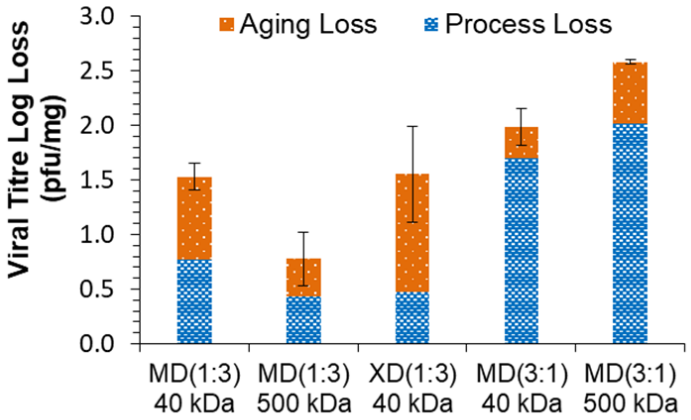


**Figure 4.3.** Viral titre log loss (pfu/mg) of spray dried AdHu5 adenoviral vector with excipient formulations using mannitol with dextran (MD) in a ratio by weight of either 1:3 or 3:1 and either a low molecular weight dextran (40 kDa) or high molecular weight dextran (500 kDa). A xylitol-dextran (XD) formulation with a 1:3 ratio using 40 kDa dextran is also shown. Process loss refers to viral titre loss from spray drying compared to the stock viral titre, while aging losses are associated with the additional viral titre loss after samples were stored at 45ºC for 72 hours prior to in vitro testing. All samples were tested in duplicate and error bars represent the resulting standard error.

Despite their valued role in hydrogen bond stabilization, mannitol and xylitol both added some crystallinity to the overall particle matrix which can negatively impact viral activity. Incorporating a lower weight fraction of these components likely prevented crystal exclusion of the adenovirus where we theorize that large amounts of crystalline excipient can force the biologic to the air-particle boundary or potentially even damage the structural integrity of the virus. If the adenovirus is located on the particle surface or any air-solid boundary, there is a greater chance of exposure to high heat during processing and higher activity losses [10,33,65,116]. Additionally, including a higher fraction of dextran promotes stronger thermal shielding upon exposure to the outlet temperature conditions to protect against structural degradation of the protein capsid for better activity retention [33]. Using a higher molecular weight dextran may further increase viscosity during drying [126], impeding molecular movement of the adenovirus that might otherwise lead to viral aggregation. However, at the 3:1 ratio, the 500 kDa dextran led to a slightly higher viral titre log loss than the 40 kDa formulation, suggesting that the molecular weight of dextran was less influential on viscosity than its concentration in the droplet.

Thermal stability was also tested in all five formulations, by analyzing viral activity retention upon exposure to accelerated aging conditions at 45 ºC for 72 hours. All mannitol-dextran formulations display similar thermal aging behaviour, based on aging losses being of similar magnitude for each of these formulations (Figure 4.3). This suggests that there were no significant differences in $T_g$ between these formulations. This observation is directly supported by $T_g$ values reported in literature, which indicate that 40 kDa and 500 kDa dextran have a $T_g$ of approximately 223 ºC and 225 ºC, respectively [49]. Mannitol-dextran formulations showed superior thermal

stability, compared to the xylitol-dextran blend which experienced 1.1 log loss during thermal aging.

Notably, the combined processing and aging losses experienced by the MD (1:3)-500 kDa formulation were below 0.8 log loss. The chemical structure of xylitol and mannitol is very similar, differing only by one C-OH group. But as an individual sugar alcohol, amorphous xylitol has a very low $T_g$ of -24 °C and will readily recrystallize at room temperature [127]. Comparatively, the reported $T_g$ of amorphous mannitol is around 12 °C [128], which significantly improves the overall $T_g$ in a dextran blend compared to xylitol. Under elevated thermal conditions, the xylitol-dextran blend likely experienced a higher degree of molecular mobility that led to viral aggregation. Xylitol recrystallization may have also forced more adenovirus towards the air-particle interfaces where thermal stresses during aging could have caused deactivation. Similarly, reorganization of the excipient crystal structure could have resulted in structural rearrangement and denaturation of the adenovirus causing poor stability [37]. Due to the significantly higher thermal aging losses observed with the use of xylitol, this formulation was considered to have poor thermal stability and was not used for further characterization. Despite past reports indicating xylitol as a promising excipient for vaccine powders [98], to the best of our knowledge this is the first study showing that the thermal aging properties of xylitol in blended systems are likely unsuitable to protect viral vectors during vaccine storage and distribution.

### *4.3.3 Moisture Content and Particle Morphology*

Since excessive water uptake can hinder dry powder stability, TGA was used to measure moisture content in each mannitol-dextran formulation after exposure to accelerated aging conditions (see Table 4.2). Moisture content for the MD (1:3)-40 kDa formulation was 4.6%,

which was slightly higher than the remaining mannitol-dextran formulations that contained closer to 3% moisture. Since moisture content was measured after 72 hours of thermal aging, these values indicate that formulations with a greater concentration of dextran had a higher capacity for moisture absorption under elevated storage temperatures. Kawaizumi et al. found that dextran hydration decreases with increasing molecular weight [118], which could explain why MD (1:3)-500 kDa did not have the same moisture content as the MD (1:3)-40 kDa formulation. As such, using a higher molecular weight dextran may also promote more effective, long-term stabilization of the encapsulated adenovirus.

**Table 4.2.** Summary of particle flowability properties of spray dried powder formulated with mannitol and dextran (MD) excipient blend in a ratio by weight of either 1:3 or 3:1, using a low molecular weight dextran (40 kDa) or high molecular weight dextran (500 kD).

| Formulation Ratio | Dextran MW | Moisture Content (%) | Bulk Density | Carr's Index |
|---|---|---|---|---|
| MD (1:3) | 40 kDa | $4.6 \pm 0.2$ % | $0.28 \pm 0.02$ | $53 \pm 4$ |
| MD (1:3) | 500 kDa | $3.5 \pm 0.2$ % | $0.33 \pm 0.01$ | $47 \pm 4$ |
| MD (3:1) | 40 kDa | $3.4 \pm 0.2$ % | $0.41 \pm 0.03$ | $48 \pm 5$ |
| MD (3:1) | 500 kDa | $2.7 \pm 0.2$ % | $0.39 \pm 0.03$ | $53 \pm 1$ |

Powder morphology of each mannitol-dextran formulation was observed by SEM (Figure 4.4). Formulations with a 1:3 mannitol-dextran ratio appeared to be highly clumped with large agglomerates observed, also indicating higher moisture content and stickiness in these powders. Handling and preparation of these powders was conducted in a lab space with increased ambient humidity directly before particle imaging, so the observed agglomeration may be further indication that increased amorphous content causes an increased capacity for moisture absorption. These particles appeared to have a rough outer surface, but solid particle structure. Agglomeration and clumping due to liquid bridge formation appears to be worse in the MD (1:3)-40 kDa sample, compared to the same ratio with 500 kDa. This qualitative observation is in direct agreement with

the measured moisture content and may also be attributed to the natural tendency of hydrophilic polymers to experience "stickiness" in the presence of water. Dextran is a hygroscopic material [118], so a higher amorphous content increased the capacity for moisture absorption when exposed to humidity.

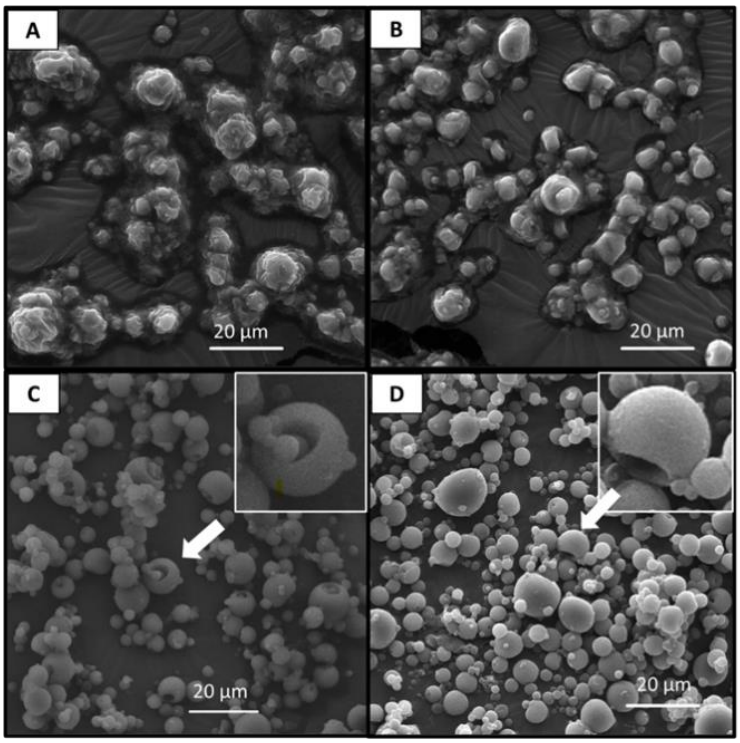


**Figure 4.4.** Scanning electron microscope (SEM) images showing particle morphology of the following mannitol-dextran (MD) spray dried powders: (A) MD (1:3)–40 kDa dextran, (B) MD (1:3)–500 kDa dextran (C) MD (3:1)–40 kDa dextran and (D) MD (3:1)–500 kDa dextran. Arrows indicate particle dimpling and indentation likely due to hollow shell formation. All images were captured at 2000 X magnification with a scale bar representing 20 µm in length.

Comparatively, formulations that contained more mannitol appeared to have a smoother particle surface, with the tendency to form hollow shells (as evidenced by the dimpling and rounded indentation observed in Figures 4.4C and 4.4D). Hollow shell formation is indicative of particles with a high *Peclet* number, in which evaporation occurs faster than solute diffusion [126]. Clumping is also less evident in the samples with higher crystalline content. Moisture absorption

can ultimately reduce the $T_g$ of the formulation through a plasticization effect, leading to reduced thermal stability and poor viral activity retention over time [129]. Therefore, protocols for handling spray dried powders with high amorphous content and some degree of crystallinity must minimize exposure to humidity as much as possible (i.e., through the use of double-wrapped powder blister packs and/or desiccants during storage).

*4.3.4 Geometric and Aerodynamic Particle Size*

To assess the suitability of these powders for inhalation, both geometric particle size and aerodynamic particle size were quantified and summarized in Table 4.3. In all formulations, the median particle diameter (D50) was either at or above 5 µm, indicating that the overall geometric particle size was slightly above our target size range for efficient pulmonary delivery to the peripheral lung [69]. However, these geometric particle sizes are not expected too substantially hinder inhalation efficiency. The MD (1:3)-40 kDa formulation had the highest D50 value of 8.7 µm with a large span indicating potential agglomeration in the sample. Agglomeration in this sample could also be a consequence of the higher dextran weight fraction, leading to the higher moisture content (Table 4.3). This presents a concern for inhalation delivery depending on the time scale for aggregation relative to patient administration. Subsequent moisture swell or particle cohesion may have resulted in the higher D50 and broader size distribution found for MD (1:3)-40 kDa. Despite these geometric particle sizes, the MMAD values ranged from 4.4 - 4.9 µm. Based on these results, all formulations have an aerodynamic particle size within the appropriate range of 1-5 µm for delivery to the lungs [108]. Since experimental MMAD was smaller than the measured geometric particle size, these powders can be considered inhalable and are therefore applicable for further study in pulmonary delivery.

**Table 4.3.** Geometric particle size compared to aerodynamic particle size of spray dried powder formulated with mannitol and dextran (MD) excipient blend in a ratio by weight of either 1:3 or 3:1, using a low molecular weight dextran (40 kDa) or high molecular weight dextran (500 kDa). Aerodynamic particle sizes are presented as MMAD based on experimental measurement using a Next Generation Impactor (NGI). A Helos R-series laser diffraction sensor was used to measure median particle diameter (D50) and span.

| Formulation Ratio | Dextran MW | Median Particle Diameter, D50 [µm] | Particle Distribution Span [µm] | MMAD [µm] |
|---|---|---|---|---|
| MD (1:3) | 40 kDa | $8.7 \pm 0.5$ | $4.0 \pm 0.3$ | 4.5 |
| MD (1:3) | 500 kDa | $5.9 \pm 0.5$ | $2.4 \pm 0.1$ | 4.4 |
| MD (3:1) | 40 kDa | $4.9 \pm 0.7$ | $1.6 \pm 0.4$ | 4.5 |
| MD (3:1) | 500 kDa | $6.1 \pm 0.1$ | $2.4 \pm 0.2$ | 4.9 |

*4.3.5 Bulk Powder Flowability*

Powder delivery via inhalation must also consider bulk powder properties like bulk density and Carr's Index (Table 4.2) to develop a successful powder delivery system. A slightly lower bulk density was observed in all formulations containing less mannitol, when testing in low ambient humidity. Lower bulk density in formulations with a 1:3 mannitol-to-dextran implies that there could be less interparticle contact and therefore less cohesion within the bulk state [130]. Bulk density was also used to calculate Carr's Index, to assess powder compressibility and flowability. Carr's Index values for each formulation were all above 47, indicating that these formulations produce highly compressible powders [131] and likely possess very poor bulk flow. Ideal powder flowability typically yields Carr's Index values less than 10, while very, very poor flow is represented by values 38 and above [132]. While this may primarily be an artifact of the small size of our particles, the relative comparison of Carr's Index values between formulations is

still insightful. Of all tested formulations, MD (1:3)-500 kDa was the least compressible and suggests that it would have higher flowability compared to the other powders. In terms of pulmonary powder delivery, the highly compressible nature of this powder requires a delivery method that minimizes powder compression during powder dosage loading. Due to this poor bulk flowability, powder delivery *in vivo* can also benefit from a delivery device that uses positive pressure or physical obstructions to interrupt particle bridging and induce aerosolization.

*4.3.6 Available Dose via Intratracheal Delivery*

Powder flowability was further analyzed through powder delivery with a hand-held, positive pressure dosator device intended for intratracheal delivery to murine animal models (Figure 4.1). Figure 4.5 shows the available dose from the custom-made dosator for each mannitol-dextran formulation, as well as the estimated delivered dose that can be sprayed through a 3D printed mouse trachea. Available dose was substantially higher in MD (1:3)-500 kDa and MD (3:1)-40 kDa formulations, with 84% and 91% emitted, respectively. The formulations with highest available dose also had the lowest Carr's Index values and particle sizes (Tables 2 and 3), predicting better flowability from the dosator tip. The other two formulations, both with a Carr's Index of 53, had significantly lower average available doses which were between 40-60%. The wide differences in available dose data further supports the claims of others that device performance is highly formulation dependent [84]. In all cases, the difference between available and delivered dose can be attributed to the larger particles or clumps that became stuck within the 3D printed trachea, representing the dose fraction unlikely to reach the lower airways. It should be noted that relative humidity during device testing was below 25% RH, allowing for relatively high available doses. Since the formulations with higher dextran content tend to absorb more moisture, it is expected that available dose would be far lower under elevated humidity conditions

[133]. Based on the high viral loading used in our formulations, a delivered powder mass between 2-4 mg should be sufficient for generating an immune response in mice, provided that viral activity remains high after spray drying [115]. With low viral log loss and a high delivered dose above 55%, the MD (1:3)-500 kDa formulation displayed sufficient viral potency within a desired powder mass for successful *in vivo* pulmonary delivery.

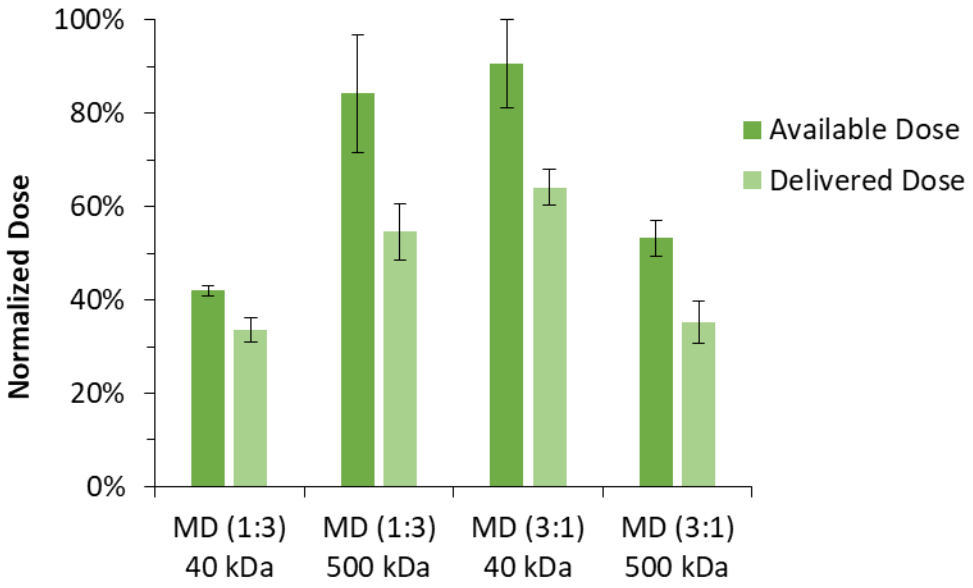


**Figure 4.5.** Available dose of spray dried dispersed from custom made dosator device (Figure 1), for each respective mannitol-dextran formulation in a ratio by weight of either 1:3 or 3:1 using a low molecular weight dextran (40 kDa) or high molecular weight dextran (500 kDa). Delivered dose represents the percentage of powder collected after powder was sprayed from the dosator and directly through a 3D printed mouse trachea, mimicking endotracheal delivery. Error bars represent standard error between replicate measurements (n=3).

## 4.4 Conclusions

Within this study, we have demonstrated how excipient ratio and molecular weight within a spray dried formulation impact particle drying dynamics and pulmonary delivery. Incorporating higher molecular weight dextran at a higher mass ratio within a spray dried mannitol-dextran blend can greatly improve retained viral activity in a thermally stable and inhalable dry powder. Increasing the dextran content relative to mannitol caused an increase in viscosity during droplet drying to limit molecular diffusion for more effective encapsulation of the viral vector within the particle core. Adding less mannitol to the blend also reduced crystal exclusion of the labile AdHu5 vector towards an air-solid interface, minimizing viral exposure to thermal stresses.

Formulations with a higher dextran ratio do have a higher capacity for moisture absorption and particle agglomeration, leading to possible challenges with powder delivery within environments of increased humidity and *in vivo* targeting at the lung. Under low humidity conditions (<25% RH), an available dose above 84% can be achieved using a custom made intratracheal dosator device that minimizes powder compression. MD (1:3)-500 kDa was the best performing formulation as it minimized processing and aging losses, while also offering suitable particle size and flowability to achieve a high available dose for intratracheal delivery. Overall, we have demonstrated that this mannitol-dextran spray dried formulation can maintain high viral potency and strong aerosolization potential, making it a promising candidate for *in vivo* pulmonary vaccine delivery.

## Appendix 4 – Chapter 3 Supplementary Material

### A1. Carr's Index Validation

Bulk and tapped density were measured using a graduated cylinder made from the body of a 1 mL syringe. The nozzle was cut off and a rubber stopper was fixed at the base of syringe at the 1 mL graduated marking (Figure A4.1). A known mass of powder was poured into the syringe using a stainless-steel funnel, secured in place using a retort stand, and the volume was recorded to obtain the bulk density.

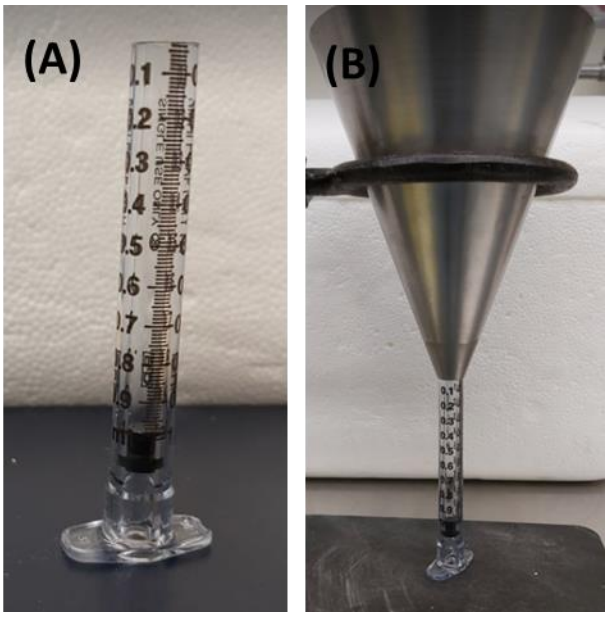


**Figure A4.1.** Graduated cylinder created from a 1 mL syringe (A) and filled with powder using a stainless-steel syringe (B) for use in bulk and tapped density measurement.

Carr's Index was determined based on the bulk and tapped density testing method described above. This method was validated based on evaluation of 7 bulk powder materials with known characteristic flow properties. Characteristic flow properties can be determined using the standard USP protocol for bulk and tapped density and calculating Carr's Index accordingly. Table

A4.1 includes the Carr's Index value calculated based on bulk and tapped density values measured using the 1 mL method described, as compared to characteristic powder flow for each material. Based on the appropriate alignment between calculated Carr's Index and reported flow properties, this testing method was considered accurate and did not require additional correction factors.

**Table A4.1**. Calculated Carr's Index and characteristic powder flow for the corresponding material.

| Material Tested | Carr's Index via 1mL Method | Characteristic Powder Flow |
|---|---|---|
| *Sucrose* | $1 \pm 1$ (*n*=3) | Excellent Flow |
| *Lactose Monohydrate (FlowLac)* | $7 \pm 2$ (*n*=3) | Excellent Flow |
| *Instant Coffee Grinds* | $13 \pm 1$ (*n*=3) | Good Flow |
| *NaCl* | $13 \pm 2$ (*n*=3) | Good Flow |
| *Mannitol* | $26 \pm 1$ (*n*=3) | Passable Flow |
| *Maltodextrin* | $28 \pm 1$ (*n*=2) | Passable Flow |
| *Cocoa Powder* | $47 \pm 2$ (*n*=3) | Poor Flow |

## A2. Method of CT Acquisition

A CT of a healthy mouse (Figure A4.2) was acquired in the McMaster Centre for Pre-clinical and Translational Imaging (MCPTI) at McMaster University (Hamilton, Canada) on a X-SPECT system (Gamma-Medica, Northridge, CA). The mouse was anesthetized with 2% isoflurane, strapped to a bed, and placed into the gantry of the X-SPECT where 1024 X-ray projections were

acquired with x-ray tube characteristics of 75 kilovoltage peak (kVp) and 175 µA. The 1024 projection images were reconstructed using a Feldkamp cone beam backprojection algorithm in COBRA (Exxim Sofware, Pleasanton, CA, USA) into 512 x 512 x 512 arrays (0.115 mm isotropic voxels).

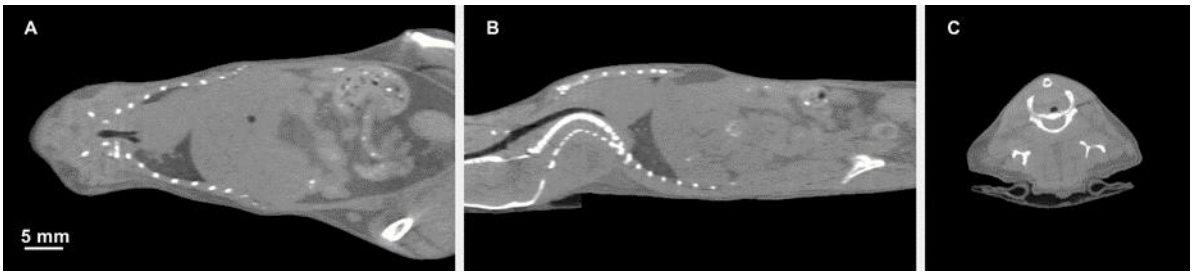


**Figure A4.2.** Individual slices from the CT image of a mouse. Slices displayed are A) at the level of the tracheal bifurcation in the coronal plane, B) mid-trachea in the sagittal plane, and C) at the level of the 1st rib in the transaxial plane.

### A3. 3D Rendering of Mouse Trachea

Using MATLAB, the following procedures were used to segment the airways from the array of projection images. The airways and lungs were segmented from the mouse body using a threshold to select a contiguous low-density area within the mouse's body (Figure A4.3). The airway segmentation was then cropped ~1.5 mm above where the trachea bifurcates (Figure A4.4). An anatomical overlay of the segmented tracheal region on the original CT scans can be seen in Figure A4.5. The tracheal region then undergoes a morphological dilation using a disk-shaped structuring element with a radius of approximately 2.5 mm. This operation expands the outer surface of the trachea by ~2.5 mm. The original tracheal region is then subtracted from the dilated region to produce a hollow tube whose inner surface matches the outer surface of the original tracheal region. The resulting isosurface is then saved as a STL file to produce a 3D printed model (Figure A4.6-A4.7).

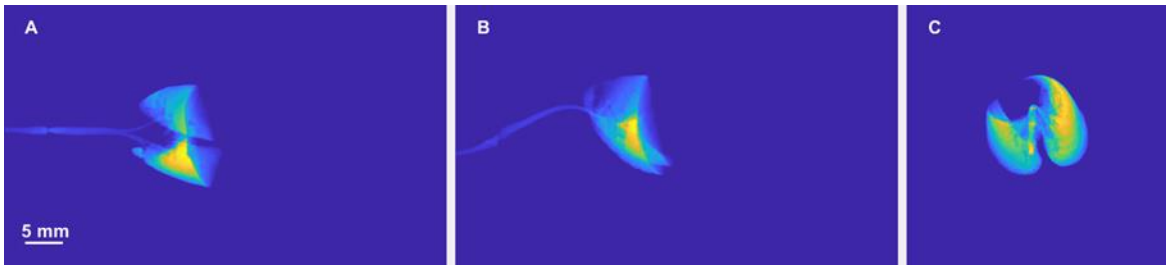


**Figure A4.3.** Images of the sum of segmented airways and lungs within the mouse body in A) coronal, B) sagittal, and C) transaxial planes.

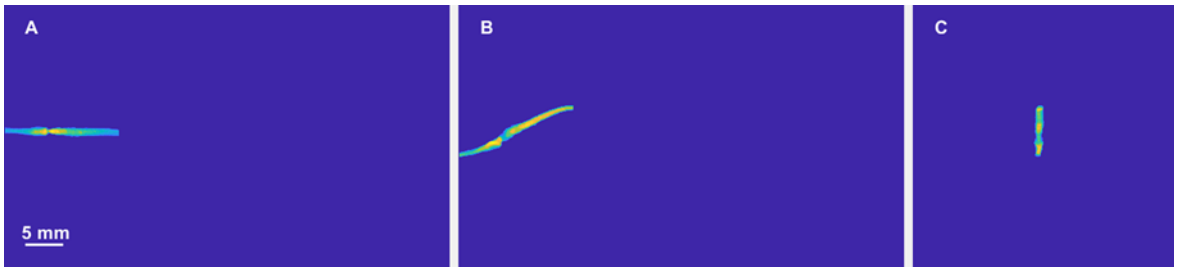


**Figure A4.4.** Images of the sum of the trachea region after cropping above the bifurcation in the A) coronal, B) sagittal, and C) transaxial planes.

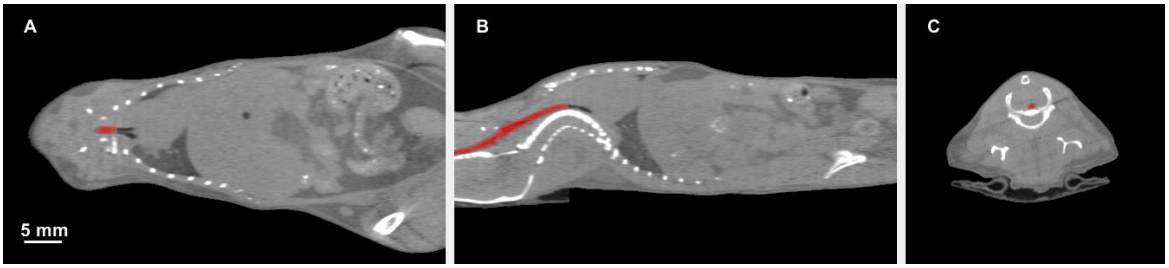


**Figure A4.5.** Overlay of tracheal region on A) coronal, B) sagittal, and C) transaxial CT slices.

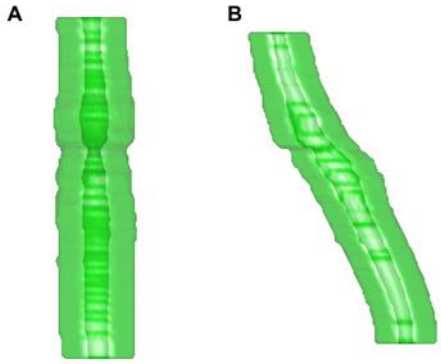


**Figure A4.6.** Isosurface of the tracheal region after dilation seen from A) the front and B) the left side.

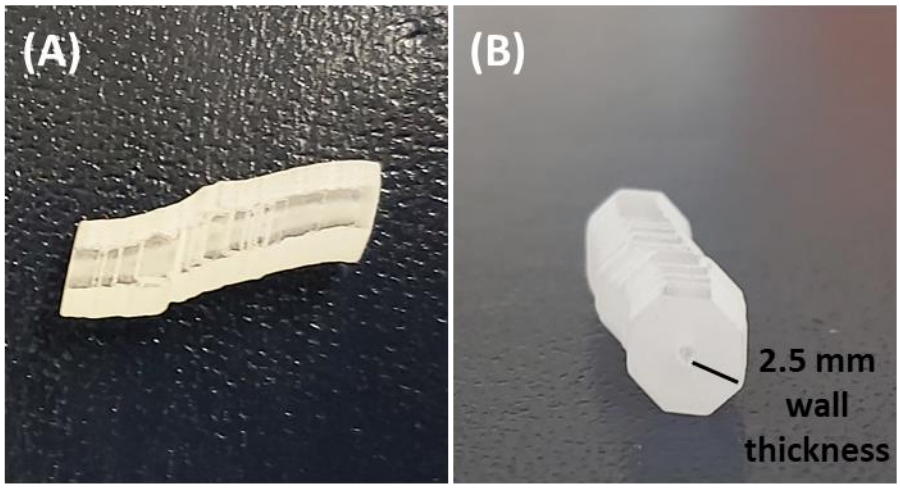


**Figure A4.7.** 3D printed mouse trachea with internal geometry printed to scale (Panel A). Cross-sectional image (Panel B) shows the increased wall thickness of 2.5 mm of the printed trachea to reduce model fragility and prevent breakage when used in repeated experimental testing.

## Chapter 5: Design Considerations of Intratracheal Delivery Devices for *in vivo* Dry Powder Vaccine Delivery in Mice

Within this chapter, the experimental design, *in vitro* dosator testing, lung tissue testing and data analysis was all conducted by myself. Co-author Vidthiya Jeyanathan conducted all *in vivo* powder delivery and mouse-related procedures. Co-author Mangalakumari Jeyanathan conducted all *in vivo* liquid delivery. The manuscript was drafted by myself and edited by supervisors Dr. Michael Thompson, Dr. Emily Cranston and Dr. Zhou Xing. This chapter will be submitted to *Pharmaceutical Research*.

**Abstract**

Intratracheal delivery of dry powder vaccines is especially challenging in mice and often associated with dose inconsistencies. To address this problem, we analyzed how material selection and actuation parameters of positive pressure dosators can affect powder flowability *in vitro*. We also evaluated *in vivo* device performance of dosators with different powder loading methods including tamp-loading, chamber-loading and pipette tip-loading. For a chamber-loading dosator assembled with stainless-steel, polypropylene or polytetrafluoroethylene (PTFE) needle tips, stainless-steel led to a 45% available dose with optimal mass loading of 6-7 mg due to its ability to dissipate state charge. Although increasing syringe air volume to 0.9 mL increased the available dose, 0.6 mL was considered safer for delivery to mice. Under high ambient humidity, storing a loaded dosator on dry ice prior to administration was found to reduce improve performance and reduce variability at prolonged storage times. Comparing dosator loading methods *in vivo*, the highest available dose (50%) was achieved with the pipette tip-loading dosator. By administering two powder doses per mouse, each of 2.4 mg of a spray dried adenovirus encapsulated in a mannitol-dextran blend, high bioactivity was observed in excised mouse lung tissue 3 days post-infection. For the first time, we have shown that a thermally stable, viral-vectored dry power can be delivered intratracheally to achieve strong bioactivity that is equivalent to intratracheal liquid delivery of reconstituted spray dried powder. Based on this success, we hope to guide the design and device selection process for murine intratracheal delivery of dry powders to help progress this promising area of therapeutics.

## 5.1 Introduction

For the prevention of respiratory infectious diseases like tuberculosis, dry powder vaccine delivery through the pulmonary route is very promising since the lungs are highly vascularized and offer high surface area for absorption [51,68,69]. By directly targeting the lungs, highly localized therapeutic doses can be delivered with reduced systemic side effects [71] and may even require a lower therapeutic dosage to initiate a mucosal immune response compared to systemic intramuscular delivery [70]. Vaccines encapsulated in dry powder form have the additional advantage of displaying thermal stability at elevated temperatures that minimizes the need for expensive cold-chain infrastructure [115]. The non-invasive nature of inhaled delivery and relative ease of self-administration makes inhalation highly desirable for dry powder vaccine administration in a clinical setting.

In early stages of vaccine development, preclinical animal models are critical for determining the immunogenicity and reactogenicity profiles of a new therapeutic [84]. Murine models are of particular importance in the preclinical screening of vaccines, serving as a relatively inexpensive mechanistic model with a short growth period [51,80,81]. However, testing inhalable dry powder vaccine products with murine models is especially challenging since active inhalation cannot be directly controlled and the small anatomical scale of mice can lead to inconsistencies in dosage delivery. Pulmonary delivery in mice is also challenging due to the lack of commercially available devices that can be used for consistent dosing. As a result, many groups have resorted to developing custom-made dosage chambers or hand-held devices with varying levels of complexity [68,72,84,87].

Current pulmonary delivery strategies used for rodents range from passive inhalation to intratracheal and endotracheal administration, often referred to as insufflation. Since mice are obligatory nose-breathers, passive inhalation requires aerosolized powder to travel through the nasal cavity prior to reaching the trachea and primary bifurcation of the lungs [83]. This approach typically utilizes a customized chamber set-up to ensure uniform powder dispersion and commonly suffers from poor delivery efficiency with very high powder mass requirements [51,68,72]. For high-cost biologics like viral-vectored vaccines that are produced in small-batch volume, passive inhalation in mice is not usually a feasible approach of delivery.

A small range of hand held insufflation devices have been developed for intratracheal dry powder delivery in mice using positive pressure from a syringe to dispel powder [84,86,87,88]. Similar to the Penn-Century Dry Powder Insufflator™, which is no longer commercially available, these intratracheal dosator devices are loaded with a small mass of dry powder that is sprayed through a small needle tip directly into the trachea. Depending on the device design, initial powder loading has been demonstrated using a tamping strategy [88], chamber loading method [87], or direct loading into a pipette needle tip [84,86]. Although these devices can be assembled with easily accessible components, there is a lack of general guidance towards material selection and resulting compatibility with a dry powder formulation. To the best of our knowledge, the impact of dosator device design and corresponding powder loading method have never been directly quantified or compared for a highly compressible dry powder vaccine.

To optimize intratracheal delivery using a custom-made dosator device, this study seeks to evaluate how design and operational parameters impact device performance. Material selection of the dosator tip, selected actuation parameters and powder loading strategy are all expected to impact the performance of custom-made intratracheal dosators in terms of achieving consistent

and sufficient powder dosage delivery into mice. By testing a chamber loading dosator design with a stainless steel, polypropylene or polytetrafluoroethylene (PTFE) needle tip, the impact of operational parameters like loaded powder mass, air volume and device storage conditions on powder flowability were evaluated *in vitro*. Assembly of a chamber-loading dosator offered the highest level of customization in terms of needle tip material and powder capacity. As such, the chamber-loading design was used as the basis for investigating the impact of actuation parameters, with the expectation that these findings are transferrable to other applicable dosator designs. Upon determining the optimal actuation parameters, we compared three different dosator designs which use tamp-loading, chamber-loading and pipette-tip loading to assess the *in vivo* intratracheal device functionality and resulting bioactivity of a thermally stable spray dried adenovirus powder. Intended as a viral-vectored vaccine, this human serotype 5 adenovirus (AdHu5) encapsulated in a binary excipient mixture of mannitol and dextran in a 1:3 ratio by mass has previously been shown to retain viral activity after 72-hour exposure to 45 °C with only 0.8 log loss in viral titre [134]. Overall, this study is intended as a guide to the design and device selection process to achieve successful intratracheal delivery of highly compressible dry powder viral biopharmaceutics into mice.

## 5.2. Materials & Methods

### *5.2.1 Chemicals and Biologics*

D-mannitol at USP grade and D-(+)-trehalose dihydrate were purchased from Millipore-Sigma (ON, Canada) and dextran ($M_r$ 500000 Da) was purchased from ThermoFisher Scientific (Waltham, MA, USA). A Barnstead GenPure Pro system (ThermoFisher Scientific, Waltham, MA,

USA) was used to purify Milli-Q® water at a resistivity of 18.2 MΩ cm. Preparation and purification of a recombinant, replication deficient human adenovirus of serotype 5 expressing Luciferase (AdHu5-Luc) was conducted at the vector facility within the McMaster University Immunology Research Centre. The adenoviral vector stock was suspended in a 5% trehalose storage buffer directly after purification with a titer of $3.5 \times 10^9\ pfu/mL$ and was stored at -80 ºC based on a previously optimized protocol [115]. Luciferase assay substrate, luciferase assay buffer and 5X cell culture lysis reagent were all purchased from Promega (Madison, WI, USA) as part of a luciferase assay system.

*5.2.2 Spray Dried Powder Preparation*

A mannitol-dextran excipient solution was prepared by dissolving mannitol and dextran at a 1:3 mass ratio in purified Milli-Q® water to a final concentration of 1% solids. This formulation was selected based on our previous study that minimized viral log loss during spray drying and thermal aging [134]. For all *in vitro* testing described in Section 2.4, a 5% trehalose placebo solution was added to the excipient blend at 60 µL/100 mg excipient, while *in vivo* testing required the addition of the AdHu5-Luc stock vector at the same concentration of 60 µL/100 mg excipient. A previous study has shown that mannitol-dextran spray dried powders have constant particle size and morphology with and without the addition of AdHu5 [65], so *in vitro* placebo testing is expected to accurately represent the powder flow of the adenoviral powder.

Once dissolved, the excipient solution was spray dried through a 0.7 mm nozzle using a B-290 Mini Spray Dryer (Büchi, Switzerland). The following processing conditions were selected based on previous optimization to maximize yield and viral activity while achieving inhalable particle size [65]: feed flow rate of 217.5 mL/h, spray gas flow rate of 439.11 L/min, aspirator

flow rate of 35 m/h and an inlet temperature of 120 ºC. An outlet temperature range between 55-65 ºC was recorded. Powder was collected immediately after drying and transferred to microcentrifuge tubes within a biosafety cabinet. A benchtop desiccator filled with Drierite® anhydrous indicating desiccant (W.A Hammond Drierite Company Ltd.) was used for short-term room temperature storage to avoid ambient moisture uptake.

*5.2.3 Intratracheal Dosator Assembly*

Three custom-made dosator designs were assembled and primarily differed based on the method of powder loading (Figure 5.1). The tamp-loading design was based on a loading method described by Stewart et al. and was fabricated using a 22 Ga blunt tip intravenous catheter with 1.5 inch stainless steel needle tip and a 1 mL syringe press-fit at the opposite end as shown in Figure 1A [88]. This device required minimal assembly using two prefabricated components, including the intravenous catheter and syringe. On average the tracheal diameter of a mouse is approximately 1.5 mm [135], which makes a 22 Ga or 23 Ga catheter needle an appropriate size for intratracheal delivery. Powder loading was accomplished using a previously described method in which the needle tip was repeatedly tamped in a small plastic tamp bucket containing approximately 20 mg of powder [88]. The dosator was weighed before and after tamping to determine the loaded powder mass.

Comparatively, the pipette tip-loading dosator design used a 3-way stopcock from Cole-Parmer (Montreal, Canada) with a luer inlet for connecting a syringe with a complementary male luer lock, adapted from similar designs reported by Ihara et al. and Qui et al. [84,86]. In this design, the 3-way stopcock serves as a connection between the prefabricated pipette tip and a 1mL syringe. As previously described, our version of the pipette tip-loading dosator uses a 10 µL Rainin

LiteTouch System polypropylene pipette tip with surface repellent (Mettler-Toledo, Oakland, CA, USA) in which powder is carefully poured using weigh paper prior to securing on the opposite end of the three-way stopcock, as indicated in Figure 5.1B [134]. All 3 components of this dosator design, including the pipette tip, 3-way stopcock and syringe were prefabricated and required minimal assembly.

Finally, the chamber-loading design (Figure 5.1C) was based directly on the described protocol by Durham et al. of a disposable dosator for pulmonary insufflation in small animals [87]. The powder loading chamber was prepared using a 0.5 mL microcentrifuge tubes with holes approximately drilled in the center of the cap and bottom of the tube with diameters of approximately 4 mm and 2mm, respectively. Blunt end 1.5 inch, luer lock-connecting 23 Ga needle tips made from stainless-steel (Amazon, Seattle, WA, USA), polypropylene (McMaster-Carr, Elmhurst, IL, USA) and PTFE (McMaster-Carr, Elmhurst, IL, USA) were used to compare the effect of tip material on powder flow from a chamber-loading dosator design (see Figure 5.1D). The needle tip was press-fit directly into the bottom of the microcentrifuge tube and with the cap open, powder was carefully loaded into the microcentrifuge chamber. A small piece of cotton was placed near the top of loading chamber before closing the cap to prevent backflow of material upon actuation of the syringe secured in the top hole of the microcentrifuge cap. A fine mesh screen between the loading chamber and needle tip was not used in this design, based on initial testing that showed poor powder flow from the device (data not shown).

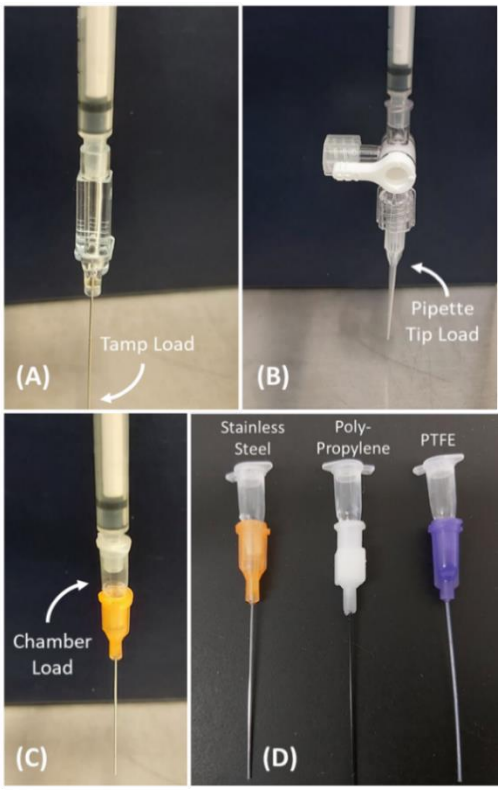


**Figure 5.1.** Assembled dosator designs intended for intratracheal dry powder delivery which differ based on the power loading strategy, including: (A) tamp-loading (B) pipette tip-loading and (C) chamber-loading. Three tip materials (D) were tested for the chamber loading design including stainless steel, polypropylene and PTFE.

### *5.2.4 Dosator Performance Testing*

To determine the impact of various operational parameters on dosator functionality, a range of syringe air volumes, loaded masses, storage times and storage conditions were evaluated. Syringe air volumes ranged from 0.3 to 0.9 mL, based on reported values that have been previously used for successful insufflation in mice [13,84]. The total lung capacity of a mouse is approximately 1 mL, which serves as the critical upper limit for aspiration volumes used for dosator actuation [136]. Dosator performance was assessed in terms of powder flowability from the device and quantified based on available dose. A testing set-up was used to vertically spray a

loaded dosator through a 3D printed mouse trachea and into a glass collection vial placed directly below, using a method previously described [134]. Each 23 Ga needle tip fit snuggly within the inner diameter of the 3D printed trachea. A retort stand with clamp was used to ensure the loaded dosator assembly was sprayed from a consistent height and properly centered above the collection vial. All testing was conducted with the chamber-loading dosator design, based on the ability to load a wider range of powder mass and easily test different needle tip materials. Available dose was used to describe the percentage of powder exiting the dosator with respect to the total amount of powder initially loaded, as indicated in Equation 5.1. Each sample condition was measured in triplicate and error bars represent standard error between repeated measurements.

$$Available\ Dose = \frac{Dosator\ Mass_{Before} - Dosator\ Mass_{After}}{Powder\ Loaded} \times 100\% \quad (5.1)$$

The expected powder dose delivered to the mouse lung tissue was approximated by the mass of powder collected within the glass vial. Here, we refer to the delivered dose as the percentage of powder that can flow through the 3D printed trachea compared to the total powder initially loaded, as seen in Equation 5.2.

$$Delivered\ Dose = \frac{Vial\ Mass_{After} - Vial\ Mass_{Before}}{Powder\ Loaded} \times 100\% \quad (5.2)$$

*5.2.5 Intratracheal Inoculation for Liquid Delivery In Vivo*

Female BALB/c mice 8-10 weeks old were purchased from Charles River (Wilmington, USA) and housed in a level B facility at McMaster University for one week prior to all *in vivo* experiments. All experimental procedures and animal handling protocols were approved and in

accordance with the guidelines of McMaster University's Animal Research and Ethics Board. To confirm suitability of our excipient blend and quantify *in vivo* bioactivity of the adenovirus following spray drying, reconstituted spray dried powder was administered as a liquid control via intratracheal inoculation using a previously described technique [137]. Following anaesthetization with isoflurane, mice were hung by their teeth on a string attached to a 45° intubation board while the tongue is held to the side to expose the trachea and prevent swallowing. A pipette was used to deliver liquid drops of reconstituted spray dried powder to the back of the mouth, allowing each drop to be individually inhaled. Two doses were administered within 1 hour, with each dose consisting of 2.4 mg of spray dried powder reconstituted in 40 µL PBS. The total viral dosage per animal was $2 \times 10^6$ PFU.

*5.2.6 Intratracheal Powder Delivery In Vivo*

For *in vivo* testing of dry powder, intratracheal dosators were loaded and stored in a plastic bag that was sealed within a glass container filled with desiccant for transport to the animal facility. For all tests conducted under ambient humidity above 10% RH, the glass container was additionally placed on dry ice during storage and transport prior to administration in animals. Spray dried powder was not directly in contact with the dry ice, as the glass container prevented exposure to $CO_2$ sublimation which is known to cause acidification that can deactivate adenovirus [34].

To deliver spray dried powder using each dosator design, endotracheal intubation was conducted using a previously described protocol in which the anesthetized mouse was suspended on a 45° intubation board by its teeth [138]. Once the tracheal opening was located, a P200 pipette containing 100 µL of water was inserted into the trachea to confirm the correct location based on the movement of the air gap during aspiration. The P200 pipette tip was then removed and replaced

with the needle tip of the loaded dosator for subsequent actuation. Each dosator was loaded with powder and weighed, prior to device administration in animals and directly afterwards. *In vivo* performance of each dosator design was determined based on the change in dosator weight before and after administration and was used to calculate emitted dose. All powder was delivered using a syringe air volume of 0.6 mL through fast actuation. Mice that did not receive any reconstituted or dry powder treatment were considered the negative control group. Spray dried placebo powder containing no added vector was also tested for baseline comparison. As with the reconstituted powder delivery, two spray dried powder doses of approximately 1-4 mg each were sprayed within a 1-hour interval for a total viral dosage between $2 \times 10^6$ and $3 \times 10^6$ PFU. Animals were sacrificed 3 days post-infection and lung tissue was removed for storage at -70 ºC.

*5.2.7 In Vivo Adenovirus Bioactivity via Luciferase Assay*

Luciferase activity within collected lung tissue was assessed after approximately 24 hours of cryo-storage. Frozen lung tissue was transferred to 14 mL polypropylene tubes containing 1mL of a 1X solution of cell culture lysis reagent, stored on ice. Samples were fully homogenized with a Brinkmann Homogenizer (Polytron, Switzerland) on ice for 30-40 seconds before centrifugation at 3000 rpm for 10 minutes at 4 ºC. Supernatants were transferred into 1 mL microcentrifuges tube on ice, while the luciferase assay reagent was thawed to room temperature. In a Corning® Costar 96-well white solid plate (Thermo Fisher Scientific, Waltham, USA), 100 µL of luciferase assay reagent mixed with 20 µL of sample supernatant per well, followed by gentle pipette mixing. Luminescence was immediately measured using a i3SpectraMax Plate Reader (Molecular Devices, CA, USA). Three wells were analyzed per sample and the average signal was used to determine

the relative luciferase units within the total lung tissue, which accounted for the sample dilution prior to homogenization.

## 5.3 Results and Discussion

### *5.3.1 Impacts of Air Volume on Chamber-Loading Dosator*

Achieving incipient flow through the needle tip with our cohesive mannitol-dextran powder requires sufficient air pressure to overcome interparticle forces and wall friction to effectively dilate the powder from its bulk stored state. To investigate the impact of syringe air volume on device performance, chamber-loading dosators were assembled from three different needle tip materials, loaded with placebo powder and sprayed using 0.3, 0.6 and 0.9 mL of air preloaded in a syringe (Figure 5.2). For both stainless-steel tip and PTFE tip, device performance was poor for the two lower air volumes but substantially improved to approximately 20% available dose when a 0.9 mL syringe volume was used. With progressively greater volumes of air, the solids were more effectively dispersed from the dosator needle tip. Comparatively, the polypropylene tip had marginally better performance at the two lower air volumes though it did not improve with 0.9 mL air volume like the other cases. Despite increased air volume, consistent dilation of the bulk solids with the polypropylene tip was likely due to the tendency of this powder formulation to build static charge during spray drying [139] which is held in balance by the dielectric properties of polypropylene [140]. Charge stabilization by PTFE was less evident than it was for polypropylene, but the significance of static charge and the resulting impact on powder flow from the dosator should not be overlooked.

For all tip materials, the delivered dose was similar to the available dose, indicating effective powder flow through the 3D printed trachea. Minimal powder losses on the tracheal walls

were observed and suggests that the powder formulation and delivery strategy are suitable for inhalation in mice. Maximizing available dose, and similarly improving delivered dose, is paramount for achieving overall delivery efficiency and reducing powder wastage within the device itself. Despite the general improvements in powder emission with 0.9 mL air volume, this volume is too close to the critical limit for safe delivery to a mouse without risk of tissue damage. Qiu et al. found that actuation of an intratracheal dosator using 1 mL of air caused weight change in BALB/c mice between 7-9 weeks old, suggesting that tissue damage should be anticipated at or beyond an air volume of 0.9 mL [84]. As a result, 0.6 mL was elected as the optimum air volume for devices in this study, with new focus placed on other actuation parameters to maximize delivery efficiency

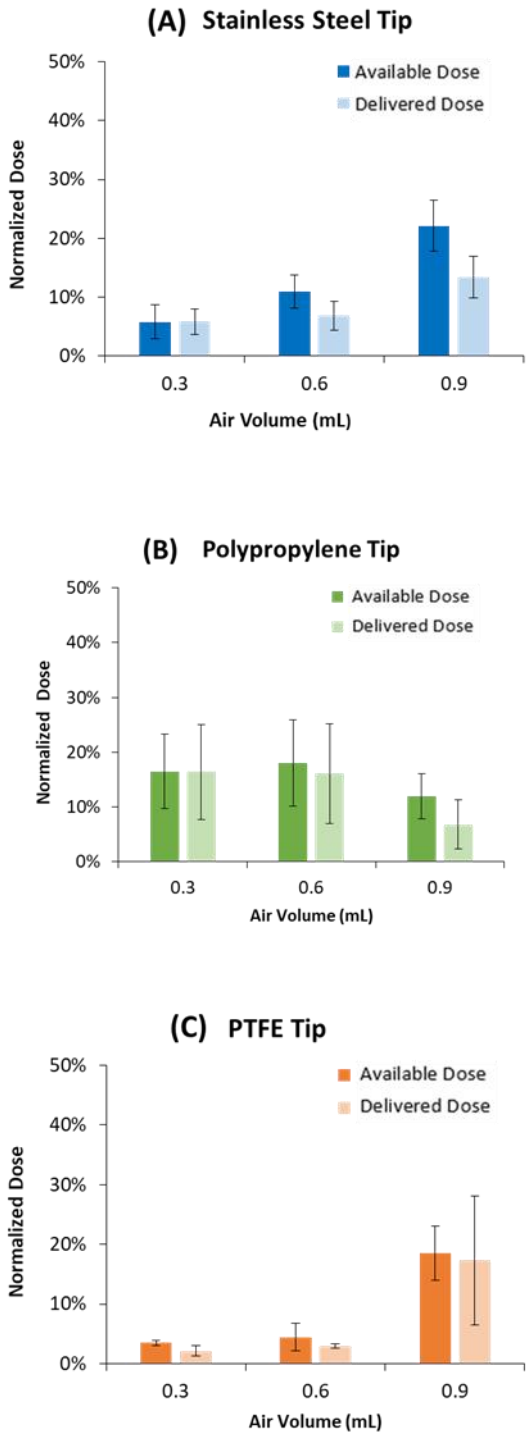


**Figure 5.2.** Available dose and estimated delivered dose collected *in vitro* from a chamber loading dosator design assembled with a (A) stainless steel tip, (B) polypropylene tip and (C) PTFE tip. Powder was administered from the dosator device using syringe air volume intervals of 0.3 mL, 0.6 mL and 0.9 mL. Dose was normalized based on the mass of powder loaded in the dosator.

### *5.3.2 Loaded Mass Optimization of Chamber-Loading Dosator*

The optimum loading mass for the chamber-loading dosator was determined by examining a range of mass intervals for each of the three needle tip materials, with the results summarized in Figure 5.3 for 0.6 mL dispensed air volume. Care was taken to minimize vibrations to the dosator during these tests to avoid accelerating the time consolidation of loaded powders. Despite all loading chambers being the same size, with similar needle tip geometry, there were distinct differences in dosator performance with different initial powder mass loading. When a stainless-steel tip was used, available dose decreased after the loading mass exceeded 7 mg. Above 7 mg, significant powder agglomeration was likely occurring at the entrance to the needle tip, causing an intermittent blockage during use. Within the optimum loading range below 7 mg, the stainless-steel tip outperformed the other tip materials in terms of available dose. Since these powders contain very low moisture content, static build-up was more effectively dissipated by the stainless-steel tip, compared to the other materials, allowing for more effective flow from the chamber-loading device.

Comparatively, the polypropylene tipped dosator had a relatively constant available dose up to 11 mg, similar to the trend seen for air volume, which suggests that it could be more effective when a high powder dosage is required to elicit an immunogenic response. The PTFE tip performed poorly across the tested mass range, but available dose improved slightly at the 10-11 mg loading. Significant build-up of powder across the inner length of the needle tip indicated that static attraction occurred between the PTFE needle tip and the charged mannitol-dextran powder. With a higher mass loading, the higher applied stresses from the syringe on the powder were

sufficient to dilate segments of the bulk solids in the PFTE needle tip to allow for better particle travel and powder emission.

As seen above, there was minimal difference between delivered dose and available dose, indicating appropriate powder flow of this formulation through the model trachea. Although the available dose percentage should be ideally maximized, the optimal mass of a viral dry powder that is delivered per dosator actuation will be highly dependent on the viral dosage required to elicit an immune response as well as the viral titre of the dry powder [115]. Conversely, due to the anatomically small scale of a mouse's lungs, too much powder delivered in a single spray can pose a choking hazard. Other studies have suggested that 1-2 mg of powder is appropriate for intratracheal delivery [13,84], but our initial tests indicated that up to 6 mg can be safely delivered intratracheally (data not shown). The delivery efficiency of the stainless-steel tip dosator reached with approximately 45% available dose when 6-7 mg of powder was loaded, which meant that approximately 3 mg of the powder could be delivered. For the polypropylene tip that achieved a delivered dose of 25% when loaded with 10-11 mg of powder, approximately 2.6 mg delivered powder was considered an acceptable powder dosage. On the other hand, the PFTE tip dosator did not dispense a suitable powder mass, with only 8% available dose at 10-11 mg loading, which meant that approximately 0.8 mg of powder was delivered. Recognizing the recommended upper limit of powder mass that can safely be delivered per dose, the loaded mass must therefore be considered in conjunction with spray efficiency to successfully deliver an appropriate powder dosage.

Initial *in vivo* testing using luciferase expression as a marker of adenovirus infection revealed that a minimum liquid dosage of $1 \times 10^6 PFU$ was required to produce a bioactive response in mice (data not shown). For the viral-vectored dry powder used in this study, the viral

titre of the dry powder after spray drying was $4.2 \times 10^5 PFU/mg$, therefore a target powder dosage of at least 2.3 mg was required for quantifiable viral infection and gene expression. Since the PTFE tip could not deliver this mass of mannitol-dextran powder with the loaded mass range tested, it was not suitable for our intended *in vivo* application. Comparatively, chamber-loading dosators outfitted with stainless steel and polypropylene needle tips could both emit at least 2.3 mg, when loaded with the optimal mass of 6-7 mg and 10-11 mg, respectively. However, the stainless- steel tip was chosen for *in vivo* testing since it offered a higher available dose with lower mass loaded, resulting in higher device efficiency and reduced powder wastage.

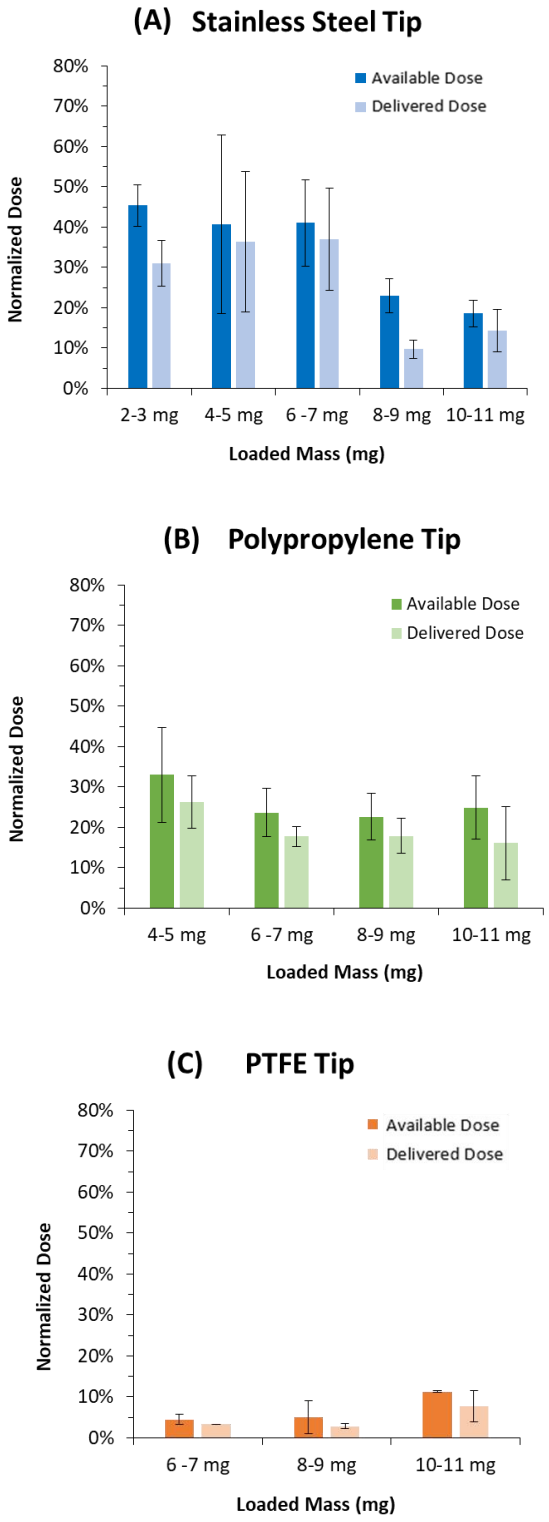


**Figure 5.3.** Available dose and estimated delivered dose collected in vitro from an intratracheal dosator with chamber loading design. Powder dose was normalized based on initial powder mass loaded into the chamber of a dosator device assembled with (A) stainless steel tip, (B) polypropylene tip and (C) PTFE tip. Dose was normalized based on the mass of powder loaded in the dosator.

### *5.3.3 Impacts of Dosator Storage Conditions*

Since the time between loading a dosator and spraying *in vivo* can vary substantially, particularly when a prepared dose must be transported to an animal testing facility, the impact of ambient storage time and consolidation was necessary to assess in terms of device efficiency (Figure 5.4). At the time of testing, ambient humidity was ~40% RH which was observed to impact powder behaviour and dosator performance. The results in Figure 5.4 show a notable decline in the available and delivered dose performance for the stainless-steel tip design over time in this humidity. Due to high amorphous content, this powder formulation was sensitive to moisture absorption causing undesirable molecular motion which promoted particle agglomeration within the dosator and a reduction in available dose. Conversely, the device with the polypropylene tip did not show the same decline in performance over time under ambient conditions, but there was notably high variability and poor repeatability between sprays. The hydrophobic nature of polypropylene may provide a beneficial water repellent effect [141], preventing water adsorption onto the interior surface of the needle tip. Once the powder was in motion, this repellent effect prevented the powder from contacting any additional water source which would have otherwise promoted further agglomeration. In comparison, the PTFE tip showed poor available dose performance overall and notably lower available and delivered dose at the 90-minute timepoint. Although PTFE is highly hydrophobic, like polypropylene, the internal luer lock geometry connecting the PTFE needle and the loading chamber seemed to induce powder consolidation that limited particle flow.

An alternative storage protocol was considered to address device performance concerns under high humidity conditions by storing the pre-loaded dosators within a glass container and placing on dry ice for various time periods prior to actuation. When using dry ice storage, significant

improvements in both available and delivered dose were observed for all tip materials, specifically at the storage higher time intervals. After 90 minutes of storage time on dry ice, the stainless-steel design yielded an available dose of 10% compared to 2% available dose when stored at ambient conditions for the same time interval. After 30 minutes of storage, the average available dose from the polypropylene tip showed a slight increase from 37% to 43% with the use of dry ice and a significant reduction in variability between measurements at most tested time points. The use of dry ice storage also improved the average available dose observed at the 90-minute timepoint for the PTFE tip design, increasing to 12% compared to 3% under ambient conditions. This improvement in dosator performance was due to the cooling effect created by dry ice sublimation which caused water vapour in the surrounding air within the glass container to condense [142]. As a result, ambient humidity decreases to prevent moisture uptake and agglomeration of the spray dried powder. Overall, careful dry ice storage was preferrable for improved dosing consistency and general performance of a chamber loading dosator when working in environments with elevated humidity.

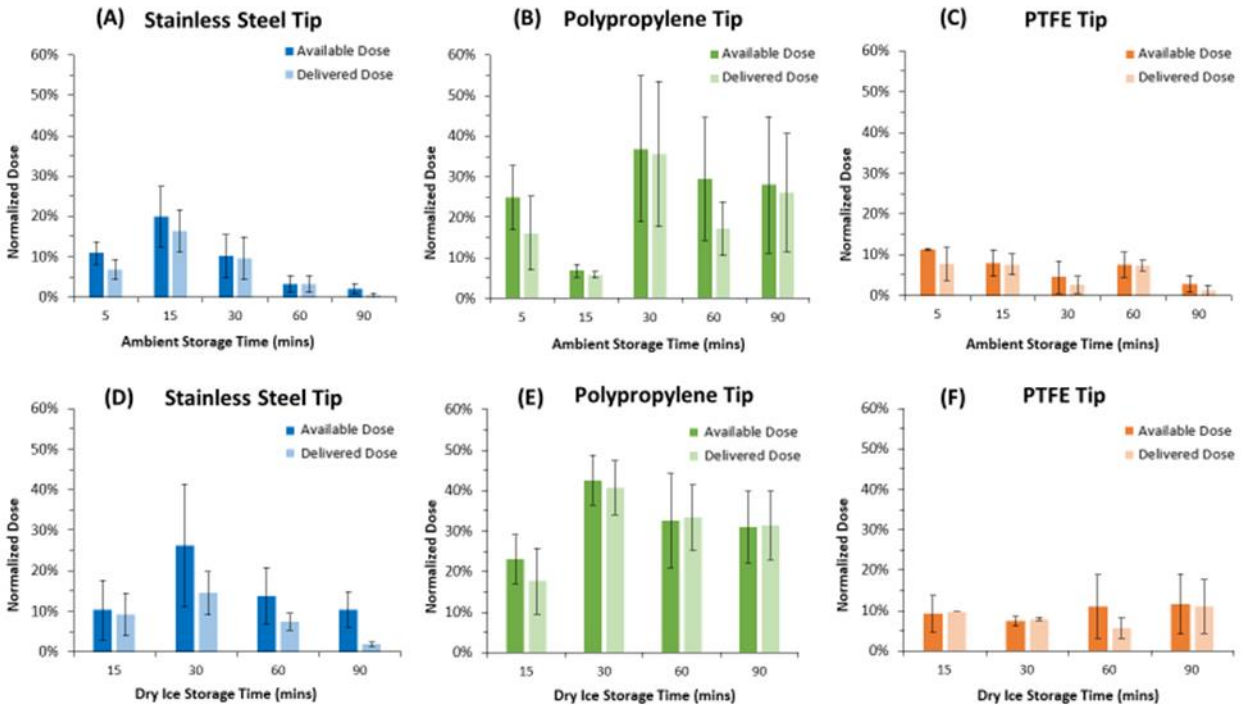


**Figure 5.4.** Performance of chamber loading dosators after loading powder and exposing the assembly to ambient conditions (A-C) or dry ice (D-F) for designated storage time intervals prior to actuation. Available dose and estimated delivered dose were normalized based on the initial powder loaded in the dosator, which was optimized based on tip material selection.

### *5.3.4 In Vivo Dosator Design Comparison*

*In vivo* evaluation of the optimal actuation parameters and storage conditions detailed above was conducted using three dosator devices with differing loading methods to determine bioactivity of a spray dried adenoviral vector upon intratracheal delivery. An air volume of 0.6 mL, optimal device loaded mass and dry ice storage for all experimentation that occurred with ambient humidity exceeding 10% RH was used to analyze dosator designs with tamp-loading, chamber-loading and pipette tip-loading. Using spray dried powder encapsulating the AdHu5-Luc vector at a viral potency of $4.2 \times 10^5\ PFU/mg$, the emitted dose of each dosator was assessed in Table 5.1. A stainless-steel needle tip was selected for the chamber-loading design to achieve a high emitted

dose, as mentioned above, while the rigid needle tip also improved the delivery accuracy when targeting the trachea.

Overall, the tamp-loading design with stainless-steel tip offered powder loading capacity, below the minimum powder dosage required and could not successfully emit powder *in vivo*. Due to the dense consolidation experienced during loading, the loaded powder solidified in the tip during tamping and could not be successfully sprayed. In addition, the close proximity of the powder to the end of the stainless-steel tip led to moisture absorption and subsequent agglomeration when the tip came into contact with the humid environment of the oropharynx. Comparatively, the chamber-loading design had a slightly higher mass loading capacity with an *in vivo* emitted dose of 15% that resulted in 0.9 mg of powder sprayed, but this was still too low to achieve sufficient viral potency for an observable bioactive response. Fortunately, the pipette tip-loading design provided a much higher emitted dose *in vivo*, allowing for sufficient viral dose delivery and assessment of adenovirus bioactivity. With a low retention pipette tip made of polypropylene, the surface coating likely increased the hydrophobicity of the interior surface, creating a water-repellent effect that helped to limit powder adhesion and encourage particle flow. When using a pipette tip-loading strategy, Qiu et al. have similarly reported strong device performance and indicated that there was negligible moisture absorption at the delivery site in the oropharynx with this method [84].

**Table 5.1.** Emitted dose determined after in vivo administration of 3 intratracheal dosator designs differing by needle tip material, loading method and optimal loaded mass.

| **Device Type** | **Needle Tip Material** | **Optimal Mass Loaded (mg)** | **Emitted Dose *In Vivo* (%)** |
|---|---|---|---|
| Tamp Loading | Stainless Steel | $2 \pm 1$ | 0 % |
| Chamber Loading | Stainless Steel | $6 \pm 1$ | $15 \pm 3$ % |
| Pipette Tip Loading | Polypropylene (with low retention coating) | $5 \pm 1$ | $50 \pm 4$ % |

Using the pipette tip-loading dosator, bioactivity of the spray dried AdHu5-Luc vector was assessed *in vivo* along with an uninfected negative control and spray dried placebo excipient blend as well as reconstituted powder delivered as a liquid (Figure 5.5). In this experiment, two powder doses were delivered to achieve a total viral dosage of $2 \times 10^6 PFU$, ensuring a strong and repeatable luciferase signal could be easily quantified. Compared to the uninfected and placebo powder controls, mice that received either reconstituted spray dried powder or spray dried powder via the pipette tip-loading dosator both showed very strong luciferase expression. This indicated that the adenoviral vector was highly bioactive within the targeted lung tissue and it is the first report, to the best of our knowledge, which demonstrates that a thermally stable, spray dried AdHu5 vector can be effectively delivered intratracheally in mice to yield a strong bioactive response. As a liquid, the reconstituted powder was also highly bioactive, indicating that the excipient formulation can successfully protect the adenovirus during spray drying at sufficient viral potency for observable infection. Previous reports have shown that for reconstituted liquid and dry powder intratracheal delivery of spray dried siRNA and mRNA, luciferase luminescence in the lungs is often higher with reconstituted liquid delivery due to the challenges of insufflation in mice [84,85]. Here we see that bioactivity was equivalently high after powder insufflation of our spray dried powder, further suggesting that there is strong powder dissolution within the distal lung to permit localized adenovirus infection and high luciferase expression. However, achieving dosage consistency between animals is still quite challenging with the pipette tip-loading dosator, leading to high variability in luciferase signals measured after dry powder delivery.

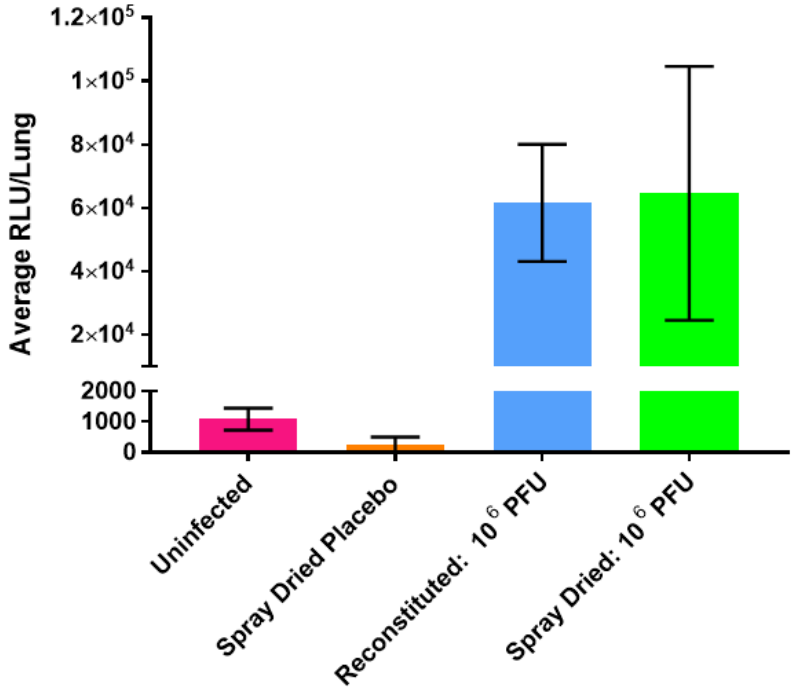


**Figure 5. 5.** Average relative luciferase units (RLU) activity measured in mouse lung tissue 3 days post-infection. All treatments were delivered intratracheally including: placebo spray dried powder, reconstituted spray dried Ad5E1 CMV Luc powder at $10^6$ PFU and spray dried Ad5E1 CMV Luc powder at $10^6$ PFU. Untreated mice are referred to as uninfected and serve as the negative control. Error bars represent the standard error between three animals (n=3).

## 5.4 Conclusion

Selecting an intratracheal dosator for delivery of powder biopharmaceutics requires careful consideration of the needle tip material and powder loading method, especially for compressible vaccine powders with a high capacity for moisture absorption. Although the small scale of powder delivery to mice can be limiting, we have shown that syringe air volume and loaded mass have a significant influence on device performance and should therefore be optimized when developing a custom-made dosator. Overall, static charge and ambient moisture both have a negative impact on device performance and the resulting powder dosage delivered. It is suggested that after loading

a dosator with moisture-sensitive powder, the loaded assembly should be immediately stored on dry ice prior to *in vivo* administration. For highly compressible dry powders, dosators that use a pipette tip-loading method, rather than a chamber-loading or tamp-loading strategy, tend to minimize powder agglomeration or solidification to achieve sufficient emitted dose for distal lung delivery. Using the pipette tip-loading method, we have demonstrated for the first time that a thermally stable, spray dried adenoviral dry powder can be delivered intratracheally in mice to yield a very strong bioactive response in the targeted lung tissue. Based on this work, we highlight the unique challenges faced during murine pulmonary delivery and offer guidance on successful strategies that can improve intratracheal dosator performance when delivering compressible dry powder pharmaceutics.

## Chapter 6: Concluding Remarks and Future Recommendations

The work presented in this thesis provides new insights and strategies that can be used to formulate a thermally stable dry powder vaccine more effectively for pulmonary delivery. With the goal of lowering the costs associated with the global vaccine supply chain, this work demonstrates that alternative manufacturing strategies like spray drying can effectively be used to stabilize labile adenoviral vectors to maintain biologic function. The research objectives outlined in Chapter 1 were achieved as follows:

1. **Analyze the impacts of cryoprotective agents on AdHu5 stabilization.**

Chapter 3 investigated the impact that cryoprotective agents like glycerol and trehalose can have when included in small amounts within a spray dried mannitol-dextran matrix. It was found that at high viral loading, viral stock suspensions containing 10% glycerol resulted in a spray dried powder with viral titre log loss of 2.8, with increased particle cohesion and poor yields, compared to 0.7 log loss using neat PBS for the viral stock suspension. Since a cryoprotective agent is necessary to ensure freeze-thaw stability of the stock vector, trehalose is a suitable alternative to glycerol and led to an improved viral log loss of 1.5 at high viral loading that would be suitable for generating an *in vivo* response.

2. **Determine the role of mass ratio and molecular weight of excipients in spray dried encapsulation of AdHu5**

Based on the results presented in Chapter 3 using a high loading of 5% trehalose AdHu5 stock suspension, Chapter 4 further improved the excipient formulation through the investigation of dextran mass ratio and molecular weight. Using a 1:3 mannitol to 500 kDa dextran ratio, processing losses related to spray drying were less than 0.5 log loss of viral titre. This formulation also had a low mass median aerodynamic diameter of 4.4 μm and could be efficiently sprayed from an intratracheal dosator device with an available dose of 84% to indicate the overall suitability of this formulation for inhalable vaccine delivery.

### 3. Evaluate dosator devices for intratracheal delivery of AdHu5 dry powder in mice

Chapter 5 investigated the design and operational factors of custom-made intratracheal devices which varied based on powder loading method and needle tip material. The best performing dry powder formulation presented in Chapter 4, with mannitol in a 1:3 ratio to 500 kDa dextran, was then validated *in vivo* using the pipette tip-loading dosator design. Compared to the liquid delivery of reconstituted powder, the AdHu5 dry powder delivery led to equivalent luciferase luminescence observed in lung tissue 3 days after dose administration to indicate high bioactivity of the AdHu5 spray dried formulation.

Overall, the findings presented in this thesis can be used to develop spray dried formulation strategies to thermally stabilize labile vectors more efficiently and at higher potency. This work also offers a suitable spray dried formulation for AdHu5-vectored vaccines that is both thermally stable and inhalable. In addition, the unique challenges faced at the preclinical testing phase of inhalable dry powder pharmaceutics are highlighted, while providing strategic guidance to deliver compressible dry powders to mice more effectively. Due to the scalable nature of spray drying, the lab-scale dry powder production that is presented in this work is also expected to be applicable for industrial scale manufacturing.

Within this presented work, the AdHu5 adenoviral vectors only expressed GFP and luciferase as biomarkers to indicate targeted cell infection and viral bioactivity. Future *in vivo* testing of the localized and systemic immunogenic response should also be conducted with the adenovirus expressing the intended tuberculosis antigen for true assessment of vaccine efficiency upon pulmonary delivery. To better understand where the powder is deposited after intratracheal delivery, fluorescent or luminescent imaging could also be used to anatomically map the location

of adenoviral expression. However, the low sensitivity of this strategy may be limiting and would require a higher delivered powder dosage or adenovirus stock solution of higher concentration to fully visualized the location of gene expression. Although the use of *in vivo* mouse models may provide important initial screening results for bioactivity and immunologic response, powder deposition and aerosolization behaviour may differ from the behaviour observed in human recipients. Primate models may provide a more representative indication pf aerosol behaviour to more accurately assess inhalable vaccine delivery prior to testing in humans.

Our spray dried adenoviral formulation and pulmonary delivery system may also hold promise for other encoded antigens against globally prominent respiratory diseases, such as COVID-19, to help prevent future pandemics. In terms of future development as an inhalable pharmaceutic, incorporating a flow aid material or carrier like lactose may also be beneficial to improve dosator or inhaler performance. Inhaler performance should also be more rigorously analyzed, particularly with the use of a blister-pack or foil to protect the powder from moisture absorption. Scaled-up manufacturing of this inhalable vaccine formulation should also consider the challenges of achieving 500 kDa dextran dissolution and the refrigeration required to dissolve this polymer prior to spray drying. Furthermore, studies may be required to assess the long-term stability of this formulation with the goal of achieving a 5-year shelf-life to satisfy the needs of the pharmaceutical industry.

## References


[1] J. Ehreth, "The value of vaccination: A global perspective," *Vaccine*, vol. 21, no. 27–30, pp. 4105–4117, 2003, doi: 10.1016/S0264-410X(03)00377-3.

[2] A. Galazka, J. B. Milstien, and M. Zaffran, "Thermostability of vaccines," 1998. doi: 10.1017/S0266462300014100.

[3] A. Fanelli, L. Mantegazza, S. Hendrickx, and I. Capua, "Thermostable Vaccines in Veterinary Medicine: State of the Art and Opportunities to Be Seized," *Vaccines*, vol. 10, no. 2, pp. 1–41, 2022, doi: 10.3390/vaccines10020245.

[4] M. M. V. X. van den Ent *et al.*, "Equity and immunization supply chain in Madagascar," *Vaccine*, vol. 35, no. 17, pp. 2148–2154, 2017, doi: 10.1016/j.vaccine.2016.11.099.

[5] A. Ashok, M. Brison, and Y. LeTallec, "Improving cold chain systems: Challenges and solutions," *Vaccine*, vol. 35, pp. 2217–2223, 2017, doi: 10.1016/j.vaccine.2016.08.045.

[6] T. Comes, K. Bergtora Sandvik, and B. Van de Walle, "Cold chains, interrupted: The use of technology and information for decisions that keep humanitarian vaccines cool," *J. Humanit. Logist. Supply Chain Manag.*, vol. 8, no. 1, pp. 49–69, 2018, doi: 10.1108/JHLSCM-03-2017-0006.

[7] F. Smaill *et al.*, "A human type 5 adenovirus-based tuberculosis vaccine induces robust T cell responses in humans despite preexisting anti-adenovirus immunity," *Sci. Transl. Med.*, vol. 5, no. 205, 2013, doi: 10.1126/scitranslmed.3006843.

[8] M. Jeyanathan, S. Afkhami, F. Smaill, M. S. Miller, B. D. Lichty, and Z. Xing, "Immunological considerations for COVID-19 vaccine strategies," *Nat. Rev. Immunol.*, vol. 20, no. 10, pp. 615–632, 2020, doi: 10.1038/s41577-020-00434-6.

[9] World Health Organization, "Global Tuberculosis Report," Geneva, 2020.

[10] D. A. Leclair, E. D. Cranston, Z. Xing, and M. R. Thompson, "Evaluation of excipients for enhanced thermal stabilization of a human type 5 adenoviral vector through spray drying," *Int. J. Pharm.*, vol. 506, pp. 289–301, 2016, doi: 10.1016/j.ijpharm.2016.04.067.

[11] J. Broadhead, S. K. Edmond Rouan, and C. T. Rhodes, "The spray drying of pharmaceuticals," *Drug Dev. Ind. Pharm.*, vol. 18, no. 11–12, pp. 1169–1206, 1992, doi: 10.3109/03639049209046327.

[12] S. Honmane, A. Hajare, H. More, R. A. M. Osmani, and S. Salunkhe, "Lung delivery of nanoliposomal salbutamol sulfate dry powder inhalation for facilitated asthma therapy," *J. Liposome Res.*, vol. 29, no. 4, pp. 332–342, 2019, doi: 10.1080/08982104.2018.1531022.

[13] T. Okuda, D. Kito, A. Oiwa, M. Fukushima, D. Hira, and H. Okamoto, "Gene silencing in a mouse lung metastasis model by an inhalable dry small interfering RNA powder prepared using the supercritical carbon dioxide technique," *Biol. Pharm. Bull.*, vol. 36, no. 7, pp. 1183–1191, 2013, doi: 10.1248/bpb.b13-00167.

[14] E. Quarta *et al.*, "Excipient-free pulmonary insulin dry powder: Pharmacokinetic and

pharmacodynamics profiles in rats," *J. Control. Release*, vol. 323, no. February, pp. 412–420, 2020, doi: 10.1016/j.jconrel.2020.04.015.

[15] J. H. Crowe, L. M. Crowe, J. F. Carpenter, and C. Aurell Wistrom, "Stabilization of dry phospholipid bilayers and proteins by sugars.," *Biochem. J.*, vol. 242, no. 1, pp. 1–10, 1987, doi: 10.1042/bj2420001.

[16] K. L. Emmer and H. C. J. Ertl, "Chapter 24: Recombinant adenovirus vectors as mucosal vaccines," in *Mucosal Vaccines: Innovation for Preventing Infectious Diseases*, Elsevier Inc., 2019, pp. 419–444.

[17] D. L. Bolton *et al.*, "Comparison of systemic and mucosal vaccination: Impact on intravenous and rectal SIV challenge," *Mucosal Immunol.*, vol. 5, no. 1, pp. 41–52, 2012, doi: 10.1038/mi.2011.45.

[18] S. Afkhami *et al.*, "Respiratory mucosal delivery of next-generation COVID-19 vaccine provides robust protection against both ancestral and variant strains of SARS-CoV-2," *Cell*, vol. 185, no. 5, pp. 896-915.e19, 2022, doi: 10.1016/j.cell.2022.02.005.

[19] J. Wang *et al.*, "Single Mucosal, but Not Parenteral, Immunization with Recombinant Adenoviral-Based Vaccine Provides Potent Protection from Pulmonary Tuberculosis," *J. Immunol.*, vol. 173, no. 10, pp. 6357–6365, 2004, doi: 10.4049/jimmunol.173.10.6357.

[20] G. Alkhatib and D. J. Briedis, "High-level eucaryotic in vivo expression of biologically active measles virus hemagglutinin by using an adenovirus type 5 helper-free vector system," *J. Virol.*, vol. 62, no. 8, pp. 2718–2727, 1988, doi: 10.1128/jvi.62.8.2718-2727.1988.

[21] R. W. Horne, S. Brenner, A. P. Waterson, and P. Wildy, "The icosahedral form of an adenovirus," *J. Mol. Biol.*, vol. 1, no. 1, pp. 84–86, 1959, doi: 10.1016/S0022-2836(59)80011-5.

[22] V. S. Reddy and G. R. Nemerow, "Structures and organization of adenovirus cement proteins provide insights into the role of capsid maturation in virus entry and infection," *Proc. Natl. Acad. Sci. U. S. A.*, vol. 111, no. 32, pp. 11715–11720, 2014, doi: 10.1073/pnas.1408462111.

[23] J. Gallardo, M. Pérez-Illana, N. Martín-González, and C. S. Martín, "Adenovirus structure: What is new?," *Int. J. Mol. Sci.*, vol. 22, no. 10, pp. 1–16, 2021, doi: 10.3390/ijms22105240.

[24] C. S. Lee *et al.*, "Adenovirus-mediated gene delivery: Potential applications for gene and cell-based therapies in the new era of personalized medicine," *Genes Dis.*, vol. 4, no. 2, pp. 43–63, 2017, doi: 10.1016/j.gendis.2017.04.001.

[25] C. Y. Teng, J. B. Millar, N. Grinshtein, J. Bassett, J. Finn, and J. L. Bramson, "T-cell immunity generated by recombinant adenovirus vaccines," *Expert Rev. Vaccines*, vol. 6, no. 3, pp. 347–356, 2007, doi: 10.1586/14760584.6.3.347.

[26] O. K. Yarosh, A. I. Wandeler, F. L. Graham, J. B. Campbell, and L. Prevec, "Human adenovirus type 5 vectors expressing rabies glycoprotein," *Vaccine*, vol. 14, no. 13. pp. 1257–1264, 1996, doi: 10.1016/S0264-410X(96)00012-6.

[27] J. E. Ledgerwood *et al.*, “Chimpanzee Adenovirus Vector Ebola Vaccine,” *N. Engl. J. Med.*, vol. 376, no. 10, pp. 928–938, 2017, doi: 10.1056/nejmoa1410863.

[28] A. Berg *et al.*, “Stability of chimpanzee adenovirus vectored vaccines (Chadox1 and chadox2) in liquid and lyophilised formulations,” *Vaccines*, vol. 9, no. 11, pp. 1–12, 2021, doi: 10.3390/vaccines9111249.

[29] S. Afkhami *et al.*, “Spray dried human and chimpanzee adenoviral-vectored vaccines are thermally stable and immunogenic in vivo,” *Vaccine*, vol. 35, no. 22, pp. 2916–2924, 2017, doi: 10.1016/j.vaccine.2017.04.026.

[30] J. A. Malik, A. H. Mulla, T. Farooqi, F. H. Pottoo, S. Anwar, and K. R. R. Rengasamy, “Targets and strategies for vaccine development against SARS-CoV-2,” *Biomed. Pharmacother.*, vol. 137, p. 111254, 2021, doi: 10.1016/j.biopha.2021.111254.

[31] H. G. Pereira, R. C. Valentine, and W. C. Russel, “The Effect of Heat on the Anatomy of the Adenovirus,” *J. gen.Virol.*, vol. 1, pp. 509–522, 1967.

[32] F. Galdiero, “Archives of Virology Adenovirus Aggregation and Preservation in Extracellular Environment,” *Arch. Virol.*, vol. 59, pp. 99–105, 1979.

[33] J. Rexroad, C. M. Wiethoff, A. P. Green, T. D. Kierstead, M. O. Scott, and C. R. Middaugh, “Structural stability of adenovirus type 5,” *J. Pharm. Sci.*, vol. 92, no. 3, pp. 665–678, 2003, doi: 10.1002/jps.10340.

[34] C. Nyberg-Hoffman and E. Aguilar-Cordova, “Instability of adenoviral vectors during transport and its implication for clinical studies,” *Nat. Med.*, vol. 5, no. 8, pp. 955–957, 1999, doi: 10.1038/11400.

[35] H. Ugai, S. Watanabe, E. Suzuki, H. Tsutsui-Nakata, K. K. Yokoyama, and T. Murata, “Stability of a recombinant adenoviral vector: Optimization of conditions for storage, transport and delivery,” *Japanese J. Cancer Res.*, vol. 93, no. 5, pp. 598–603, 2002, doi: 10.1111/j.1349-7006.2002.tb01296.x.

[36] K. Gekko and S. N. Timasheff, “Mechanism of Protein Stabilization by Glycerol: Preferential Hydration in Glycerol-Water Mixtures,” *Biochemistry*, vol. 20, no. 16, pp. 4667–4676, 1981, doi: 10.1021/bi00519a023.

[37] Z. Hubálek, “Protectants used in the cryopreservation of microorganisms,” *Cryobiology*, vol. 46, pp. 205–229, 2003, doi: 10.1016/S0011-2240(03)00046-4.

[38] S. S. Renteria, C. C. Clemens, and M. A. Croyle, “Development of a nasal adenovirus-based vaccine: Effect of concentration and formulation on adenovirus stability and infectious titer during actuation from two delivery devices,” *Vaccine*, vol. 28, no. 9, pp. 2137–2148, 2010, doi: 10.1016/j.vaccine.2009.12.025.

[39] R. K. Evans *et al.*, “Development of stable liquid formulations for adenovirus-based vaccines,” *J. Pharm. Sci.*, vol. 93, no. 10, pp. 2458–2475, 2004, doi: 10.1002/jps.20157.

[40] L. Yu, “Amorphous pharmaceutical solids: Preparation, characterization and stabilization,” *Adv. Drug Deliv. Rev.*, vol. 48, no. 1, pp. 27–42, 2001, doi: 10.1016/S0169-409X(01)00098-9.

[41] A. Newman and G. Zografi, “Commentary: Considerations in the Measurement of Glass Transition Temperatures of Pharmaceutical Amorphous Solids,” *AAPS PharmSciTech*, vol. 21, no. 1, pp. 1–13, 2020, doi: 10.1208/s12249-019-1562-1.

[42] B. C. Hancock and S. L. Shamblin, “Water vapour sorption by pharmaceutical sugars,” *Pharm. Sci. Technol. Today*, vol. 1, no. 8, pp. 345–351, 1998, doi: 10.1016/S1461-5347(98)00088-1.

[43] K. E. Uhrich, Y. Zhang, J. W. Chan, and A. Moretti, “Designing polymers with sugar-based advantages for bioactive delivery applications,” *J Control Release*, vol. 10, no. 219, pp. 355–368, 2015, doi: 10.1016/j.jconrel.2015.09.053.Designing.

[44] C. Schebor, M. F. Mazzobre, and M. del P. Buera, “Glass transition and time-dependent crystallization behavior of dehydration bioprotectant sugars,” *Carbohydr. Res.*, vol. 345, no. 2, pp. 303–308, 2010, doi: 10.1016/j.carres.2009.10.014.

[45] J. Gupta, C. Nunes, and S. Jonnalagadda, “A molecular dynamics approach for predicting the glass transition temperature and plasticization effect in amorphous pharmaceuticals,” *Mol. Pharm.*, vol. 10, no. 11, pp. 4136–4145, 2013, doi: 10.1021/mp400118v.

[46] N. Schafroth and M. Meuri, “Laboratory scale spray-drying of lactose: A review,” *Ind. Pharm.*, no. 36, pp. 4–8, 2012.

[47] R. W. Hartel, R. Ergun, and S. Vogel, “Phase/State Transitions of Confectionery Sweeteners: Thermodynamic and Kinetic Aspects,” *Compr. Rev. Food Sci. Food Saf.*, vol. 10, pp. 17–32, 2011, doi: 10.1111/j.1541-4337.2010.00136.x.

[48] A. Lechanteur and B. Evrard, “Influence of composition and spray-drying process parameters on carrier-free DPI properties and behaviors in the lung: A review,” *Pharmaceutics*, vol. 12, no. 1, 2020, doi: 10.3390/pharmaceutics12010055.

[49] B. S. Larsen, J. Skytte, A. J. Svagan, H. Meng-Lund, H. Grohganz, and K. Löbmann, “Using dextran of different molecular weights to achieve faster freeze-drying and improved storage stability of lactate dehydrogenase,” *Pharm. Dev. Technol.*, vol. 24, no. 3, pp. 323–328, 2019, doi: 10.1080/10837450.2018.1479866.

[50] N. Carrigy and R. Vehring, “Engineering Stable Spray Dried Biologic Powder for Inhalation,” in *Pharmaceutical Inhalation Aerosol Technology*, 3rd ed., CRC Press, Taylor & Francis Group, 2019, p. 36.

[51] M. Gomez *et al.*, “Development and Testing of a Spray-Dried Tuberculosis Vaccine Candidate in a Mouse Model,” *Front. Pharmacol.*, vol. 12, no. January, pp. 1–23, 2022, doi: 10.3389/fphar.2021.799034.

[52] D. Coucke *et al.*, “Spray-dried powders of starch and crosslinked poly(acrylic acid) as carriers for nasal delivery of inactivated influenza vaccine,” *Vaccine*, vol. 27, no. 8, pp. 1279–1286, 2009, doi: 10.1016/j.vaccine.2008.12.013.

[53] D. A. Leclair, E. D. Cranston, B. D. Lichty, Z. Xing, and M. R. Thompson, “Consecutive Spray Drying to Produce Coated Dry Powder Vaccines Suitable for Oral Administration,” *ACS Biomater. Sci. Eng.*, vol. 4, no. 5, pp. 1669–1678, 2018, doi: 10.1021/acsbiomaterials.8b00117.

[54] M. P. M. Vierboom *et al.*, “Stronger induction of trained immunity by mucosal BCG or MTBVAC vaccination compared to standard intradermal vaccination,” *Cell Reports Med.*, vol. 2, no. 1, 2021, doi: 10.1016/j.xcrm.2020.100185.

[55] X. Tang and M. J. Pikal, “Design of Freeze-Drying Processes for Pharmaceuticals: Practical Advice,” *Pharm. Res.*, vol. 21, no. 2, pp. 191–200, 2004, doi: 10.1023/B:PHAM.0000016234.73023.75.

[56] J. C. Kasper and W. Friess, “The freezing step in lyophilization: Physico-chemical fundamentals, freezing methods and consequences on process performance and quality attributes of biopharmaceuticals,” *Eur. J. Pharm. Biopharm.*, vol. 78, no. 2, pp. 248–263, 2011, doi: 10.1016/j.ejpb.2011.03.010.

[57] F. Geeraedts *et al.*, “Preservation of the immunogenicity of dry-powder influenza H5N1 whole inactivated virus vaccine at elevated storage temperatures,” *AAPS J.*, vol. 12, no. 2, pp. 215–222, 2010, doi: 10.1208/s12248-010-9179-z.

[58] D. Xiao and Q. Zhong, “In vitro release kinetics of nisin as affected by Tween 20 and glycerol co-encapsulated in spray-dried zein capsules,” *J. Food Eng.*, vol. 106, pp. 65–73, 2011, doi: 10.1016/j.jfoodeng.2011.04.009.

[59] R. Murugesan and V. Orsat, “Spray Drying for the Production of Nutraceutical Ingredients-A Review,” *Food Bioprocess Technol.*, vol. 5, no. 1, pp. 3–14, 2012, doi: 10.1007/s11947-011-0638-z.

[60] V. Nekkanti, T. Muniyappan, P. Karatgi, M. S. Hari, S. Marella, and R. Pillai, “Spray-drying process optimization for manufacture of drug-cyclodextrin complex powder using design of experiments,” *Drug Dev. Ind. Pharm.*, vol. 35, no. 10, pp. 1219–1229, 2009, doi: 10.1080/03639040902882264.

[61] R. Vehring, “Pharmaceutical particle engineering via spray drying,” *Pharm. Res.*, vol. 25, no. 5, pp. 999–1022, 2008, doi: 10.1007/s11095-007-9475-1.

[62] V. Saluja, J. P. Amorij, J. C. Kapteyn, A. H. de Boer, H. W. Frijlink, and W. L. J. Hinrichs, “A comparison between spray drying and spray freeze drying to produce an influenza subunit vaccine powder for inhalation,” *J. Control. Release*, vol. 144, no. 2, pp. 127–133, 2010, doi: 10.1016/j.jconrel.2010.02.025.

[63] S. Ohtake *et al.*, “Heat-stable measles vaccine produced by spray drying,” *Vaccine*, vol. 28, pp. 1275–1284, 2010, doi: 10.1016/j.vaccine.2009.11.024.

[64] S. Saboo *et al.*, “Optimized Formulation of a Thermostable Spray-Dried Virus-Like Particle Vaccine against Human Papillomavirus,” *Mol. Pharm.*, vol. 13, no. 5, pp. 1646–1655, 2016, doi: 10.1021/acs.molpharmaceut.6b00072.

[65] D. A. LeClair, E. D. Cranston, Z. Xing, and M. R. Thompson, “Optimization of Spray Drying Conditions for Yield, Particle Size and Biological Activity of Thermally Stable Viral Vectors,” *Pharm. Res.*, vol. 33, pp. 2763–2776, 2016, doi: 10.1007/s11095-016-2003-4.

[66] J. Liu *et al.*, “Solid lipid nanoparticles for pulmonary delivery of insulin,” *Int. J. Pharm.*, vol. 356, no. 1–2, pp. 333–344, 2008, doi: 10.1016/j.ijpharm.2008.01.008.

[67] K. Miwata *et al.*, "Intratracheal Administration of siRNA Dry Powder Targeting Vascular Endothelial Growth Factor Inhibits Lung Tumor Growth in Mice," *Mol. Ther. - Nucleic Acids*, vol. 12, no. September, pp. 698–706, 2018, doi: 10.1016/j.omtn.2018.07.009.

[68] J. Kaur *et al.*, "A hand-held apparatus for 'nose-only' exposure of mice to inhalable microparticles as a dry powder inhalation targeting lung and airway macrophages," *Eur. J. Pharm. Sci.*, vol. 34, no. 1, pp. 56–65, 2008, doi: 10.1016/j.ejps.2008.02.008.

[69] B. Chaurasiya and Y. Y. Zhao, "Dry powder for pulmonary delivery: A comprehensive review," *Pharmaceutics*, vol. 13, no. 1, pp. 1–28, 2021, doi: 10.3390/pharmaceutics13010031.

[70] J. L. Rau, "The inhalation of drugs: Advantages and problems," *Respir. Care*, vol. 50, no. 3, pp. 367–382, 2005.

[71] A. J. Hickey, P. G. Durham, A. Dharmadhikari, and E. A. Nardell, "Inhaled drug treatment for tuberculosis: Past progress and future prospects," *J. Control. Release*, vol. 240, pp. 127–134, 2016, doi: 10.1016/j.jconrel.2015.11.018.

[72] P. J. Kuehl *et al.*, "Regional particle size dependent deposition of inhaled aerosols in rats and mice," *Inhal. Toxicol.*, vol. 24, no. 1, pp. 27–35, 2012, doi: 10.3109/08958378.2011.632787.

[73] C. Duret *et al.*, "In vitro and in vivo evaluation of a dry powder endotracheal insufflator device for use in dose-dependent preclinical studies in mice," *Eur. J. Pharm. Biopharm.*, vol. 81, no. 3, pp. 627–634, 2012, doi: 10.1016/j.ejpb.2012.04.004.

[74] M. Hänsel, T. Bambach, and H. Wachtel, "Reduced Environmental Impact of the Reusable Respimat® Soft Mist™ Inhaler Compared with Pressurised Metered-Dose Inhalers," *Adv. Ther.*, vol. 36, no. 9, pp. 2487–2492, 2019, doi: 10.1007/s12325-019-01028-y.

[75] N. A. Wiggins, "The development of a mathematical approximation technique to determine the mass median aerodynamic diameter (MMAD) and geometric standard deviation (GSD) of drug particles in an inhalation aerosol sprat," *Drug Dev. Ind. Pharm.*, vol. 17, no. 14, pp. 1971–1986, 1991, doi: 10.3109/03639049109048062.

[76] N. El-Gendy and C. Berkland, "Combination chemotherapeutic dry powder aerosols via controlled nanoparticle agglomeration," *Pharm. Res.*, vol. 26, no. 7, pp. 1752–1763, 2009, doi: 10.1007/s11095-009-9886-2.

[77] D. A. Edwards *et al.*, "Large porous particles for pulmonary drug delivery," *Science (80-. ).*, vol. 276, no. 5320, pp. 1868–1871, 1997, doi: 10.1126/science.276.5320.1868.

[78] Y. B. Wang, A. B. Watts, J. I. Peters, S. Liu, A. Batra, and R. O. Williams, "In vitro and in vivo performance of dry powder inhalation formulations: Comparison of particles prepared by thin film freezing and micronization," *AAPS PharmSciTech*, vol. 15, no. 4, pp. 981–993, 2014, doi: 10.1208/s12249-014-0126-7.

[79] S. J. Yang *et al.*, "Activation of M1 Macrophages in Response to Recombinant TB Vaccines With Enhanced Antimycobacterial Activity," *Front. Immunol.*, vol. 11, no. June, pp. 1–12, 2020, doi: 10.3389/fimmu.2020.01298.

[80] H. Golding, S. Khurana, and M. Zaitseva, “What is the predictive value of animal models for vaccine efficacy in humans? The importance of bridging studies and species-independent correlates of protection,” *Cold Spring Harb. Perspect. Biol.*, vol. 10, no. 4, pp. 1–8, 2018, doi: 10.1101/cshperspect.a028902.

[81] A. Armando *et al.*, “The importance of animal models in tuberculosis vaccine development,” *Malaysian J. Med. Sci.*, vol. 18, no. 5, pp. 5–12, 2011.

[82] A. S. Jiménez, K. S. Galea, and R. J. Aitken, “Guidance for collection of relevant particle size distribution data of workplace aerosols-Cascade Impactor Measurements,” 2011. [Online]. Available: http://www.nickelconsortia.eu/assets/files/library/Guidances/IOM Report 2-June 2011.pdf.

[83] J. Grimaud and V. N. Murthy, “How to monitor breathing in laboratory rodents: A review of the current methods,” *J. Neurophysiol.*, vol. 120, no. 2, pp. 624–632, 2018, doi: 10.1152/jn.00708.2017.

[84] Y. Qiu, Q. Liao, M. Y. T. Chow, and J. K. W. Lam, “Intratracheal administration of dry powder formulation in mice,” *J. Vis. Exp.*, vol. 2020, no. 161, pp. 1–12, 2020, doi: 10.3791/61469.

[85] Y. Qiu, R. C. H. Man, Q. Liao, K. L. K. Kung, M. Y. T. Chow, and J. K. W. Lam, “Effective mRNA pulmonary delivery by dry powder formulation of PEGylated synthetic KL4 peptide,” *J. Control. Release*, vol. 314, no. September, pp. 102–115, 2019, doi: 10.1016/j.jconrel.2019.10.026.

[86] D. Ihara *et al.*, “Histological Quantification of Gene Silencing by Intratracheal Administration of Dry Powdered Small-Interfering RNA/Chitosan Complexes in the Murine Lung,” *Pharm. Res.*, vol. 32, no. 12, pp. 3877–3885, 2015, doi: 10.1007/s11095-015-1747-6.

[87] P. G. Durham, S. N. Hanif, L. G. Contreras, E. F. Young, M. S. Braunstein, and A. J. Hickey, “Disposable dosators for pulmonary insufflation of therapeutic agents to small animals,” *J. Vis. Exp.*, vol. 2017, no. 121, pp. 4–9, 2017, doi: 10.3791/55356.

[88] I. E. Stewart *et al.*, “Development and Characterization of a Dry Powder Formulation for Anti-Tuberculosis Drug Spectinamide 1599,” *Pharm. Res.*, vol. 36, no. 9, 2019, doi: 10.1007/s11095-019-2666-8.

[89] P. Kroger, A Bahta, L Hunter, “General Best Practice Guidelines for Immunization: Best Practices Guidance of the Advisory Committee on Immunization Practices (ACIP). Contraindications and Precautions.,” *Centers Dis. Control Prev.*, pp. 146–169, 2020, [Online]. Available: www.cdc.gov/vaccines/hcp/acip-recs/general-recs/downloads/general-%0Ahttps://www.cdc.gov/vaccines/hcp/acip-recs/general-recs/downloads/general-recs.pdf%0Awww.cdc.gov/vaccines/hcp/acip-recs/general-recs/contraindications.pdf.

[90] H. A. Bogale, A. F. Amhare, and A. A. Bogale, “Assessment of factors affecting vaccine cold chain management practice in public health institutions in east Gojam zone of Amhara region,” *BMC Public Health*, vol. 19, no. 1, pp. 1–6, 2019, doi: 10.1186/s12889-019-7786-x.

[91] R. Alcock *et al.*, “Long-term thermostabilization of live poxviral and adenoviral vaccine vectors at supraphysiological temperatures in carbohydrate glass,” *Sci. Transl. Med.*, vol. 2, no. 19, pp. 1–9, 2010, doi: 10.1126/scitranslmed.3000490.

[92] K. Radošević *et al.*, “Protective immune responses to a recombinant adenovirus type 35 tuberculosis vaccine in two mouse strains: CD4 and CD8 T-cell epitope mapping and role of gamma interferon,” *Infect. Immun.*, vol. 75, no. 8, pp. 4105–4115, 2007, doi: 10.1128/IAI.00004-07.

[93] E. O. Ronan, L. N. Lee, P. C. L. Beverley, and E. Z. Tchilian, “Immunization of mice with a recombinant adenovirus vaccine inhibits the early growth of mycobacterium tuberculosis after infection,” *PLoS One*, vol. 4, no. 12, 2009, doi: 10.1371/journal.pone.0008235.

[94] M. Thompson, Z. Xing, D. LeClair, and E. Cranston, “PCT Patent Application WO 2017/035664,” 2017.

[95] S. P. Toniolo *et al.*, “Excipient selection for thermally stable enveloped and non-enveloped viral vaccine platforms in dry powders,” *Int. J. Pharm.*, vol. 561, pp. 66–73, 2019, doi: 10.1016/j.ijpharm.2019.02.035.

[96] T. H. Jin, E. Tsao, J. Goudsmit, V. Dheenadhayalan, and J. Sadoff, “Stabilizing formulations for inhalable powders of an adenovirus 35-vectored tuberculosis (TB) vaccine (AERAS-402),” *Vaccine*, vol. 28, no. 27, pp. 4369–4375, 2010, doi: 10.1016/j.vaccine.2010.04.059.

[97] A. S. Tyne *et al.*, “TLR2-targeted secreted proteins from Mycobacterium tuberculosis are protective as powdered pulmonary vaccines,” *Vaccine*, vol. 31, no. 40, pp. 4322–4329, 2013, doi: 10.1016/j.vaccine.2013.07.022.

[98] B. A. Morgan, Z. Xing, E. D. Cranston, and M. R. Thompson, “Acoustic levitation as a screening method for excipient selection in the development of dry powder vaccines,” *Int. J. Pharm.*, vol. 563, pp. 71–78, 2019, doi: 10.1016/j.ijpharm.2019.03.026.

[99] M. A. Croyle, D. J. Anderson, B. J. Roessler, and G. L. Amidon, “Development of a highly efficient purification process for recombinant adenoviral vectors for oral gene delivery,” *Pharm. Dev. Technol.*, vol. 3, no. 3, pp. 365–372, 1998, doi: 10.3109/10837459809009864.

[100] Y. Kanegae, M. Makimura, and I. Saito, “A simple and efficient method for purification of infectious recombinant adenovirus,” *Japanese J. Med. Sci. Biol.*, vol. 47, pp. 157–166, 1994, doi: 10.7883/yoken1952.47.157.

[101] N. E. Altaras, J. G. Aunins, R. K. Evans, A. Kamen, J. O. Konz, and J. J. Wolf, “Production and formulation of adenovirus vectors,” *Adv. Biochem. Eng. Biotechnol.*, vol. 99, pp. 193–260, 2005, doi: 10.1007/10_008.

[102] C. Sene, “PCT Patent Application WO1998/002522,” 1998.

[103] M. Pelliccia *et al.*, “Additives for vaccine storage to improve thermal stability of adenoviruses from hours to months,” *Nat. Commun.*, vol. 7, pp. 1–7, 2016, doi: 10.1038/ncomms13520.

[104] M. A. Croyle, X. Cheng, and J. M. Wilson, “Development of formulations that enhance physical stability of viral vectors for gene therapy,” *Gene Ther.*, vol. 8, no. 17, pp. 1281–1290, 2001, doi: 10.1038/sj.gt.3301527.

[105] B. A. Morgan, M. Manser, M. Jeyanathan, Z. Xing, E. D. Cranston, and M. R. Thompson, “Effect of Shear Stresses on Adenovirus Activity and Aggregation during Atomization To Produce Thermally Stable Vaccines by Spray Drying,” *ACS Biomater. Sci. Eng.*, vol. 6, no. 7, pp. 4304–4313, 2020, doi: 10.1021/acsbiomaterials.0c00317.

[106] L. S. C. Wan, P. W. S. Heng, and C. G. H. Chia, “Plasticizers and their effects on microencapsulation process by spray-drying in an aqueous system,” *J. Microencapsul.*, vol. 9, no. 1, pp. 53–62, 1992, doi: 10.3109/02652049209021222.

[107] K. B. Preston and T. W. Randolph, “Stability of lyophilized and spray dried vaccine formulations,” *Adv. Drug Deliv. Rev.*, vol. 171, pp. 50–61, 2021, doi: 10.1016/j.addr.2021.01.016.

[108] C. Darquenne, “Aerosol deposition in health and disease,” *J. Aerosol Med. Pulm. Drug Deliv.*, vol. 25, no. 3, pp. 140–147, 2012, doi: 10.1089/jamp.2011.0916.

[109] P. Chen, L. Zhang, and F. Cao, “Effects of moisture on glass transition and microstructure of glycerol-plasticized soy protein,” *Macromol. Biosci.*, vol. 5, pp. 872–880, 2005, doi: 10.1002/mabi.200500072.

[110] K. D. Foster, J. E. Bronlund, and A. H. J. (Tony. Paterson, “Glass transition related cohesion of amorphous sugar powders,” *J. Food Eng.*, vol. 77, no. 4, pp. 997–1006, 2006, doi: 10.1016/j.jfoodeng.2005.08.028.

[111] D. J. O’Callaghan and S. A. Hogan, “The physical nature of stickiness in the spray drying of dairy products - A review,” *Dairy Sci. Technol.*, vol. 93, no. 4–5, pp. 331–346, 2013, doi: 10.1007/s13594-013-0114-9.

[112] L. Maggi, R. Bruni, and U. Conte, “Influence of the moisture on the performance of a new dry powder inhaler,” *Int. J. Pharm.*, vol. 177, pp. 83–91, 1999, doi: 10.1016/S0378-5173(98)00326-3.

[113] S. Ohtake *et al.*, “Heat-stable measles vaccine produced by spray drying,” *Vaccine*, vol. 28, no. 5, pp. 1275–1284, 2010, doi: 10.1016/j.vaccine.2009.11.024.

[114] S. P. Toniolo *et al.*, “Spray dried VSV-vectored vaccine is thermally stable and immunologically active in vivo,” *Sci. Rep.*, vol. 10, pp. 1–8, 2020, doi: 10.1038/s41598-020-70325-2.

[115] M. M. Manser, X. Feng, Z. Xing, E. D. Cranston, and M. R. Thompson, “Cryoprotective agents influence viral dosage and thermal stability of inhalable dry powder vaccines,” *Int. J. Pharm.*, vol. 617, no. December 2021, p. 121602, 2022, doi: 10.1016/j.ijpharm.2022.121602.

[116] B. A. Morgan, E. Niinivaara, Z. Xing, M. R. Thompson, and E. D. Cranston, “Validation of a diffusion-based single droplet drying model for encapsulation of a viral-vectored vaccine using an acoustic levitator,” *Int. J. Pharm.*, vol. 605, no. June, p. 120806, 2021, doi: 10.1016/j.ijpharm.2021.120806.

[117] H. H. Y. Tong, S. Y. S. Wong, M. W. L. Law, K. K. W. Chu, and A. H. L. Chow, "Anti-hygroscopic effect of dextrans in herbal formulations," *Int. J. Pharm.*, vol. 363, no. 1–2, pp. 99–105, 2008, doi: 10.1016/j.ijpharm.2008.07.016.

[118] F. Kawaizumi, N. Nishio, H. Nomura, and Y. Miyahara, "Calorimetric and compressibility study of aqueous solutions of dextran with special reference to hydration and structural change of water," *Polym. J.*, vol. 13, no. 3, pp. 209–213, 1981, doi: 10.1295/polymj.13.209.

[119] M. Odziomek, T. R. Sosnowski, and L. Gradoń, "Conception, preparation and properties of functional carrier particles for pulmonary drug delivery," *Int. J. Pharm.*, vol. 433, no. 1–2, pp. 51–59, 2012, doi: 10.1016/j.ijpharm.2012.04.067.

[120] J. G. Weers, T. E. Tarara, and A. R. Clark, "Design of fine particles for pulmonary drug delivery," *Expert Opin. Drug Deliv.*, vol. 4, no. 3, pp. 297–313, 2007, doi: 10.1517/17425247.4.3.297.

[121] World Health Organization, "Bulk density and tapped density of powders," in *The International Pharmacopoeia, Tenth Edition*, Geneva, 2020.

[122] H. Hughes, M. M. Leane, M. Tobyn, J. F. Gamble, S. Munoz, and P. Musembi, "Development of a Material Sparing Bulk Density Test Comparable to a Standard USP Method for Use in Early Development of API's," *AAPS PharmSciTech*, vol. 16, no. 1, pp. 165–170, 2014, doi: 10.1208/s12249-014-0215-7.

[123] L. Masaro and X. X. Zhu, *Physical models of diffusion for polymer solutions, gels and solids*, vol. 24, no. 5. 1999.

[124] A. Mazzarotta, T. M. Caputo, L. Raiola, E. Battista, P. A. Netti, and F. Causa, "Small oligonucleotides detection in three-dimensional polymer network of dna-peg hydrogels," *Gels*, vol. 7, no. 3, pp. 1–16, 2021, doi: 10.3390/gels7030090.

[125] G. Meerdink and K. van't Riet, "Modeling segregation of solute material during drying of liquid foods," *AIChE J.*, vol. 41, no. 3, pp. 732–736, 1995, doi: 10.1002/aic.690410331.

[126] K. Kadota *et al.*, "Development of porous particles using dextran as an excipient for enhanced deep lung delivery of rifampicin," *Int. J. Pharm.*, vol. 555, no. May 2018, pp. 280–290, 2019, doi: 10.1016/j.ijpharm.2018.11.055.

[127] E. Palomäki, P. Ahvenainen, H. Ehlers, K. Svedström, S. Huotari, and J. Yliruusi, "Monitoring the recrystallisation of amorphous xylitol using Raman spectroscopy and wide-angle X-ray scattering," *Int. J. Pharm.*, vol. 508, no. 1–2, pp. 71–82, 2016, doi: 10.1016/j.ijpharm.2016.04.074.

[128] L. Yu, D. S. Mishra, and D. R. Rigsbee, "Determination of the glass properties of D-mannitol using sorbitol as an impurity," *J. Pharm. Sci.*, vol. 87, no. 6, pp. 774–777, 1998, doi: 10.1021/js970224o.

[129] A. Prudic, Y. Ji, C. Luebbert, and G. Sadowski, "Influence of humidity on the phase behavior of API/polymer formulations," *Eur. J. Pharm. Biopharm.*, vol. 94, pp. 352–362, 2015, doi: 10.1016/j.ejpb.2015.06.009.

[130] M. E. Aulton, “Part 2: Particle Science and Powder Technology - Powder Flow,” in *Aulton’s Pharmaceutics: The Design and Manufacture of Medicines*, Fifth Edit., M. E. Aulton and K. M. G. Taylor, Eds. 2018, pp. 189–192.

[131] M. C. Sarraguça, A. V. Cruz, S. O. Soares, H. R. Amaral, P. C. Costa, and J. A. Lopes, “Determination of flow properties of pharmaceutical powders by near infrared spectroscopy,” *J. Pharm. Biomed. Anal.*, vol. 52, no. 4, pp. 484–492, 2010, doi: 10.1016/j.jpba.2010.01.038.

[132] C. Turchiuli *et al.*, “Oil encapsulation by spray drying and fluidised bed agglomeration,” *Innov. Food Sci. Emerg. Technol.*, vol. 6, no. 1, pp. 29–35, 2005, doi: 10.1016/j.ifset.2004.11.005.

[133] P. C. L. Kwok and H. K. Chan, “Effect of relative humidity on the electrostatic charge properties of dry powder inhaler aerosols,” *Pharm. Res.*, vol. 25, no. 2, pp. 277–288, 2008, doi: 10.1007/s11095-007-9377-2.

[134] M. M. Manser *et al.*, “Dextran mass ratio helps to control particle drying dynamics in a thermally stable dry powder vaccine for pulmonary delivery,” Submitted to: *Pharm. Res.*, Submission ID: PHAM-D-22-00378, 2022.

[135] K. Kishimoto and M. Morimoto, “Mammalian tracheal development and reconstruction: Insights from in vivo and in vitro studies,” *Dev.*, vol. 148, no. 13, 2021, doi: 10.1242/DEV.198192.

[136] C. G. Irvin and J. H. T. Bates, “Measuring the lung function in the mouse: The challenge of size,” *Respir. Res.*, vol. 4, pp. 1–9, 2003, doi: 10.1186/rr199.

[137] M. Jeyanathan *et al.*, “Novel chimpanzee adenovirus-vectored respiratory mucosal tuberculosis vaccine: Overcoming local anti-human adenovirus immunity for potent TB protection,” *Mucosal Immunol.*, vol. 8, no. 6, pp. 1373–1387, 2015, doi: 10.1038/mi.2015.29.

[138] V. Jeyanathan, M. Jeyanathan, and Z. Xing, Manuscript in Preparation, 2022.

[139] M. Murtomaa, M. Savolainen, L. Christiansen, J. Rantanen, E. Laine, and J. Yliruusi, “Static electrification of powders during spray drying,” *J. Electrostat.*, vol. 62, no. 1, pp. 63–72, 2004, doi: 10.1016/j.elstat.2004.05.001.

[140] T. C. Mike Chung, “Functionalization of Polypropylene with High Dielectric Properties: Applications in Electric Energy Storage,” *Green Sustain. Chem.*, vol. 02, no. 02, pp. 29–37, 2012, doi: 10.4236/gsc.2012.22006.

[141] M. M. Mehanna, S. M. Mohyeldin, and N. A. Elgindy, “Rifampicin-carbohydrate spray-dried nanocomposite: A futuristic multiparticulate platform for pulmonary delivery,” *Int. J. Nanomedicine*, vol. 14, pp. 9089–9112, 2019, doi: 10.2147/IJN.S211182.

[142] X. R. Zhang and H. Yamaguchi, “An experimental study on heat transfer of CO2 solid-gas two phase flow with dry ice sublimation,” *Int. J. Therm. Sci.*, vol. 50, no. 11, pp. 2228–2234, 2011, doi: 10.1016/j.ijthermalsci.2011.05.019.

[143] N. Carrigy and R. Vehring, “Engineering Stable Spray-Dried Biologic Powder for

Inhalation," in *Pharmaceutical Inhalation Aerosol Technology*, 3rd ed., A. J. Hickey and S. R. da Rocha, Eds. Boca Raton, FL: CRC Press, Taylor & Francis Group, 2019, pp. 291–320.